NIST Technical Note
NIST TN 2334

Suspect Screening of Per- and Polyfluoroalkyl Substances in New Firefighter Turnout Gear Textiles

Andrew Maizel
Andre Thompson
Benjamin Place
Alix Rodowa
Jessica Reiner
Audrey Tombaugh
Halen Solomon
Brittany Stinger
Michelle Donnelly
Rick Davis

This publication is available free of charge from:
https://doi.org/10.6028/NIST.TN.2334

NIST NATIONAL INSTITUTE OF STANDARDS AND TECHNOLOGY
U.S. DEPARTMENT OF COMMERCE

NIST Technical Note
NIST TN 2334

Suspect Screening of Per- and Polyfluoroalkyl Substances in New Firefighter Turnout Gear Textiles

Rick Davis
Michelle Donnelly
Andrew Maizel
Halen Solomon
Brittany Stinger
Andre Thompson
Audrey Tombaugh
Fire Research Division
Engineering Laboratory

Benjamin Place
Jessica Reiner
Alix Rodowa
Chemical Sciences Division
Material Measurement Laboratory

This publication is available free of charge from:
https://doi.org/10.6028/NIST.TN.2334

March 2025

U.S. Department of Commerce
Howard W. Lutnick, Secretary

National Institute of Standards and Technology
Craig Burkhardt, Acting Under Secretary of Commerce for Standards and Technology and Acting NIST Director

NIST TN 2334
March 2025

Certain equipment, instruments, software, or materials, commercial or non-commercial, are identified in this paper in order to specify the experimental procedure adequately. Such identification does not imply recommendation or endorsement of any product or service by NIST, nor does it imply that the materials or equipment identified are necessarily the best available for the purpose.

Publication History
Approved by the NIST Editorial Review Board on 2025-03-18

How to Cite this NIST Technical Series Publication
Maizel, A., Thompson, A., Place, B., Rodowa, A., Reiner, J., Tombaugh, A., Solomon, H., Stinger, B., Donnelly, M., Davis, R. (2025) Suspect Screening of Per- and Polyfluoroalkyl Substances in New Firefighter Turnout Gear Textiles. (National Institute of Standards and Technology, Gaithersburg, MD), NIST Technical Note (TN) NIST TN 2334. https://doi.org/10.6028/NIST.TN.2334

Author ORCID iDs
Rick Davis: 0000-0003-2264-0490
Michelle Donnelly: 0000-0003-1800-5515
Andrew Maizel: 0000-0002-2981-5241
Benjamin Place: 0000-0003-0953-5215
Alix E. Rodowa: 0000-0002-3990-2111
Jessica L. Reiner: 0000-0002-1419-6062
Halen Solomon: 0000-0002-8664-9577
Brittany Stinger: 0009-0000-7231-8307
Andre Thompson: 0000-0001-5717-6902
Audrey Tombaugh: 0009-0008-4656-2742

Contact Information
rick.davis@nist.gov

Abstract

Turnout gear protects firefighters from exposure to flames, heat, and liquids and is made from textiles which have been found to contain per- and polyfluoroalkyl substances (PFAS). Previous examinations of PFAS in turnout gear have predominantly utilized targeted analytical approaches, which quantify a limited number of PFAS with established quantitative methods. This NIST Technical Note describes the first use of liquid chromatography high-resolution mass spectrometry combined with suspect screening to search for the presence of over 4,000 PFAS in firefighter turnout gear textiles. PFAS were ionized with negative mode electrospray and the resulting mass spectral features were screened against the NIST PFAS Suspect List as either deprotonated ions ($[M-H]^-$) or acetate adducts ($[M+C_2H_3O_2]^-$), which enabled the detection of a highly chemically diverse set of PFAS. Molecular formulas were assigned to mass spectral features by comparison of precursor ion spectra against predicted isotopic distributions while chemical identities were determined and evaluated by comparison of precursor and product ion spectra against previously collected spectra using the NIST Database Infrastructure for Mass Spectrometry (DIMSpec) application MSMatch. Six PFAS compound identities were confirmed in firefighter gear textiles with high confidence, including four that were not quantified in a previously reported targeted analysis of the same textiles. Additionally, this is the first reported identification of three PFAS (perfluorobutane sulfonamido ethanol, perfluorobutane sulfonamido diethanol, and 6:2 fluorotelomer sulfate) in any outerwear textile. Overall, this NIST Technical Note demonstrates the need for PFAS screening techniques can discern a broader swath of PFAS than targeted analysis alone and also the capability of DIMspec and MSMatch to provide and evaluate PFAS compound annotations.

Keywords

Firefighter; firefighter gear; high resolution-mass spectrometry; nontargeted analysis; per- and polyfluoroalkyl substances; PFAS; suspect screening; turnout gear.

Table of Contents

List of Tables

List of Figures

Author Contributions

Andrew Maizel: Conceptualization, Formal Analysis, Investigation, Methodology, Writing – original draft. **Andre Thompson**: Conceptualization, Investigation, Methodology. **Benjamin Place**: Investigation, Writing- Reviewing and Editing. **Alix Rodowa**: Writing- Reviewing and Editing, Validation. **Jessica Reiner**: Writing- Reviewing and Editing, Validation. **Audrey Tombaugh**: Writing – Reviewing and Editing. **Halen Solomon**: Writing- Reviewing and Editing. **Brittany Stinger**: Writing – Reviewing and Editing. **Michelle Donnelly**: Resources, Writing – Reviewing and Editing. **Rick Davis**: Conceptualization, Funding Acquisition, Project Administration, Resources

1. Introduction

Per- and polyfluoroalkyl substances (PFAS) are a diverse class of thousands of anthropogenically derived compounds, including many that have been observed in consumer goods [1-3]. For example, firefighter turnout gear textiles have been found to contain numerous PFAS [4-8] as well as fluoropolymer membranes and side-chain fluorinated polymer treatments [7]. While little is known about the toxicological effects of most PFAS, some have been found to produce negative health effects such as endocrine disruption, growth defects, and immunosuppression [9].

Due to the number and chemical diversity of PFAS that are known or speculated to be present in consumer goods and the environment, a variety of analytical approaches have been applied to their identification and quantification [10, 11]. Total fluorine concentrations in consumer goods have been reported with combustion ion chromatography (CIC), instrumental neutron activation analysis (INAA), and particle-induced gamma ray emission (PIGE) [7, 8, 12-15], while concentrations of individual PFAS are typically determined by targeted analysis with liquid chromatography-tandem mass spectrometry (LC-MS/MS) or gas chromatography-mass spectrometry (GC-MS) [4-8, 13-15]. However, while targeted approaches are able to determine the concentration of previously specified compounds at extremely low concentrations, only nontargeted analytical approaches can identify PFAS without previously selecting analytes and has been used to identify hundreds of individual PFAS in consumer products as well as environmental and human matrices [16, 17].

Multiple strategies have been employed for the nontargeted identification of PFAS with high resolution mass spectrometry (HRMS) [17], but nontargeted approaches are generally divided into two workflows: nontarget screening and suspect screening. Broadly, nontarget screening involves prioritizing mass spectral features according to defined protocols (e.g., mass defects, presence of specific tandem mass spectrometry (MS/MS) fragments, statistical analysis such as clustering, or effect-directed methods such as bioassays), then annotating molecular formulas and structures by evaluation of the mass spectrometry (MS) precursor ion mass spectra and MS/MS fragmentation spectra, respectively [18, 19]. Conversely, suspect screening prioritizes features by screening extracted ion chromatograms (XICs) for those that match the predicted *m/z* of species from a predetermined list of “suspects” [18]. Numerous PFAS suspect lists have been released [20]. For example, the National Institute of Standards and Technology (NIST) has aggregated a list of 4,967 PFAS (as of February 27, 2025) from a variety of public sources and correspondence with PFAS researchers [21]. Once potential suspect matches have been identified, the confidence with which formula and structural annotations (i.e., chemical characteristics determined from mass spectra) are assigned can be expressed with confidence scales that are general to nontargeted analysis [22] or specific to PFAS [23].

Previous investigations have quantified nonvolatile PFAS in firefighter turnout gear by LC-MS/MS or liquid chromatography-quadrupole time-of-flight mass spectrometry (LC-QTOF-MS), volatile PFAS by GC-MS or GC-QTOF-MS, and total fluorine by PIGE or INAA [4-8]. Paired measurements of total fluorine and summed PFAS concentrations in firefighter turnout gear typically reveal large discrepancies, suggesting that most of the fluorine in firefighter gear is not present as the analytes that are quantified by targeted PFAS analysis [7, 8]. While two previous reports have utilized nontargeted analytical approaches to identify volatile PFAS in firefighter gear, there are

no similar reports for nonvolatile PFAS [6, 7]. Similarly, reports of nonvolatile PFAS in fire station dust or wipe samples of turnout gear [24], as well as waterproof outerwear [13, 25-28] or other textiles such as school uniforms [14] and car seat covers [15] have not utilized nontargeted analytical approaches.

Therefore, the objective of this study was to identify previously unnoticed non- and semivolatile PFAS in firefighter turnout gear textiles with LC-HRMS. The specific objectives included collecting LC-HRMS spectra from the analysis of firefighter turnout gear textiles, applying a suspect screening workflow built with open-source tools to identify novel PFAS, and evaluate the confidence of the determined compound annotations.

2. Materials and Methods

Experimental chemicals and consumables (Section 2.1) were identical to those used in three previous NIST Technical Notes (NIST TN), which reported the occurrence and concentration of PFAS in various firefighter textiles [4, 5, 29]. Seventeen firefighter turnout gear textiles were obtained from a distributor of firefighter gear (Section 2.2). PFAS analytical standards (Sections 2.3 and A.1), and extraction techniques (Section 2.4) were also as used in previous NIST TNs related to PFAS in firefighter gear [4].

2.1. Chemicals and Consumables

Ammonium acetate (Optima LC-MS grade), ammonium hydroxide (Optima grade), methanol (Optima LC-MS grade), and water (Optima LC-MS grade) were obtained from Thermo Fisher Scientific (Waltham, MA).[1] Nitrogen gas (Ultra High Purity grade) was obtained from Roberts Oxygen (Rockville, MD).

Amber glass 2 mL capacity high-performance liquid chromatography (HPLC) vials and 250 µL capacity glass vial inserts were obtained from Agilent Technologies (Santa Clara, CA). Polyethylene caps for HPLC analysis were obtained from Phenomenex (Torrence, CA). HPLC vials, inserts, and caps were used as received from their vendors. Supelco Supelclean ENVI-Carb solid phase extraction (SPE) tubes (6 mL x 500 mg) were obtained from MilliporeSigma (St. Louis, MO) and rinsed with 20 mL of 0.1 mol/L ammonium hydroxide in methanol prior to use. Glass 20 mL capacity borosilicate glass vials, glass Pasteur pipettes, and polypropylene 15 mL capacity centrifuge tubes (Antylia Scientific, Vernon Hills, IL) were used as received. Syringes (1 mL capacity) and syringe filters (0.22 µm, nylon) were obtained from Thermo Fisher Scientific and rinsed with 1 mL methanol prior to use.

2.2. Structural Firefighter Turnout Gear Textiles

Seventeen turnout gear textiles, including four thermal liner (TL-A, TL-B, TL-C, TL-D), six moisture barrier (MB-A, MB-B, MB-C, MB-D, MB-E, MB-F) and seven outer shell textiles (OS-A, OS-B, OS-C, OS-D, OS-E, OS-F, OS-G) were obtained in 2020 from a distributor and repairer of firefighter gear, prior to their assembly into turnout gear and without regard to color. All textiles were compliant with relevant performance requirements of NFPA 1971, the relevant standard for firefighter gear performance when they were manufactured. All textiles are the same and given the same identifiers as in NIST TNs 2248 and 2260 [4, 5].

2.3. Analytical Standards

Various isotopically labeled PFAS solutions were obtained from Wellington Laboratories (ON, Canada) and are listed in Table A.1.

[1] Certain commercial equipment, instruments, or materials are identified in this paper to foster understanding. Such identification does not imply recommendation or endorsement by the National Institute of Standards and Technology, nor does it imply that the materials or equipment identified are necessarily the best available for the purpose.

2.4. PFAS Extraction

Internal standard PFAS (IS) were gravimetrically combined and diluted in methanol to create a working IS spike solution (Table A.2). PFAS were then extracted from firefighter turnout gear textiles by a method discussed in previous NIST publications [4, 5, 29]. Briefly, two sections, each approximately 0.1 g (masses known; Table 1), were cut from each textile and placed into individual 15 mL centrifuge tubes. Approximately 0.1 mL (masses known; Table 1) of IS working solution was added to each centrifuge tube. After approximately an hour had elapsed, 5 mL of methanol was added to each centrifuge tube. The centrifuge tubes were capped and vortexed, before being sonicated at 25 °C for 30 min. The tubes were then centrifuged for 5 min at 2325 relative centrifugal field and the supernatants were decanted into the barrels of methanol-rinsed ENVI-Carb SPE cartridges (500 mg sorbent, 6 mL capacity) and pushed through the ENVI-Carb sorbent material into 20 mL capacity borosilicate glass vials with positive pressure. Methanol addition, vortexing, sonication, centrifugation, and passage through ENVI-Carb SPE cartridges were repeated two additional times to each centrifuge tube; then each SPE cartridge was rinsed with 5 mL 0.1 mol/L ammonium hydroxide in methanol, which was collected in the same borosilicate glass vials used for the three rounds of methanol extraction. The combined extracts were stored at -20 °C overnight before being evaporated to dryness at 40 °C under nitrogen gas in an N-EVAP nitrogen evaporator (Organomotion, Berlin, MA). The extracts were reconstituted in 0.5 mL of methanol before filtration through a methanol-rinsed 0.22 µm pore-size nylon filter.

Table 1. Extraction information including textile sources, measured masses of each cut sample, and measured mass of added internal standard working solution.

Sample	Extract	Textile Mass (g)	IS Working Standard Mass (g)
Extraction Blank	529	-	0.0707
Extraction Blank	530	-	0.0750
OS-A	533	0.1206	0.0742
OS-A	534	0.0978	0.0740
OS-B	538	0.0782	0.0748
OS-B	539	0.0886	0.0750
OS-C	541	0.0864	0.0748
OS-C	543	0.0879	0.0751
OS-D	545	0.0851	0.0750
OS-D	546	0.0988	0.0747
OS-E	549	0.1176	0.0754
OS-E	550	0.1328	0.0752
OS-F	553	0.1387	0.0753
OS-F	554	0.1137	0.0751
OS-G	557	0.1281	0.0757
OS-G	558	0.1164	0.0756
MB-A	561	0.1031	0.0742
MB-A	562	0.0893	0.0747
MB-B	565	0.0993	0.0759
MB-B	566	0.0954	0.0749
MB-C	569	0.1256	0.0752
MB-C	570	0.1292	0.0754
MB-D	573	0.1305	0.0753
MB-D	574	0.1120	0.0746
MB-E	577	0.0807	0.0751
MB-E	578	0.0779	0.0751
MB-F	581	0.0910	0.0753
MB-F	582	0.0966	0.0753
TL-A	585	0.1363	0.0746
TL-A	586	0.1372	0.0759
TL-B	589	0.0992	0.0750
TL-B	590	0.1146	0.0749
TL-C	593	0.1131	0.0743
TL-C	594	0.0970	0.0750
TL-D	597	0.0809	0.0750
TL-D	598	0.1025	0.0753

2.5. Liquid Chromatography High-Resolution Mass Spectrometry

Sample extracts were analyzed as prepared. Liquid chromatography high-resolution mass spectrometry was performed with an UltiMate 3000 Liquid Chromatograph (Thermo Fisher Scientific) and Q-Exactive High-Resolution Mass Spectrometer (Thermo Fisher Scientific). Autosampler vials were kept at 7 °C and 5 µL was injected of each sample extract. Liquid chromatography used a Poroshell 120 EC-C18 analytical column (Agilent Technologies; 3.0 x 50 mm, 2.1 µm) which was kept at a constant temperature of 40 °C. A gradient elution was performed with an aqueous (A) mobile phase consisting of 9.5 mM ammonium acetate, 0.5 mM ammonium hydroxide in water, and a solvent (B) mobile phase consisting of 9.5 mM ammonium acetate, 0.5 mM ammonium hydroxide in methanol. The mobile phase flow was kept at 0.6 mL/min for the entirety of each run and consisted of 10 % B from 12 min prior to each injection to 1 min after each injection and was then increased linearly to 99 % B over 20 min before being held at 95 % B for 7.5 min.

Mass spectrometer settings are shown in Table 2 for both MS1 and data-dependent scans. Only measurements made with negative mode electrospray ionization are reported here. Mass calibration was performed within 24 hours of all analyzed extracts to verify mass accuracy and resolution.

Table 2. Mass spectrometer settings for PFAS suspect screening analysis of firefighter gear textiles.

Sample	**Extract**
Ionization Polarity	Negative
Spray Voltage (V)	3000
Temperature (°C)	250
Sheath Gas	8.25
Auxiliary Gas	0
Default charge state	1
Microscans	1
MS1 Scan Range (*m/z*)	150 to 1200
MS1 Resolution	70,000
MS1 AGC Target (count)	3e6
MS1 Maximum IT (ms)	100
MS2 Resolution	17,500
MS2 AGC Target (count)	1e5
MS2 Maximum IT (ms)	50
TopN	5
Isolation Window (*m/z*)	4.0
Normalized Collision Energy	15, 30, 45
dd AGC Target (count)	8e3
dd Intensity Threshold	1.6e5
dd Dynamic Exclusion (s)	1.0

2.6. PFAS Suspect Screening

Following data collection, the resulting 36 data files for all were converted from .raw to .mzML format with Proteowizard MSConvert (version 3.0.21063; [30]) with the following filters: Peak Picking for MS Levels 1-2 with vendor algorithm and Threshold Peak Filter with Threshold type: Absolute intensity, Orientation: Most intense, and Value: 1.

Following data format conversion, suspect screening was performed within the patRoon software platform [31] in R (version 4.3.2; [32]) with RStudio (version 2023.09.1; [33]). For suspect screening, a list of 4,967 unique PFAS structures was obtained from the NIST PFAS Suspect List [21]. The R script used for feature identification, grouping, and filtering, as well as suspect screening, is in Appendix A.2, with a summary of settings in Table 3. Briefly, feature identification within individual data files was performed with the patRoon function findFeatures(), using the OpenMS FeatureFinderMetabo tool [34], while features from different data files were grouped with the patRoon function groupFeatures(), using the OpenMS FeatureLinkerUnlabelled tool (

Table 3). Feature groups were then filtered for minimum intensity, relative replicate abundance, and relative intensity between samples and blanks with the filter() function. Finally, all remaining features were screened against the 4,967 unique PFAS on the NIST PFAS Suspect List with the screenSuspects() function (Table 3) and only features within 0.001 *m/z* of a predicted suspect *m/z* were considered further.

Features groups were excluded if they were not associated with extracted ion chromatograms that showed reasonably smooth and symmetrical bell-curve-shaped peaks or if they appeared to be the higher mass isotope of a different feature. Additionally, feature groups were excluded if they were associated with suspect compounds that could not plausibly take on the assigned ionization state (e.g., compounds that lacked H but were identified as deprotonated ions ($[M-H]^-$) or if they were identified as acetate adducts but which lacked an MS/MS fragment with *m/z* 59 (i.e., the monoisotopic mass of acetate).

Table 3. patRoon functions and settings used in PFAS suspect screening.

Setting	Corresponding Action
findFeatures(algorithm= "openms",…)	Specifies OpenMS FeatureFinderMetabo tool.
findFeatures(noiseThrInt = 1e4,…)	Sets noise intensity threshold, the minimum peak height to be distinct from baseline noise, at 1e4.
findFeatures(chromSNR = 10,…)	Sets the minimum peak signal-to-noise ratio at 10.
findFeatures(chromFWHM = 20,…)	Expected full width at half chromatographic peak height = 20 s.
findFeatures(minFWHM = 5,…)	Minimum peak width at half chromatographic peak height = 5 s.
findFeatures(maxFWHM = 60,…)	Maximum peak width at half chromatographic peak height = 60 s.
groupFeatures (algorithm = "openms",…)	Specifies OpenMS FeatureLinkerUnlabeled tool for feature grouping.
groupFeatures(rtalign = TRUE,…)	Specifies OpenMS MapAlignerPoseClustering tool for feature retention time alignment.
filter(preAbsMinIntensity =100,…)	Minimum peak intensity prior to other filtering = 100.
filter(AbsMinIntensity = 1e6,…)	Minimum peak intensity for feature consideration = 1,000,000.
filter(relMinReplicateAbundance =1,…)	Minimum feature abundance across all samples = 1 (feature must be present in all replicates).
filter(maxReplicateIntRSD =0.75,…)	Maximum relative standard deviation of feature intensities within a replicate group = 0.75.
filter(blankThreshold = 5,…)	Features present in blanks must be present in other samples with 5 times greater intensity for suspect consideration.
filter(removeBlanks = TRUE,…)	Removes features identified in blanks from consideration.
filter(retentionRange = c(180,1800),…)	Only features with retention times between 180 s and 1,800 s will be considered for suspect screening.
screenSuspects (mzWindow = 0.002,…)	Suspect screening window width = 0.002 *m/z*.
screenSuspects (adduct = "[M-H]-"…)	Sets assumed adduct of suspect compounds, i.e., "[M-H]-" or "[M+C2H3O2]-."
screenSuspects (onlyHits = TRUE,…)	Removes features without suspect list match.

2.7. PFAS Suspect Screening Confidence Assessment

Confidence assessment of compound annotations was expressed with the scale of Charbonnet *et al.* [23], where 5b indicates the lowest level of confidence and 1a the highest. In this scale, compound assignments are evaluated based on agreement between the observed and expected monoisotopic *m/z* and isotopic pattern, the appearance of diagnostic MS/MS fragments, and comparison of the observed spectra against previously collected reference spectra. PFAS identifications reach the highest level of 1a when a compound assignment is confirmed by chromatography-mass spectrometry analysis with a reference standard. Following the recommendations of Charbonnet *et al*., only compound assignments of level 4 and above are reported here. Assigning level 4 or above requires the observed *m/z* and isotopic pattern to provide unequivocal evidence supporting the putative formula assignment. For this NIST TN, level 4 assignments were given when the exact monoisotopic *m/z* was observed along with at least two higher mass isotopes present at the exact *m/z* and at accurate relative intensities.

Features with at least level 4 confidence assignments were noted and the associated MS/MS fragmentation spectra were compared against previously collected PFAS reference spectra with Mass Spectral Match for Non-Targeted Analysis (MSMatch; a [35]), a web application built as an example tool of the Data Infrastructure for Mass Spectrometry (DIMSpec) project. MSMatch provides two functions for matching experimental mass spectra with 351 consensus reference mass spectra from 132 individual PFAS. The compound matching function compares the observed fragmentation spectra against previously collected spectra and provides match scores for both the MS1 and MS2 spectra [21]. Additionally, the fragment matching function matches individual MS/MS fragments with previously annotated fragments and provides a match score. Settings for MSMatch compound and fragment search functions are in Table 4.

Where available, commercially available analytical standards and NIST Reference Materials were obtained for PFAS identified by the above process, and either the same extracts analyzed here, or identically prepared extracts, were analyzed with those standards by LC-HRMS or LC-MS/MS to provide further confirmation of compound annotations.

Table 4. MSMatch data input settings for compound and fragment match functions.

Setting	Value
MS Experiment Type	DDA (data-dependent acquisition)
Relative Error (ppm)	5
Minimum Error (Da)	0.002
Isolation Width (Da)	0.7
Data were collected with an instrumental lock mass	Not selected
Search Type (Compound Match):	Precursor Search

3. Results

Suspect screening for $[M-H]^-$ ions identified 152 features (i.e., corresponding features in both replicate samples; Table A.3). These features were grouped into 38 feature groups (Table A.4), and each feature group was associated with between 1 and 3 suspect PFAS (Table A.5). Similarly, the formation of acetate adduct ions (i.e., $[M+C_2H_3O_2]^-$) during electrospray ionization was presumed to occur due to the presence of acetate in the mobile phase solutions and suspect screening for these adduct ions initially identified 112 features (Table A.6) which were grouped into 26 feature groups (Table A.7), with each feature group associated with between 1 and 40 suspect PFAS (Table A.8). After evaluating the compound assignments, which included considering peak shapes, the plausibility of assigned ionization states, and determination of structural annotation confidence, six compound annotations were assigned confidence levels of 4 or above including four as $[M-H]^-$ ions and two as $[M+C_2H_3O_2]^-$ adducts

Table 5).

Table 5. Compound assignments from PFAS suspect screening that were found to have confidence assignments above level 5, including the assumed ionization state, the feature group identifier, the group *m/z*, group retention time, and matched NIST PFAS Suspect List compounds.

[M-H]- Suspect Matches			
Group	**Group *m/z***	**Group RT (s)**	**Suspect Match(es)**
M299_R226_3160	298.94400	226.2	1,1,2,2-Tetrafluoro-2-(1,1,2,2-tetrafluoroethoxy)ethane-1-sulfonyl fluoride -and- 1,1,2,3,3,3-Hexa-fluoro-2-(trifluoromethyl) propanesulfonic acid -and- Perfluorobutane sulfonic acid
M342_R363_4318	341.98643	363.3	1,1,2,2,3,3,4,4,4-Nonafluoro-N-(2-hydroxyethyl)-1-butanesulfonamide
M427_R466_6072	426.96924	465.6	6:2 Fluorotelomer sulfonic acid
M443_R450_6484	442.96451	449.8	6:2 fluorotelomer sulfate -and- 1-Hydroxy-6:2 fluorotelomer sulfonate
$[M+C_2H_3O_2]$- Suspect Matches			
Group	**Group *m/z***	**Group RT (s)**	**Suspect Match(es)**
M416_R452_5807	416.02396	451.7	1,1,2,2,3,3,4,4,4-Nonafluoro-N-(2-hydroxyethyl)-N-methyl-1-butanesulfonamide -and- N-(2-hydroxyethyl)-N-Methylperfluoro-2-methylpropanesulfonamide
M446_R395_6558	446.03444	395.4	1,1,2,2,3,3,4,4,4-Nonafluoro-N,N-bis(2-hydroxyethyl)butane-1-sulphonamide -and- 1,1,2,3,3,3-Hexafluoro-N,N-bis(2-hydroxyethyl)-2-(trifluoromethyl)propane-1-sulphonamide

3.1. Feature Group M299_R226_3160

Feature group M299_R226_3160 with retention time of 226.2 s (3.77 min.) and *m/z* 298.94400 (Figure 1a, Table A.3, Table A.4) was observed in both extracts of MB-E and matched as an [M-H]- ion with three structural isomers from the NIST PFAS suspect list that shared the uncharged molecular formula $C_4HF_9O_3S$: 1,1,2,2-Tetrafluoro-2-(1,1,2,2-tetrafluoroethoxy) ethane-1-sulfonyl fluoride, 1,1,2,3,3,3-hexa-fluoro-2-(trifluoromethyl) propanesulfonic acid, and perfluorobutane sulfonic acid (PFBS; Figure 1b, Table A.5).

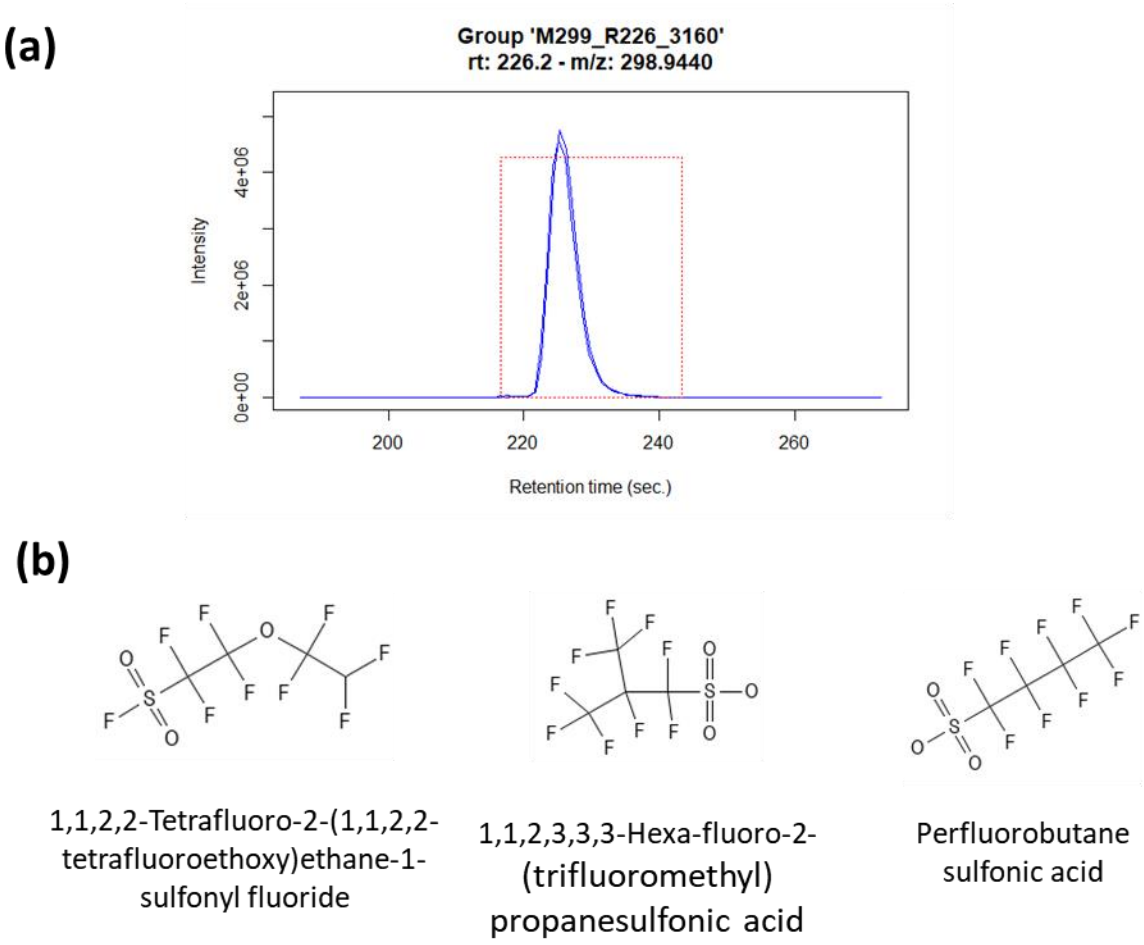

Figure 1. (a) Extracted ion chromatogram for feature group M299_R226_3160 in extracts of moisture barrier textile MB-E and (b) molecular structures for the NIST PFAS Suspect List compounds tentatively matched with this group.

The formula annotation was confirmed by exact mass match of the precursor ion *m/z* (mass error: 3.08 ppm; Table 6), as well as the similarity between the observed MS1 mass spectra and predicted relative intensities of the higher mass isotopes $^{13}C_1$-$C_3F_9O_3S$ and $^{34}S_1$-$C_4F_9O_3$ (Table 6). Also present in the precursor ion mass spectra is the feature corresponding to the mass labeled $^{13}C_3$-PFBS internal standard, which co-eluted with this feature group (Figure A.2a, Table 6).

Table 6. Predicted and observed *m/z*, and associated measured mass error, as well as the predicted and observed relative abundances associated with the feature corresponding to group M299_R226_3160, as observed in extract 577. The observed *m/z* and associated mass error for the monoisotopic mass are taken from the feature group, while the higher mass isotope *m/z* and associated mass error are taken from the mass spectra of extract 577 (MB-E), integrated from 3.64 min - 3.92 min. (Figure A.1).

Isotope	Predicted *m/z*	Observed *m/z*	Error (ppm)	Predicted Rel. Abundance	Observed Rel. Abundance
$C_4F_9O_3S$	298.94299	298.94391	3.08	100 %	100 %
^{13}C-$C_3F_9O_3S$	299.94635	299.94777	4.73	4.33 %	4.11 %
^{34}S-$C_4F_9O_3$	300.93879	300.94004	4.15	4.43 %	4.29 %
$^{13}C_3$-PFBS (IS)	301.95306	301.95423	3.87	N/A	21.38 %

Compound annotation was evaluated with the Mass Spectral Match (MSMatch) application of the Database Infrastructure for Mass Spectrometry (DIMSpec) project [35]. Feature group M299_R226_3160 was evaluated with the .mzML file from the analysis of extract 577, considering precursor *m/z* 298.944, with a retention time window of 3.70 min -3.90 min (Figure 2). The MSMatch compound match function determined 10 compound matches, all of which were mass spectra previously identified as PFBS and obtained from the analysis of analytical standards, aqueous film-forming foams, or commercial formulations (Figure A.2b, Table A.9). The fragment match function associated structures to 6 of the 15 observed fragments, which were all plausible for the fragmentation of PFBS, including diagnostic fragments such as *m/z* 79.9561 (annotated fragment formula: $[SO_3]^-$, mass error: -9.17 ppm) and 168.9886 ($[C_3F_7]^-$; -0.99 ppm; Figure A.2c, Table A.10, Table A.11). An additional 3 fragments were further associated with molecular formulas by manual annotation (Table A.12).

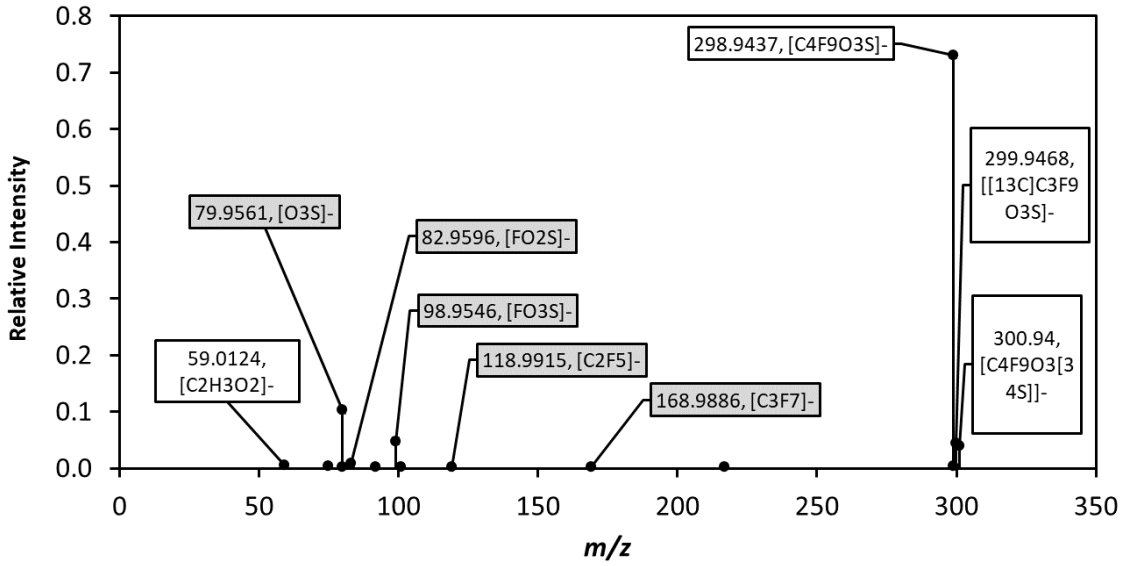

Figure 2. MS/MS fragmentation spectrum from precursor *m/z* 298.944, retention time window of 3.70 min – 3.90 min, from extract 577 of MB-E. Annotations in grey were determined by the fragment match tool of MSMatch, while annotations in white were determined manually.

The compound annotation was further investigated by comparison of the observed extracted ion chromatogram associated with this feature with the observed ion chromatogram of the internal standard compound $^{13}C_3$-PFBS, which was present at a nominal concentration of 1.84 ng/mL. The retention time and peak shape of this feature showed excellent agreement with that of $^{13}C_3$-PFBS (Figure A.2a).

The two extracts where this feature was identified were subsequently analyzed for PFBS with LC-MS/MS by comparison with commercially available analytical standards and NIST Reference Material 8447. PFBS was found to be present in these extracts at approximately 5.3 ng/mL, which was above the recorded concentrations of PFBS in any of the other extracts in this batch. Additionally, NIST TN 2248 determined the concentration of PFBS in MB-E to be 34 µg/kg ± 10 µg/kg, which was the highest PFBS concentration of any firefighter gear textile in that report [4].

Given the matching retention time of this feature and $^{13}C_3$-PFBS, the agreement between the observed precursor ion spectra and the predicted isotopic distribution of PFBS, the MS2 fragmentation spectra which both matches previously collected spectra for PFBS and contains multiple diagnostic fragments, and the subsequent targeted LC-MS/MS analysis which confirmed PFBS to be present by comparison with a NIST reference standard, this feature group is annotated as PFBS with confidence level 1a – confirmed by reference standard.

3.2. Feature Group M342_R363_4318

Feature group M342_R363_4318, with a retention time of 363.3 s (6.06 min) and *m/z* 341.98643 (Figure 3a, Table A.3, Table A.4) was present in both extracts of MB-E and was matched as an [M-H]- ion with suspect PFAS 1,1,2,2,3,3,4,4,4-nonafluoro-N-(2-hydroxyethyl)-1-butanesulfonamide (FBSEE; Figure 3b).

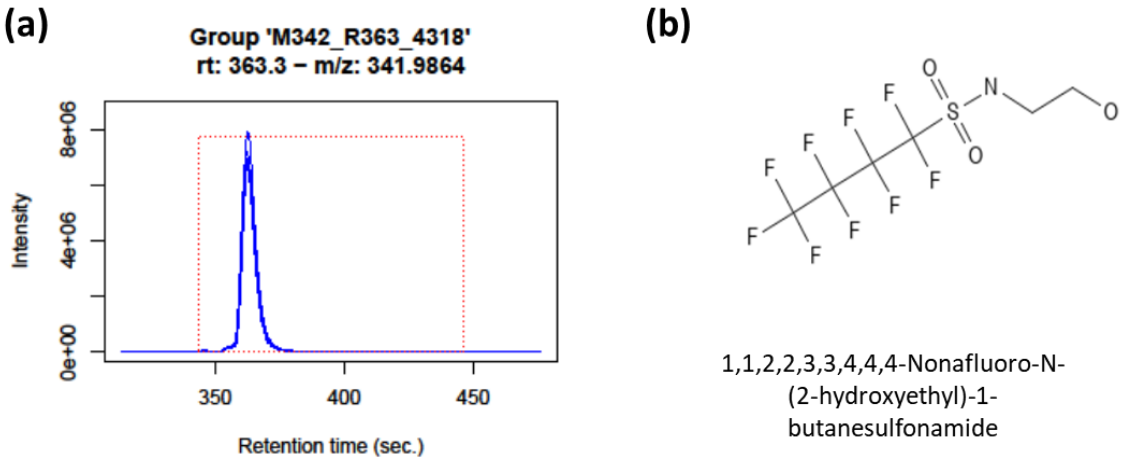

Figure 3. (a) Extracted ion chromatogram for feature group M342_R363_4318 in extracts of moisture barrier textile MB-E and (b) molecular structure for the NIST PFAS Suspect List compound tentatively matched with this group.

The formula annotation was confirmed by observation of the precursor ion *m/z* (mass error: 3.63 ppm; Table 7**Error! Reference source not found.**), as well as the similarity between the observed and predicted *m/z* and relative intensities of the precursor higher mass isotopes $^{13}C_1$-$C_3F_9O_3S$ and $^{34}S_1$-$C_4F_9O_3$.

Table 7. Predicted and observed *m/z*, and associated measured mass error, as well as the predicted and observed relative abundances associated with the feature corresponding to group M342_R363_4318, as observed in extract 577 (MB-E). The observed *m/z* and associated mass error for the monoisotopic mass are taken from the feature group averaged values, while the higher mass isotope *m/z* and associated mass error are taken from the mass spectra of extract 577, integrated from 5.98 min – 6.17 min. (Figure A.3).

Isotope	Predicted *m/z*	Observed *m/z*	Mass Error (ppm)	Predicted Rel. Abundance (%)	Observed Rel. Abundance (%)
$C_6F_9H_5NO_3S$	341.98519	341.98643	3.63	100 %	100 %
^{13}C-$C_5F_9H_5NO_3S$	342.98855	342.99013	4.61	6.49 %	6.35 %
^{34}S-$C_6F_9H_5NO_3$	343.98099	343.98211	3.26	4.43 %	4.32 %

Compound annotation was again evaluated with MSMatch using the extract 577 mzML file, and considering precursor *m/z* 341.986 with a retention time window of 5.90 min – 6.20 min. No matches were obtained with the compound match function, while the fragment match function identified 21 peaks and annotated 2: one with *m/z* 82.9596 was matched with $[FO_2S]^-$, while another with *m/z* 218.9862 was matched with $[C_4F_9]^-$ (Figure 4, Table A.13, Table A.14). Manual annotation matched a further 8 peaks with likely formulas (Table A. 15).

Given the agreement between the observed precursor ion spectra and the predicted isotopic distribution of FBSE as well as the presence of more than 3 diagnostic fragments in the MS/MS fragmentation spectra, this feature group is annotated as FBSE with confidence level 2b – probable by diagnostic fragmentation evidence.

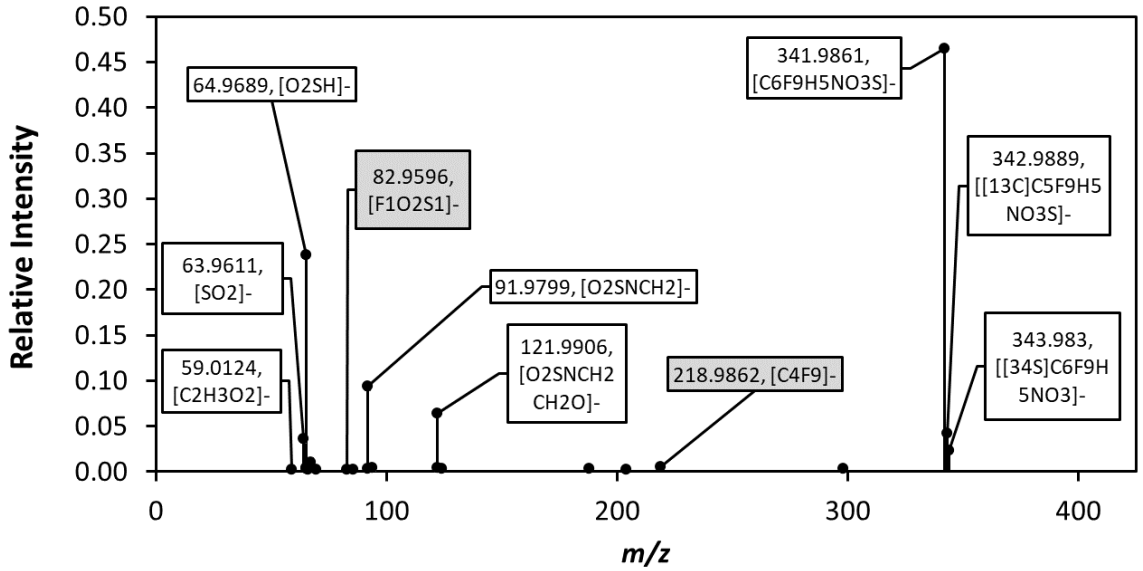

Figure 4. MS/MS fragmentation spectrum from precursor *m/z* 341.986, with a retention time window of 5.90 min – 6.20 min, in extract 577. Annotations in grey were determined by the fragment match tool of MSMatch, while annotations in white were determined manually.

3.3. Feature Group M427_R466_6072

Feature group M427_R466_6072, with a retention time of 465.6 s (7.76 min) and *m/z* 426.96924 was present in both extracts of MB-E (Figure 5a, Table A.3, Table A.4) and was matched as an $[M-H]^-$ ion with suspect PFAS 6:2 fluorotelomer sulfonic acid (6:2 FTS; Figure 5b).

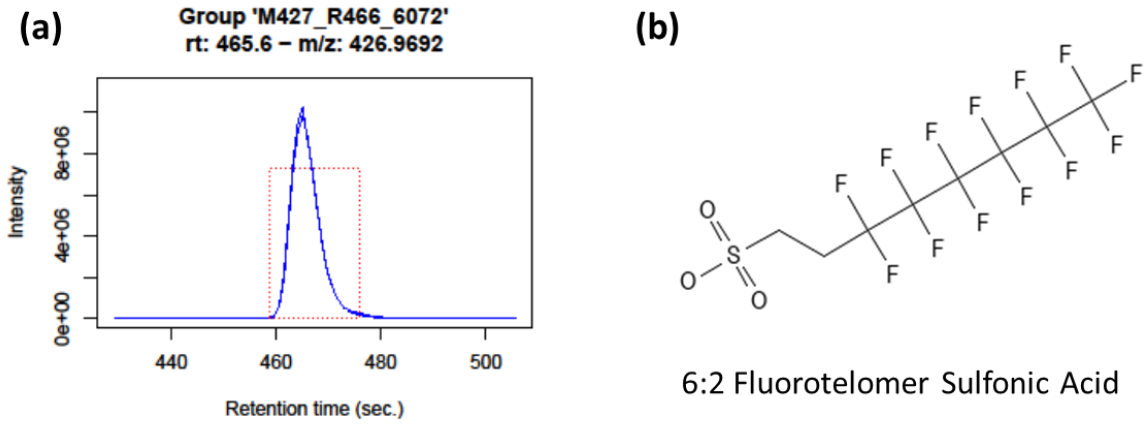

Figure 5. (a) Extracted ion chromatogram for feature group M427_R466_6072 in extracts of MB-E and (b) molecular structures for the NIST PFAS Suspect List compounds tentatively matched with this group.

The formula annotation was confirmed by observation of the precursor ion *m/z* as well as the similarity between the predicted and observed precursor ion spectra and relative intensities of the higher mass isotopes ^{13}C - $C_7H_4F_{13}O_3S$ and ^{34}S - $C_8H_4F_{13}O_3$ (Table 8). Also present in the mass spectra is a feature corresponding to the mass labeled internal standard $^{13}C_2$ - 6:2 FTS, which co-eluted with this feature (Figure A.4c).

Table 8. Predicted and observed *m/z*, and associated measured mass error, as well as the predicted and observed relative abundances associated with the feature corresponding to group M427_R466_6072, as observed in extract 577 (MB-E). The observed *m/z* and associated mass error for the monoisotopic mass are taken from the feature group, while the higher mass isotope *m/z* and associated mass error are taken from the mass spectra of extract 577, integrated from 7.66 min – 7.84 min (Figure A.4a).

Isotope	Predicted *m/z*	Observed *m/z*	Mass Error (ppm)	Predicted Rel. Abundance	Observed Rel. Abundance
$C_8H_4F_{13}O_3S$	426.96733	426.96924	4.47	100 %	100 %
^{13}C - $C_7H_4F_{13}O_3S$	427.97069	427.97253	4.30	8.65 %	9.39 %
^{34}S - $C_8H_4F_{13}O_3$	428.96313	428.96505	4.48	4.43 %	3.84 %
$^{13}C_2$ - 6:2 FTS (IS)	428.97404	428.97594	4.43	N/A	1.93 %

Compound annotation was evaluated with MSMatch using the extract 577 .mzML file, considering precursor *m/z* 426.969 and a peak retention time window of 7.70 min – 7.85 min (Figure 6). The MSMatch compound match function determined 5 compound matches, with MS1 match scores up to 0.9647 and MS2 match scores up to 0.7238, all of which were from mass spectra produced from the analysis of 6:2 FTS analytical standards or an aqueous film-forming foam known to contain 6:2 FTS (Table A.16, Figure A.5). The fragment match function associated structures with 4 of the 21 identified fragment peaks and associated a molecular formula with an additional fragment peak (Table A.17, Table A.18), including diagnostic fragments such as *m/z* 79.9561 (SO_3^-). An additional 5 peaks were manually annotated (Table A.19), including fragments corresponding to $[M\text{-}HF]^-$ and $[M\text{-}H_2F_2]^-$.

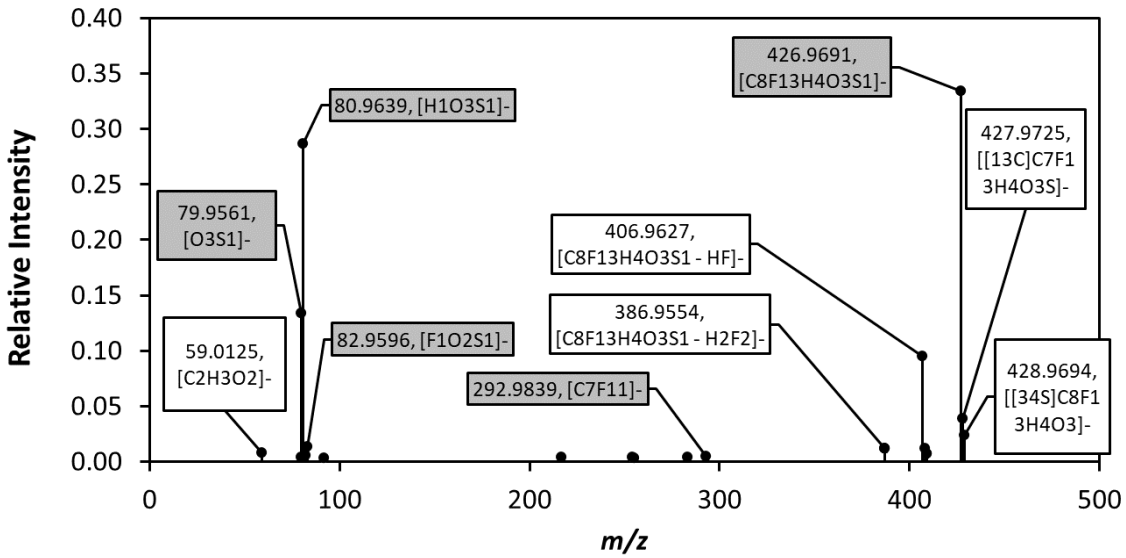

Figure 6. MS/MS fragmentation spectrum from precursor *m/z* 426.969, a retention time window of 7.70 min – 7.85 min, in extract 577. Annotations in grey were determined by the fragment match tool of MSMatch, while annotations in white were determined manually.

The two MB-E extracts which were analyzed here were subsequently analyzed for 6:2 FTS with LC-MS/MS by comparison with commercially available analytical standards and 6:2 FTS was found to be present in these extracts at approximately 20 ng/mL, which was above the recorded concentrations of 6:2 FTS in any of the other extracts in this batch. Additionally, NIST TN 2248 determined the concentration of 6:2 FTS in MB-E to be 613 µg/kg ± 15 µg/kg, which was the highest 6:2 FTS concentration of any firefighter gear textile in that report [4].

Given the matching retention time of this feature and $^{13}C_2$-6:2 FTS, the agreement between the observed precursor ion spectra and the predicted isotopic distribution of 6:2 FTS, the fragmentation spectra which both matches previously collected spectra for 6:2 FTS and contains multiple diagnostic fragments, and the subsequent targeted LC-MS/MS analysis which confirmed 6:2 FTS to be present by comparison with analytical standards, this feature group is annotated as 6:2 FTS with confidence level 1a – confirmed by reference standard.

3.4. Feature Group M443_R450_6484

Feature group M443_R450_6484 with *m/z* 442.96451 and a retention time of 449.8 s (7.50 min.; Figure 7a, Table A.3, Table A.4) was present in both extracts of OS-B (i.e., 538, 539) and OS-F (i.e., 553, 554) and was matched as an $[M-H]^-$ ion with suspect PFAS 6:2 fluorotelomer sulfate (6:2FTSa) and 1-hydroxy-6:2 fluorotelomer sulfonate (1OH-6:2 FTS; Figure 7b).

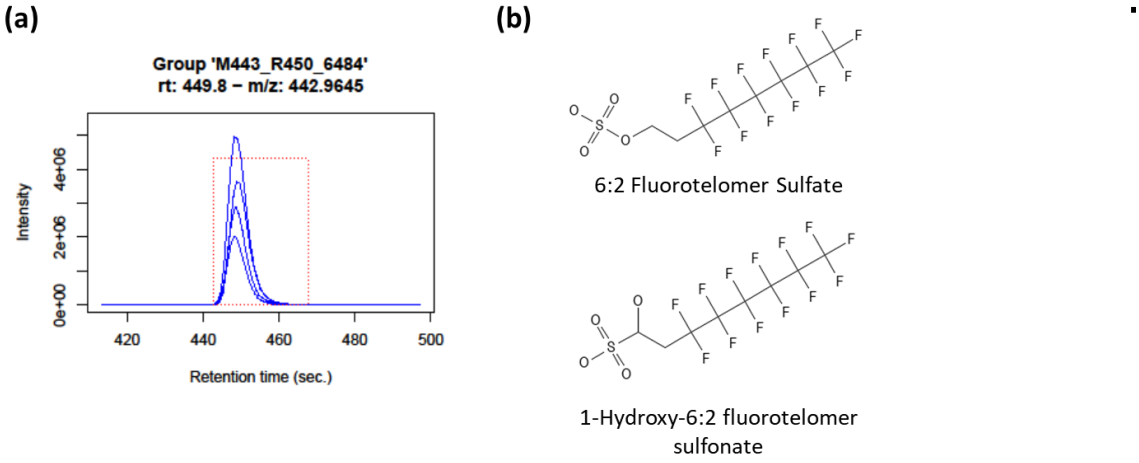

Figure 7. Extracted ion chromatogram for feature group M443_450_6484 in extracts of OS-B and OS-F, (b) molecular structures for the NIST PFAS Suspect List compounds tentatively matched with this group.

The shared formula annotation was confirmed by exact mass match of the monoisotopic *m/z* as well as the similarity between the observed precursor ion mass spectra and the predicted *m/z* and relative abundances of the higher mass isotopes ^{13}C-$C_7H_5F_{13}O_4S$ and ^{34}S-$C_8H_5F_{13}O_4$ (Table 9).

Table 9. Predicted and observed *m/z*, and associated measured mass error, as well as the predicted and observed relative abundances associated with the feature corresponding to group M427_R466_6072, as observed in extract 553 (OS-F). The observed *m/z* and associated mass error for the monoisotopic mass are taken from the feature group, while the higher mass isotope *m/z* and associated mass error are taken from the mass spectra of extract 553, integrated from 7.41 min – 7.59 min (Figure A.6a).

Isotope	Predicted *m/z*	Observed *m/z*	Mass Error (ppm)	Predicted Rel. Abundance	Observed Rel. Abundance
$C_8H_4F_{13}O_4S$	442.96282	442.96451	3.82	100 %	100 %
^{13}C-$C_7H_4F_{13}O_4S$	443.96617	443.96788	3.85	8.65 %	8.97 %
^{34}S-$C_8H_4F_{13}O_4$	444.95862	444.95944	1.84	4.43 %	3.76 %

Compound annotation was evaluated with MSMatch using the extract 553 .mzML file, considering precursor *m/z* 442.965 with retention time window of 7.40 min – 7.75 min (Figure 8). No matches were obtained with the compound match function, while the fragment match function annotated 2 fragments with structures: one with *m/z* 79.9561 was matched with $[O_3S]^-$, while another with *m/z* 98.9547 was matched with $[FO3S]^-$ (Table A.20, Table A.21). Manual annotation matched a further 4 peaks with likely formulas, as well as an alternative annotation for the peak with *m/z* 98.9547 (Table A.22). This peak was matched with the structure $[FO_3S]^-$ (mass error: -5.31 ppm) by the fragment match function, but an alternative annotation of

$[H^{34}SO_4]^-$ (mass error: -12.13 ppm) appears more likely given the relative intensity between this peak and the peak with *m/z* 96.9589 (i.e., measured $^{34}S/^{32}S$: 3.99 % vs. predicted: 4.43 %). Given the fragmentation precursor *m/z* of 442.965, the presence of fragment higher mass isotopes was not expected, however, the appearance of a peak corresponding to $C_8H_4F_{13}O_4{}^{34}S$ in the MS/MS spectrum at a relative abundance of 5.48 % of the peak corresponding to $C_8H_4F_{13}O_4{}^{32}S$ confirms the presence of higher mass isotopes in this spectrum at relative intensities near their predicted values (Figure 8).

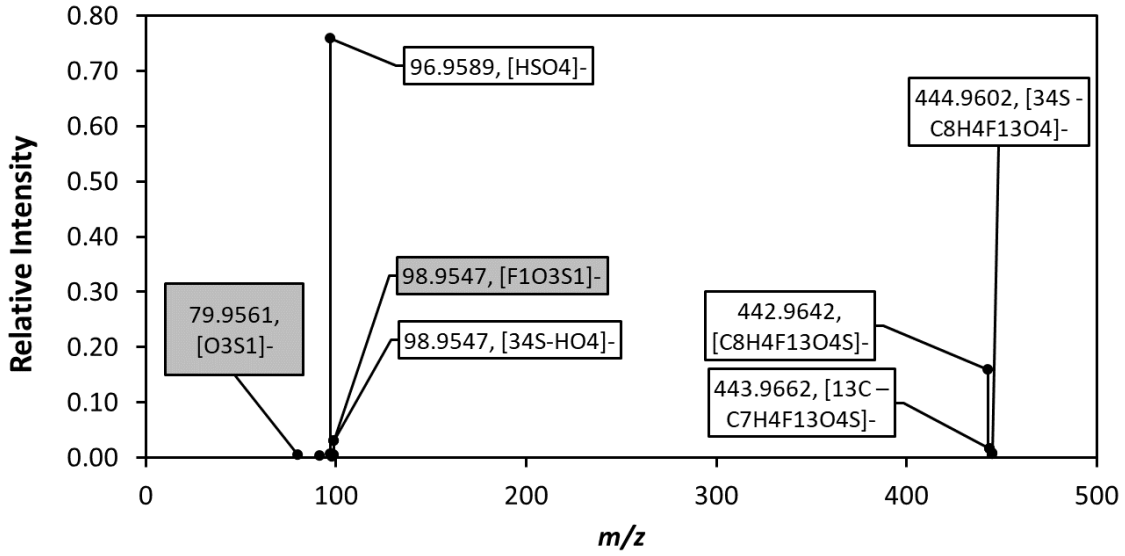

Figure 8. MS/MS fragmentation spectrum from precursor *m/z* 442.965, retention time window of 7.40 min – 7.75 min, in extract 553. Annotations in grey were determined by the fragment match tool of MSMatch, while annotations in white were determined manually. Note the double annotation for the peak with *m/z* 98.9547.

This feature is annotated as 6:2 FTSa with confidence level 2b - probable by diagnostic fragmentation evidence, due to the agreement between the observed and predicted precursor ion mass spectra and the observation of at least 3 diagnostic MS/MS fragments.

3.5. Feature Group M416_R452_5807

Feature group M416_R452_5807, with *m/z* 416.0240 and a retention time of 451.7 s (7.53 min) was present in both extracts of moisture barrier textile MB-C (Figure 9a, Table A.6, Table A.7), matched as an $[M+C_2H_3O_2]^-$ adduct with two structural isomers from the NIST PFAS Suspect List which shared the molecular formula $C_7H_8F_9NO_3S$: N-(2-hydroxyethyl)-N-methylperfluoro-2-methylpropane-sulfonamide (br-MeFBSE) and 1,1,2,2,3,3,4,4,4-nonafluoro-N-(2-hydroxyethyl)-N-methyl-1-butane-sulfonamide (n-MeFBSE; Figure 9b, Table A.6 - Table A.8).

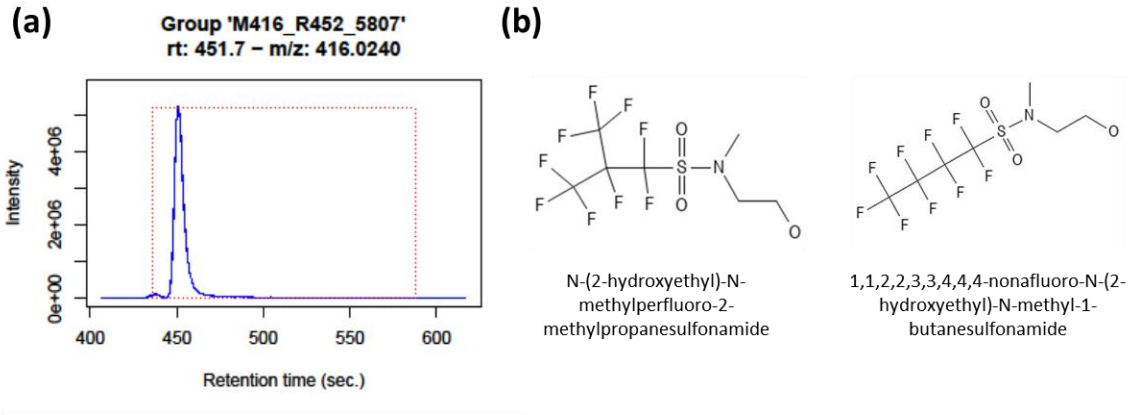

Figure 9. Extracted ion chromatogram for feature group M416_R452_5807 in extracts 569 and 570 of moisture barrier textile MB-C and (b) molecular structures for the NIST PFAS Suspect List compounds tentatively matched with this group.

The shared formula annotation was confirmed by observation of the precursor ion *m/z* (Table 10), as well as the similarity between the observed and predicted *m/z* and relative intensities of the higher mass isotopes ^{13}C-$C_6H_8F_9NO_3S$ and ^{34}S-$C_7H_8F_9NO_3$.

Table 10. Predicted and observed *m/z*, and associated measured mass error, as well as the predicted and observed relative abundances associated with the feature corresponding to group M416_R452_5807, as observed in extract 569 (MB-C). The observed *m/z* and associated mass error for the monoisotopic mass are taken from the feature group, while the higher mass isotope *m/z* and associated mass error are taken from the mass spectra of extract 569, integrated from 7.40 min – 7.76 min (Figure A.7. (a) Mass spectra from extract 569 (MB-C), integrated from 7.40 min – 7.76 min and (b) MS/MS fragmentation spectra, from extract 569 (MB-C), averaged from 7 scans, collected from 7.46 min – 7.64 min with precursor *m/z* 416.0239.Figure A.7a).

Isotope	Predicted *m/z*	Observed *m/z*	Error (ppm)	Predicted Rel. Abundance	Observed Rel. Abundance
$C_7H_8F_9NO_3S$-$C_2H_3O_2$	416.02197	416.02396	4.78	100 %	100 %
^{13}C-$C_6H_8F_9NO_3S$ -$C_2H_3O_2$	417.02533	417.02744	5.06	9.73 %	9.81 %
^{34}S- $C_7H_8F_9NO_3$-$C_2H_3O_2$	418.01777	418.01878	2.42	4.43 %	3.81 %

The extracted ion chromatogram of feature group M416_R452_5807 also contained a preceding peak with an elution time of 7.28 min with a similar isotopic pattern to the main peak at 7.53 min. (Figure A.8), though no MS/MS fragmentation spectra was collected for the earlier eluting peak. The two peaks could indicate the presence of isomers with branched (i.e., br-MeFBSE; Figure 9b) and linear (i.e., n-MeFBSE) perfluorinated carbon chains. The presence of branched and linear isomers would be expected from a compound produced by electrochemical fluorination [36].

Also present in the MS1 spectra of this feature was a peak potentially corresponding to the $[M\text{-}H]^-$ ion, which had a similar retention time and similar isotopic distribution (Figure A.9a, Table 11), but a peak intensity of 1.2 % of that corresponding to the $[M+C_2H_3O_2]^-$ feature.

Table 11. Predicted and observed *m/z*, and associated measured mass error, as well as the predicted and observed relative abundances associated with the feature corresponding to the $[M-H]^-$ ion of the same molecule as group M416_R452_5807, as observed in extract 569. The observed *m/z* and associated mass error all are taken from the mass spectra of extract 569 (MB-C), integrated from 7.45 min – 7.61 min.

Isotope	Predicted *m/z*	Observed *m/z*	Error (ppm)	Predicted Rel. Abundance	Observed Rel. Abundance
$C_7H_7F_9NO_3S$	356.00084	356.00257	4.86	100 %	100 %
^{13}C- $C_6H_7F_9NO_3S$	357.00420	357.00558	3.87	4.81 %	9.81 %
^{34}S- $C_7H_7F_9NO_3$	357.99664	Not observed	-	4.43 %	- %

Compound annotation was evaluated with MSMatch using the extract 569 mzML file and considering precursor *m/z* 416.024 with a retention time window of 7.40 min – 7.75 min (Figure 10). Only a single prominent peak was present in the MS/MS spectra and no matches were obtained with the compound match or fragment match functions (Table A.23). Manual annotation identified peaks corresponding to $[C_2H_3O_2]^-$, as well as the ^{13}C- and ^{18}O-containing isotopes of the same formula (Table A.24).

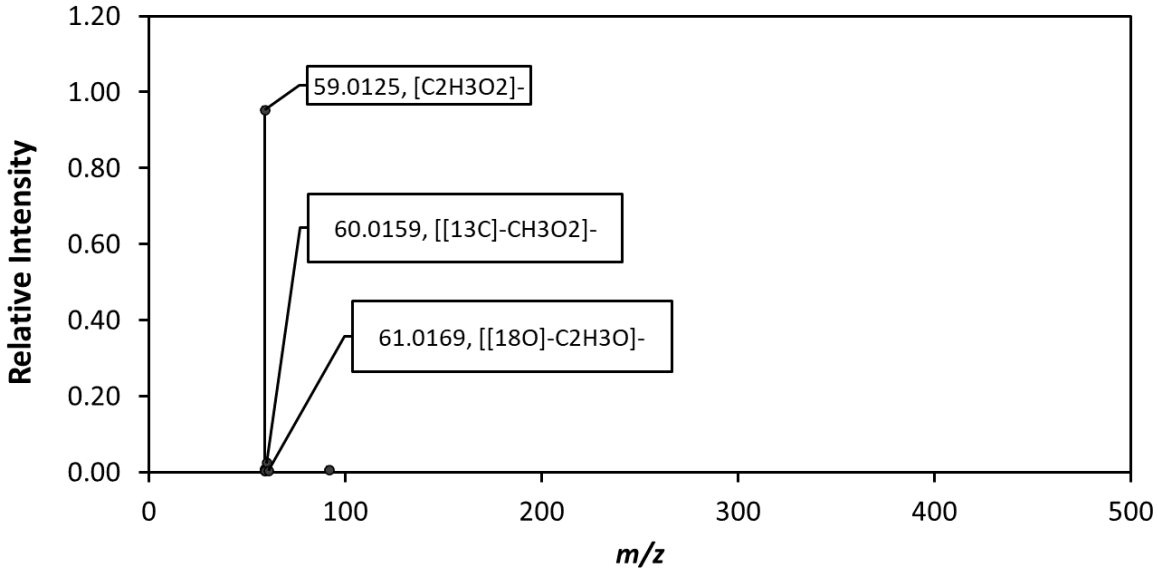

Figure 10. MS/MS fragmentation spectrum from precursor with *m/z* 416.024, a retention time window of 7.40 min – 7.75 min, in extract 569. Annotations in white were determined manually.

Subsequent LC-HRMS and LC-MS/MS analysis of extracts prepared similarly to those analyzed here which used commercially available analytical standards measured n-MeFBSE concentrations of approximately 460 ng/g in MB-E extracts, equivalent to an n-MeFBSE concentration of approximately 92 ng/mL in the extracts analyzed here.

The primary peak in this feature is assigned compound annotation n-MeFBSE with confidence level 1a - confirmed by reference standard due to the quantification of n-MeFBSE in the MB-E extracts by LC-HRMS and LC-MS/MS analysis with commercial analytical standards as well as the

agreement in *m/z* and relative intensity of the observed precursor ion mass spectra with the predicted isotopic signature. Further, the fragmentation spectra agree with the fragmentation spectra observed from the analysis of n-MeFBSE commercial analytical standards with LC-HRMS and LC-MS/MS. The extracted ion chromatograph of this feature shows a small peak which precedes this feature. This peak is annotated as br-MeFBSE but can only be assigned this compound annotation with confidence level 4 – unequivocal molecular formula – due to the lack of associated MS2 fragmentation spectra.

3.6. Feature Group M446_R395_6558

A feature group with mean *m/z* 446.03444 and a retention time of 395.4 s (6.59 min) was present in both extracts of MB-C and MB-E and was matched as an $[M+C_2H_3O_2]^-$ adduct with two structural isomers from the NIST PFAS Suspect List: 1,1,2,2,3,3,4,4,4-nonafluoro-N,N-bis(2-hydroxyethyl)butane-1-sulphonamide (n-FBSEE) and 1,1,2,3,3,3-hexafluoro-N,N-bis(2-hydroxyethyl)-2-(trifluoromethyl)propane-1-sulphonamide (br-FBSEE) Figure 11).

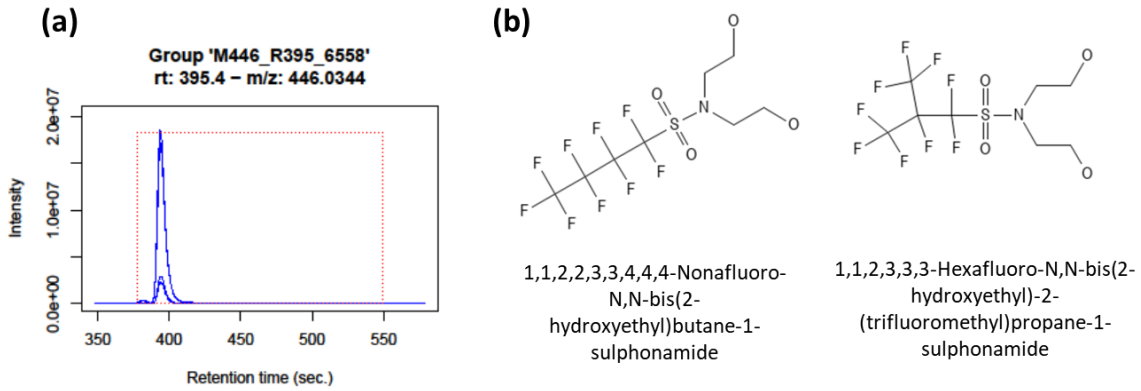

Figure 11. (a) Extracted ion chromatogram for feature group M446_R395_6558 in extracts of MB-B and MB-E as well as (b) molecular structures for the NIST PFAS Suspect List compounds tentatively matched with this group.

The shared molecular formula annotation was confirmed by observation of the precursor ion *m/z*, as well as the similarity between the observed and predicted *m/z* and relative intensities of peaks corresponding to higher mass isotopes $[^{13}C_1\text{-}C_7F_9O_4S\text{-}C_2H_3O_2]^-$ and $[^{34}S_1\text{-}C_8F_9O_4\text{-}C_2H_3O_2]^-$

Table 12).

Table 12. Predicted and observed *m/z*, and associated measured mass error, as well as the predicted and observed relative abundances associated with the feature corresponding to group M446_R395_6558, as observed in extract 569 (MB-C). The observed *m/z* and associated mass error for the monoisotopic mass are taken from the feature group, while the higher mass isotope *m/z* and associated mass error are taken from the mass spectra of extract 569, integrated from 6.50 min - 6.69 min (Figure A. 11b).

Isotope	Predicted *m/z*	Observed *m/z*	Error (ppm)	Predicted Rel. Abundance	Observed Rel. Abundance
$C_8H_{10}F_9NO_4S\text{-}C_2H_3O_2$	446.03253	446.03444	4.28	100 %	100 %
$^{13}C\text{-}C_7H_{10}F_9NO_3S\text{-}C_2H_3O_2$	447.03589	447.03786	4.41	10.82 %	11.52 %

^{34}S- $C_8H_{10}F_9NO_3$-$C_2H_3O_2$	448.02833	448.02870	0.83	4.43 %	3.76 %

Preceding this feature in the extracted ion chromatograph was a peak with an elution time of 6.36 min that possessed a similar isotopic pattern (Figure A. 11), though no MS/MS fragmentation spectra was collected. Due to the slightly earlier elution time with reversed-phase chromatography and matched isotopic pattern, this peak could indicate a branched isomer (i.e., br-FBSEE) of the primary feature (i.e., n-FBSEE), which would be expected for compounds derived from electrochemical fluorination [36].

Also present in the mass spectra of this feature was a peak potentially corresponding to the $[M-H]^-$ ion, which had a similar retention time and similar isotopic distribution (Figure A. 12, Table 13), though at roughly 0.7 % of the intensity of the $[M+C_2H_3O_2]^-$ peak.

Table 13. Predicted and observed *m/z*, and associated measured mass error, as well as the predicted and observed relative abundances associated with the feature corresponding to group M446_R395_6558, as observed in extract 569 (MB-C). The observed *m/z* and associated mass error all isotopes are taken from the mass spectra of extract 569, integrated from 6.50 min – 6.66 min. (Figure A. 12b).

Isotope	Predicted *m/z*	Observed *m/z*	Error (ppm)	Predicted Rel. Abundance	Observed Rel. Abundance
$C_8H_9F_9NO_4S$	386.01141	386.01372	5.98	100 %	100 %
^{13}C-$C_7H_9F_9NO_3S$	387.01476	387.01697	5.71	8.65 %	8.74 %
^{34}S- $C_8H_9F_9NO_3$	388.00720	388.00940	5.67	4.43 %	4.27 %

Compound annotation was investigated with the MSMatch functions compound match and fragment match, for peak with *m/z* 446.034 and a retention time window of 6.53 min - 6.86 min. While compound match returned no matches, the fragment match function identified 32 fragment peaks and assigned structures to 4 of them (Table A.25, Table A.26). Manual annotation identified a further 11 additional formula assignments and one alternative formula assignment to one matched by MSMatch (Table A.27), including numerous diagnostic fragments.

Figure 12. MS/MS fragmentation spectrum from precursor *m/z* 446.034, retention time window of 6.53 min - 6.86 min, in extract 569. Annotations in grey were determined by the fragment match tool of MSMatch, while annotations in white were determined manually. Note the double annotation for the peak with *m/z* 82.9597.

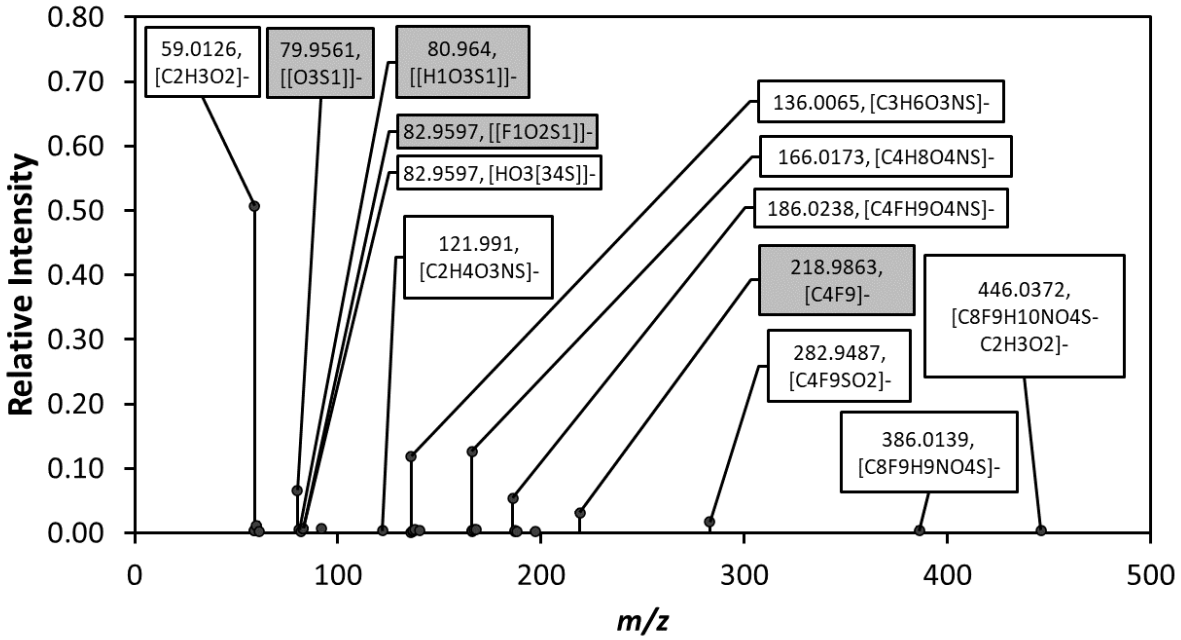

Given the agreement between the observed precursor ion spectra and the predicted isotopic distribution of n-FBSEE as well as the presence of more than 3 diagnostic fragments in the MS/MS fragmentation spectra, this feature group is annotated as n-FBSEE with confidence level 2b – probable by diagnostic fragmentation evidence. The presence of multiple peaks in the feature extracted ion chromatograph suggests the presence of branched and linear isomers of the same compound, and the earlier eluting peak is annotated as br-FBSEE with confidence level 4 - unequivocal molecular formula – due to the lack of associated MS2 fragmentation spectra.

4. Discussion

Among all examined firefighter gear extracts, six feature groups were associated with compounds from the NIST PFAS Suspect List at a confidence assessment better than level 4 (Table 14). Of these, four were associated with compounds containing four perfluorinated carbons and sulfate, sulfonamide, or sulfonate groups while two were associated with compounds containing six perfluorinated carbons connected to two non-fluorinated carbons and sulfate or sulfonate groups. These findings agree with a previously reported targeted PFAS analysis of the same textiles, which found electrochemical fluorination-derived PFAS with four perfluorinated carbons and fluorotelomerization-derived PFAS with six perfluorinated carbons to be present at the highest concentrations of all quantified PFAS [4]. Similarly, other reports of firefighter gear textiles have found MeFBSE [7] or PFBS [8] to be present at the highest concentrations of all examined nonvolatile PFAS while 6:2 FTS and PFBS have been observed in dust collected from fire station living rooms, gear locker areas, and apparatus bays [24]. To the authors knowledge, this report describes the first nontargeted analysis for nonvolatile PFAS, and the first reported identification of FBSE, FBSEE, and 6:2 FTSa in firefighter gear or any high-performance outer wear.

Table 14. Summary of suspect compounds identified in firefighter gear textile extracts, including the suspect compound name, the ions observed, and the confidence assessment of the compound annotation.

Feature Group (Textile)	Suspect Compound Match (Abbreviation)	Ion(s) Observed	Confidence Assessment
M299_R226_3160 (MB-E)	Perfluorobutane sulfonic acid (*n*-PFBS)	$[M-H]^-$	1a
M342_R363_4318 (MB-E)	1,1,2,2,3,3,4,4,4-nonafluoro-N-(2-hydroxyethyl)-1-butanesulfonamide (*n*-FBSE)	$[M-H]^-$	2b
M427_R466_6072 (MB-E)	6:2 Fluorotelomer sulfonic acid (6:2 FTS)	$[M-H]^-$	1a
M443_R450_6484 (OS-B, OS-F)	6:2 Fluorotelomer sulfate (6:2 FTSa)	$[M-H]^-$	2b
M416_R452_5807 (MB-C)	N-(2-hydroxyethyl)-N-methylperfluoro-2-methylpropanesulfonamide (br-MeFBSE)	$[M+C_2H_3O_2]^-$	4
	1,1,2,2,3,3,4,4,4-Nonafluoro-N-(2-hydroxyethyl)-N-methyl-1-utanesulfonamide (n-MeFBSE)	$[M+C_2H_3O_2]^-$, $[M-H]^-$	1a
M446_R395_6558 (MB-B, MB-E)	1,1,2,2,3,3,4,4,4-Nonafluoro-N,N-bis(2-hydroxyethyl)butane-1-sulfonamide (br-FBSEE)	$[M+C_2H_3O_2]^-$	4
	1,1,2,3,3,3-Hexafluoro-N,N-bis(2-hydroxyethyl)-2-(trifluoromethyl)propane-1-sulfonamide (n-FBSEE)	$[M+C_2H_3O_2]^-$, $[M-H]^-$	2b

A previous targeted analysis of PFAS in the same textiles analyzed here found 24 individual non- and semivolatile PFAS to be present above reporting limits in at least one textile [4]. As all 24 previously identified PFAS were present on the NIST PFAS Suspect List, their absence from this report could indicate that some PFAS were incorrectly excluded. However, their absence here likely stems from their relatively lower concentration in textile extracts coupled with the exclusion of features with peak heights below 1,000,000 intensity units from this report. This exclusion was performed so that only features with apparent higher mass isotopes and recorded fragmentation spectra were selected for suspect screening. The identification here of the two highest concentration non- and semivolatile PFAS from the targeted analysis of the same textiles suggests that the method utilized here is capable of identifying non- and semivolatile PFAS that are present at relatively high concentrations.

FBSE, FBSEE, and MeFBSE are all raw materials or intermediates in the electrochemical fluorination-based production of fluorochemicals and surface protection products such as FBSA and PFBS [36, 37]. The presence of peaks corresponding to branched and linear isomers for FBSEE and MeFBSE is further confirmation of their annotation as electrochemical fluorinated-derived compounds.

The presence of FBSE, FBSEE, and MeFBSE in moisture barrier textiles could indicate they were added to firefighter gear textiles intentionally or that they were residuals from the manufacturing process of other PFAS. While MeFBSE and PFBS have been previously identified in consumer goods [2, 7] and the environment [38], FBSE and FBSEE have been less commonly identified. FBSE is a wet etching agent for manufacturing semiconductor devices [2] while FBSEE has been previously identified in waste streams from semiconductor [39, 40] and fluorochemical manufacturing [37]. Little is known about the risk associated with exposure to these compounds, however toxicological studies for FBSA, FBSE, and FBSEE have been announced [41].

n:2 FTSs have been widely identified in consumer goods and the environment while n:2 FTSas have been patented for use in food contact materials [2] and the 6:2, 8:2, and 10:2 members of this class have been observed food contact and writing paper products [42]. This appears to be the first observation of n:2 FTSas in outerwear textiles and it is not known if their presence indicates an intended use.

FBSEE and MeFBSE were both observed most intensely as $[M+C_2H_3O_2]^-$ adducts, with $[M-H]^-$ ions present at much lower intensities. Despite not being included in recent guides on PFAS analysis with high-resolution mass spectrometry [43, 44], the inclusion of $[M+C_2H_3O_2]^-$ adducts during suspect screening widens the chemical diversity of PFAS that can be detected with negative mode electrospray ionization. For example, FBSEE and MeFBSE both contain tertiary amines and hydroxyl groups as ionizable functional groups, neither of which are especially well ionized by negative mode electrospray when only $[M-H]^-$ ions are considered. The ability to observe these compounds with negative mode electrospray is advantageous because that is the most commonly used ionization technique for PFAS that are regulated or have established negative health effects. Perhaps due to their poor ionization as $[M-H]^-$ ions with electrospray ionization, recent investigations of perfluoroalkane sulfonamido ethanols (FASEs) have largely relied on either gas chromatography [7, 45] or atmospheric pressure chemical- or photoionization [45]. However, a previous examination of PFAS in high-performance outerwear quantified n-methyl

perfluorooctane sulfonamido ethanol (MeFOSE) as $[M+C_2H_3O_2]^-$ adducts by targeted LC-MS/MS analysis [28] and two recent examinations of PFAS in semiconductor waste with high resolution mass spectrometry included $[M+C_2H_3O_2]^-$ adducts in their compound annotation workflow and were able to identify FBSEE and MeFBSE with negative mode electrospray [39, 40]. To the authors knowledge, this is the first report identifying PFAS in consumer goods as $[M+C_2H_3O_2]^-$ adducts with LC-ESI(-)-HR-MS and demonstrates the utility of including a broader range of nontarget workflows than those that assume PFAS are only present as $[M-H]^-$ ions when ionized by negative mode electrospray.

5. Summary

To identify per- and polyfluoroalkyl substances (PFAS) that may be missed by targeted analysis, this study utilized a suspect screening approach with liquid chromatography high-resolution mass spectrometry to examine 17 firefighter turnout gear moisture barrier, outer shell, and thermal liner textiles for the presence of over 4,900 PFAS from the NIST PFAS Suspect List. This report follows NIST Technical Note 2248, which used targeted analysis to quantify 53 PFAS in the same textiles and is the first reported nontargeted PFAS analysis with LC-HRMS in outerwear textiles.

Six PFAS were identified with high confidence in at least one textile including four which were not previously reported by targeted analysis: 6:2 fluorotelomer sulfate (6:2 FTSa), methyl perfluorobutane sulfonamido ethanol (MeFBSE), perfluorobutane sulfonamido diethanol (FBSEE), and perfluorobutane sulfonamido ethanol (FBSE) as well as two which were previously reported by targeted analysis: 6:2 fluorotelomer sulfonate (6:2 FTS) and perfluorobutane sulfonic acid (PFBS). The identity of these compounds was confirmed by isotopic pattern matching of their molecular ions as well as a comparison of the observed fragmentation spectra against previously collected spectra of the same compounds using the NIST Database Infrastructure for Mass Spectrometry (DIMSpec) application MSMatch. Additionally, the identities of 6:2 FTS, MeFBSE, and PFBS were confirmed by comparison with commercial analytical standards and a NIST reference material.

This study provides further insight into the PFAS present in firefighter turnout gear by greatly expanding the chemical diversity of PFAS that can be identified compared with typical targeted analytical approaches and detecting PFAS that are not commonly included in targeted PFAS analyte lists. The combination of this study with the previously reported targeted analysis provides a more complete assessment of the PFAS present in firefighter turnout gear and also demonstrates the necessity of including nontargeted analytical approaches when seeking to fully characterize the PFAS present in consumer goods.

6. Future Work

Future work will apply the suspect screening approach described here to other potential sources of PFAS exposure to firefighters such as materials present at fire scenes or in fire stations. Additionally, other approaches to feature prioritization will be utilized to search for PFAS which are not present on the NIST PFAS Suspect List, such as searching for previously identified MS/MS fragments that are commonly associated with PFAS.

References

[1] Schymanski EL, Zhang J, Thiessen PA, Chirsir P, Kondic T, Bolton EE (2023) Per- and polyfluoroalkyl substances (PFAS) in PubChem: 7 million and growing. *Environmental Science & Technology* 57(44):16918-16928. https://doi.org/10.1021/acs.est.3c04855

[2] Gluge J, Scheringer M, Cousins IT, DeWitt JC, Goldenman G, Herzke D, Lohmann R, Ng CA, Trier X, Wang Z (2020) An overview of the uses of per- and polyfluoroalkyl substances (PFAS). *Environmental Science: Processes & Impacts* 22(12):2345-2373. https://doi.org/10.1039/d0em00291g

[3] Buck RC, Korzeniowski SH, Laganis E, Adamsky F (2021) Identification and classification of commercially relevant per- and poly-fluoroalkyl substances (PFAS). *Integrated Environmental Assessment and Management* 17(5):1045-1055. https://doi.org/10.1002/ieam.4450

[4] Maizel A, Thompson A, Tighe M, Escobar Veras S, Rodowa A, Falkenstein-Smith R, Benner B, Hoffman K, Donnelly M, Hernandez O, Wetzler N, Ngu T, Reiner J, Place B, Kucklick J, Rimmer C, Davis R (2023) Per- and Polyfluoroalkyl Substances in New Firefighter Turnout Gear Textiles. (National Institute of Standards and Technology, Gaithersburg, MD), NIST TN 2248. https://doi.org/10.6028/nist.Tn.2248

[5] Maizel A, Thompson A, Tighe M, Escobar Veras S, Rodowa AE, Falkenstein-Smith R, Benner B, Hoffman K, Donnelly M, Hernandez O, Wetzler N, Ngu T, Reiner J, Place B, Kucklick J, Rimmer C, Davis RD (2024) Per- and Polyfluoroalkyl Substances in Firefighter Turnout Gear Textiles Exposed to Abrasion, Elevated Temperature, Laundering, or Weathering. (National Institute of Standards and Technology, Gaithersburg, MD), NIST TN 2260. https://doi.org/10.6028/nist.Tn.2260

[6] Rewerts JN, Morre JT, Massey Simonich SL, Field JA (2018) In-vial extraction large volume gas chromatography mass spectrometry for analysis of volatile PFASs on papers and textiles. *Environmental Science & Technology* 52(18):10609-10616. https://doi.org/10.1021/acs.est.8b04304

[7] Muensterman DJ, Titaley IA, Peaslee GF, Minc LD, Cahuas L, Rodowa AE, Horiuchi Y, Yamane S, Fouquet TNJ, Kissel JC, Carignan CC, Field JA (2022) Disposition of fluorine on new firefighter turnout gear. *Environmental Science & Technology* 56(2):974-983. https://doi.org/10.1021/acs.est.1c06322

[8] Peaslee GF, Wilkinson JT, McGuinness SR, Tighe M, Caterisano N, Lee S, Gonzales A, Roddy M, Mills S, Mitchell K (2020) Another pathway for firefighter exposure to per- and polyfluoroalkyl substances: Firefighter textiles. *Environmental Science & Technology Letters* 7(8):594-599. https://doi.org/10.1021/acs.estlett.0c00410

[9] Fenton SE, Ducatman A, Boobis A, DeWitt JC, Lau C, Ng C, Smith JS, Roberts SM (2021) Per- and Polyfluoroalkyl Substance Toxicity and Human Health Review: Current State of Knowledge and Strategies for Informing Future Research. *Environmental Toxicology and Chemistry* 40(3):606-630. https://doi.org/10.1002/etc.4890

[10] McDonough CA, Guelfo JL, Higgins CP (2019) Measuring total PFASs in water: The tradeoff between selectivity and Iinclusivity. *Current Opinion in Environmental Science & Health* 7:13-18. https://doi.org/10.1016/j.coesh.2018.08.005

[11] Rehman AU, Crimi M, Andreescu S (2023) Current and emerging analytical techniques for the determination of PFAS in environmental samples. *Trends in Environmental Analytical Chemistry* 37. https://doi.org/10.1016/j.teac.2023.e00198

[12] Schultes L, Peaslee GF, Brockman JD, Majumdar A, McGuinness SR, Wilkinson JT, Sandblom O, Ngwenyama RA, Benskin JP (2019) Total fluorine measurements in food packaging: How do current methods perform? *Environmental Science & Technology Letters* 6(2):73-78. https://doi.org/10.1021/acs.estlett.8b00700

[13] Robel AE, Marshall K, Dickinson M, Lunderberg D, Butt C, Peaslee G, Stapleton HM, Field JA (2017) Closing the mass balance on fluorine on papers and textiles. *Environmental Science & Technology* 51(16):9022-9032. https://doi.org/10.1021/acs.est.7b02080

[14] Xia C, Diamond ML, Peaslee GF, Peng H, Blum A, Wang Z, Shalin A, Whitehead HD, Green M, Schwartz-Narbonne H, Yang D, Venier M (2022) Per- and polyfluoroalkyl substances in North American school uniforms. *Environmental Science & Technology* 56(19):13845-13857. https://doi.org/10.1021/acs.est.2c02111

[15] Wu Y, Miller GZ, Gearhart J, Peaslee G, Venier M (2021) Side-chain fluorotelomer-based polymers in children car seats. *Environmental Pollution* 268(Pt B):115477. https://doi.org/10.1016/j.envpol.2020.115477

[16] Stroski KM, Sapozhnikova Y, Taylor RB, Harron A (2024) Non-targeted analysis of per- and polyfluorinated substances in consumer food packaging. *Chemosphere* 360:142436. https://doi.org/10.1016/j.chemosphere.2024.142436

[17] Liu Y, D'Agostino LA, Qu G, Jiang G, Martin JW (2019) High-resolution mass spectrometry (HRMS) methods for nontarget discovery and characterization of poly- and per-fluoroalkyl substances (PFASs) in environmental and human samples. *Trends in Analytical Chemistry* 121:115420. https://doi.org/10.1016/j.trac.2019.02.021

[18] Hollender J, Schymanski EL, Ahrens L, Alygizakis N, Béen F, Bijlsma L, Brunner AM, Celma A, Fildier A, Fu Q, Gago-Ferrero P, Gil-Solsona R, Haglund P, Hansen M, Kaserzon S, Kruve A, Lamoree M, Margoum C, Meijer J, Merel S, Rauert C, Rostkowski P, Samanipour S, Schulze B, Schulze T, Singh RR, Slobodnik J, Steininger-Mairinger T, Thomaidis NS, Togola A, Vorkamp K, Vulliet E, Zhu L, Krauss M (2023) NORMAN guidance on suspect and non-target screening in environmental monitoring. *Environmental Sciences Europe* 35(1). https://doi.org/10.1186/s12302-023-00779-4

[19] Casey JS, Jackson SR, Ryan J, Newton SR (2023) The use of gas chromatography - high resolution mass spectrometry for suspect screening and non-targeted analysis of per- and polyfluoroalkyl substances. *Journal of Chromatography A* 1693:463884. https://doi.org/10.1016/j.chroma.2023.463884

[20] Williams AJ, Gaines LGT, Grulke CM, Lowe CN, Sinclair GFB, Samano V, Thillainadarajah I, Meyer B, Patlewicz G, Richard AM (2022) Assembly and curation of lists of per- and polyfluoroalkyl substances (PFAS) to support environmental science research. *Frontiers in Environmental Science* 10:1-13. https://doi.org/10.3389/fenvs.2022.850019

[21] Place BJ (2021) Development of a Data Analysis Tool to Determine the Measurement Variability of Consensus Mass Spectra. *J Am Soc Mass Spectrom* 32(3):707-715. https://doi.org/10.1021/jasms.0c00423

[22] Schymanski EL, Jeon J, Gulde R, Fenner K, Ruff M, Singer HP, Hollender J (2014) Identifying small molecules via high resolution mass spectrometry: communicating

confidence. *Environmental Science & Technology* 48(4):2097-2098. https://doi.org/10.1021/es5002105

[23] Charbonnet JA, McDonough CA, Xiao F, Schwichtenberg T, Cao D, Kaserzon S, Thomas KV, Dewapriya P, Place BJ, Schymanski EL, Field JA, Helbling DE, Higgins CP (2022) Communicating confidence of per- and polyfluoroalkyl substance identification via high-resolution mass spectrometry. *Environmental Science & Technology Letters* 9(6):473-481. https://doi.org/10.1021/acs.estlett.2c00206

[24] Young AS, Sparer-Fine EH, Pickard HM, Sunderland EM, Peaslee GF, Allen JG (2021) Per- and polyfluoroalkyl substances (PFAS) and total fluorine in fire station dust. *Journal of Exposure Science & Environmental Epidemiology* 31(5):930-942. https://doi.org/10.1038/s41370-021-00288-7

[25] van der Veen I, Weiss JM, Hanning AC, de Boer J, Leonards PE (2016) Development and validation of a method for the quantification of extractable perfluoroalkyl acids (PFAAs) and perfluorooctane sulfonamide (FOSA) in textiles. *Talanta* 147:8-15. https://doi.org/10.1016/j.talanta.2015.09.021

[26] van der Veen I, Hanning AC, Stare A, Leonards PEG, de Boer J, Weiss JM (2020) The effect of weathering on per- and polyfluoroalkyl substances (PFASs) from durable water repellent (DWR) clothing. *Chemosphere* 249:126100. https://doi.org/10.1016/j.chemosphere.2020.126100

[27] van der Veen I, Schellenberger S, Hanning AC, Stare A, de Boer J, Weiss JM, Leonards PEG (2022) Fate of per- and polyfluoroalkyl substances from durable water-repellent clothing during use. *Environmental Science & Technology* 56(9):5886-5897. https://doi.org/10.1021/acs.est.1c07876

[28] Gremmel C, Fromel T, Knepper TP (2016) Systematic determination of perfluoroalkyl and polyfluoroalkyl substances (PFASs) in outdoor jackets. *Chemosphere* 160:173-180. https://doi.org/10.1016/j.chemosphere.2016.06.043

[29] Thompson AL, Maizel AC, Tighe M, Escobar Veras S, Rodowa AE, Benner B, Tombaugh AF, Reiner J, Donnelly M, Falkenstein-Smith R, Kucklick J, Rimmer C, Davis RD (2024) Per- and Polyfluoroalkyl Substances in Textiles Present in Firefighter Gloves, Hoods, and Wildland Gear. (National Insitute of Standards and Technology, Gaithersburg, MD), NIST TN 2313. https://doi.org/10.6028/nist.Tn.2313

[30] Chambers MC, Maclean B, Burke R, Amodei D, Ruderman DL, Neumann S, Gatto L, Fischer B, Pratt B, Egertson J, Hoff K, Kessner D, Tasman N, Shulman N, Frewen B, Baker TA, Brusniak MY, Paulse C, Creasy D, Flashner L, Kani K, Moulding C, Seymour SL, Nuwaysir LM, Lefebvre B, Kuhlmann F, Roark J, Rainer P, Detlev S, Hemenway T, Huhmer A, Langridge J, Connolly B, Chadick T, Holly K, Eckels J, Deutsch EW, Moritz RL, Katz JE, Agus DB, MacCoss M, Tabb DL, Mallick P (2012) A cross-platform toolkit for mass spectrometry and proteomics. *Nature Biotechnology* 30(10):918-920. https://doi.org/10.1038/nbt.2377

[31] Helmus R, Ter Laak TL, van Wezel AP, de Voogt P, Schymanski EL (2021) patRoon: open source software platform for environmental mass spectrometry based non-target screening. *Journal of Cheminformatics* 13(1):1-25. https://doi.org/10.1186/s13321-020-00477-w

[32] R Core Team (2023) *R: A Language and Environment for Statistical Computing*. Available at https://www.R-project.org/.

[33] Racine JS (2012) RStudio: A platform-independent IDE for R and SWEAVE. *Journal of Applied Econometrics* 27(1):167-172. https://doi.org/10.1002/jae.1278

[34] Rost HL, Sachsenberg T, Aiche S, Bielow C, Weisser H, Aicheler F, Andreotti S, Ehrlich HC, Gutenbrunner P, Kenar E, Liang X, Nahnsen S, Nilse L, Pfeuffer J, Rosenberger G, Rurik M, Schmitt U, Veit J, Walzer M, Wojnar D, Wolski WE, Schilling O, Choudhary JS, Malmstrom L, Aebersold R, Reinert K, Kohlbacher O (2016) OpenMS: A flexible open-source software platform for mass spectrometry data analysis. *Nature Methods* 13(9):741-748. https://doi.org/10.1038/nmeth.3959

[35] Ragland JM , Place BJ (2024) A portable and reusable database infrastructure for mass spectrometry, and its associated toolkit (The DIMSpec Project). *Journal of the American Society for Mass Spectrometry* 35(6):1282-1291. https://doi.org/10.1021/jasms.4c00073

[36] Buck RC, Franklin J, Berger U, Conder JM, Cousins IT, de Voogt P, Jensen AA, Kannan K, Mabury SA, van Leeuwen SP (2011) Perfluoroalkyl and polyfluoroalkyl substances in the environment: Terminology, classification, and origins. *Integrated Environmental Assessment and Management* 7(4):513-541. https://doi.org/10.1002/ieam.258

[37] Hogue C (2019) 3M admits to unlawful release of PFAS in Alabama. *Chemical & Engineering News*. https://cen.acs.org/environment/persistent-pollutants/3M-admits-unlawful-release-PFAS-in-Alabama/97/i26

[38] Vento SD, Halsall C, Gioia R, Jones K, Dachs J (2012) Volatile per- and polyfluoroalkyl compounds in the remote atmosphere of the western Antarctic Peninsula: an indirect source of perfluoroalkyl acids to Antarctic waters? *Atmospheric Pollution Research* 3(4):450-455. https://doi.org/10.5094/apr.2012.051

[39] Chen Y-J, Yang J-S, Lin AY-C (2024) Comprehensive nontargeted analysis of fluorosurfactant byproducts and reaction products in wastewater from semiconductor manufacturing. *Sustainable Environment Research* 34(1). https://doi.org/10.1186/s42834-024-00221-1

[40] Chen YJ, Wang RD, Shih YL, Chin HY, Lin AY (2024) Emerging perfluorobutane sulfonamido derivatives as a new trend of surfactants used in the Semiconductor industry. *Environmental Science & Technology* 58(3):1648-1658. https://doi.org/10.1021/acs.est.3c04435

[41] Hogue C (2020) 3M to cut PFAS releases from Alabama plant. *Chemical & Engineering News*. https://cen.acs.org/environment/persistent-pollutants/3M-cut-PFAS-releases-Alabama/98/i30

[42] Chen YF, Liu T, Hu LX, Chen CE, Yang B, Ying GG (2024) Unveiling per- and polyfluoroalkyl substance contamination in Chinese paper products and assessing their exposure risk. *Environment International* 185:108540. https://doi.org/10.1016/j.envint.2024.108540

[43] Strynar M, McCord J, Newton S, Washington J, Barzen-Hanson K, Trier X, Liu Y, Dimzon IK, Bugsel B, Zwiener C, Munoz G (2023) Practical application guide for the discovery of novel PFAS in environmental samples using high resolution mass spectrometry. *Journal of Exposure Science & Environmental Epidemiology* 33(4):575-588. https://doi.org/10.1038/s41370-023-00578-2

[44] Partington JM, Rana S, Szabo D, Anumol T, Clarke BO (2024) Comparison of high-resolution mass spectrometry acquisition methods for the simultaneous quantification and identification of per- and polyfluoroalkyl substances (PFAS). *Analytical and Bioanalytical Chemistry* 416(4):895-912. https://doi.org/10.1007/s00216-023-05075-x

[45] Ayala-Cabrera JF, Moyano E, Santos FJ (2020) Gas chromatography and liquid chromatography coupled to mass spectrometry for the determination of fluorotelomer olefins, fluorotelomer alcohols, perfluoroalkyl sulfonamides and sulfonamido-ethanols in water. *J Chromatogr A* 1609:460463. https://doi.org/10.1016/j.chroma.2019.460463

Appendix A. Experimental

For the chemical analysis described in this work, isotopically labeled internal standard solutions were obtained and added to textile extracts (Section A.1).

A.1. Materials

Isotopically labeled internal standards were added to the firefighter gear textiles prior to extraction. These internal standards were originally obtained from Wellington Laboratories and are detailed in Table A.1 then mixed into a working solution as in Table A.2.

Table A.1. Isotopically labeled internal standard solutions used in PFAS suspect screening, including commercial reference standard name, specific isotopes and abbreviations, and reference concentration.

Standard	Contents	Concentration
MPFAC-24ES	Perfluoro-n-[$^{13}C_4$]-butanoic acid (MPFBA), Perfluoro-n-[$^{13}C_5$]-pentanoic acid (MPFPeA), Perfluoro-n-[1,2,3,4,6-$^{13}C_5$]-hexanoic acid (MPFHxA), Perfluoro-n-[1,2,3,4-$^{13}C_4$]-heptanoic acid (MPFHpA), Perfluoro-n-[$^{13}C_8$]-octanoic acid (MPFOA), Perfluoro-n-[$^{13}C_9$]-nonanoic acid (MPFNA), Perfluoro-n-[1,2,3,4,5,6-$^{13}C_5$]decanoic acid (MPFDA), Perfluoro-n-[1,2,3,4,5,6,7-$^{13}C_7$]undecanoic acid (MPFUnDA), Perfluoro-n-[1,2-$^{13}C_2$] dodecanoic acid (MFPDoDA), Perfluoro-n-[1,2-$^{13}C_2$]tetradecanoic acid (MPFTeDA), Sodium perfluoro-1-[2,3,4-$^{13}C_3$]-butanesulfonate (MPFBS), Sodium perfluoro-1-[1,2,3-$^{13}C_3$]-hexanesulfonate (MPFHxS), Sodium perfluoro-1-[$^{13}C_8$]-octanesulfonate (MPFOS), Perfluoro-1-[$^{13}C_8$]octane-sulfonamide (MFOSA), N-methyl-d3-perlfuoro-1-octanesulfonamid acetic acid (dMeFOSAA), N-ethyl-d5-perfluoro-1-octanesulfonamido acetic acid (dEtFOSAA), Sodium 1H, 1H, 2H, 2H-perfluoro-1-[1,2-$^{13}C_2$]-hexane sulfonate (M4:2 FTOH), Sodium 1H, 1H, 2H, 2H-perfluoro-1-[1,2-$^{13}C_2$]-octane sulfonate (M6:2 FTOH), Sodium 1H, 1H, 2H, 2H-perlfuoro-1-[1,2-$^{13}C_2$]-decane sulfonate (M8:2 FTOH)	(1.00 µg/mL ± 0.05 µg/mL) in methanol/ isopropanol (2%)/water (<1%)
M3HFPO-DA	Tetrafluoro(heptafluoropropoxy)[$^{13}C_3$]-propanoic acid (M3HFPO-DA)	(50.0 µg/mL ± 2.5 µg/mL) in methanol
d-N-MeFOSA-M	N-methy-d3-perflouro-1-octanesulfonamide (dMeFOSA)	(50 µg/mL ± 2.5 µg/mL) in methanol
d-N-EtFOSA	N-ethyl-d5-perfluoro-1-octanesulfonamide (dEtFOSA)	(50 µg/mL ± 2.5 µg/mL) in methanol

Table A.2 Concentrations of isotopically labeled internal standards in IS working solution, assuming they are present in the acid form.

Compounds	Concentration (ng/mL)
MPFBA, MPFPeA, MPFHxA, MPFHpA, MPFOA, MPFNA, MPFDA, MPFUnDA, MPFDoDA, MPFTeDA, MFOSA, dMeFOSAA, dEtFOSAA	204.7
MPFBS	190.1
MPFHxS	194.1
MPFOS	196.1
M4:2FTS	192.0
M6:2FTS	194.7
M8:2FTS	196.5
MHFPO-DA	187.9
dMeFOSA	189.1
dEtFOSA	191.5

A.2. R Markdown Script for PatRoon

The script used for suspect screening in R (version 4.3.2) with RStudio (version 2023.09.1) with the patRoon platform is shown below. This script generated the tables shown in Section A.3.

```
library(patRoon)
# -------------------------
# initialization
# -------------------------
workPath <- "*/R Working Directory/Susp Scr Textiles"
setwd(workPath)

# -------------------------
# features
# -------------------------

fList <- findFeatures(anaInfo, "openms",
                      noiseThrInt = 1e4,
                      chromSNR = 10,
                      chromFWHM = 20,
                      minFWHM = 5,
                      maxFWHM = 60)

fGroups <- groupFeatures(fList, "openms", rtalign = TRUE)

fGroups <- filter(fGroups,
                  preAbsMinIntensity = 100,
                  absMinIntensity = 1e6,
                  relMinReplicateAbundance = 1,
                  maxReplicateIntRSD = 0.75,
                  blankThreshold = 5,
                  removeBlanks = TRUE,
                  retentionRange = c(180,1800))

# -------------------------
# suspect screening
# -------------------------

# Load suspect list
suspList <- read.csv("suspectlist.csv", stringsAsFactors = FALSE)

fGroups <- screenSuspects(fGroups,
                          suspList,
                          mzWindow = 0.002,
                          adduct = c("[M-H]-"),
                          onlyHits = TRUE)

write.csv(do.call(rbind,lapply(fGroups@features@features,data.frame)), "featu
res.csv")
write.csv(fGroups@screenInfo, "exportscreeninfo.csv")
write.csv(fGroups@groupInfo, "exportgroupinfo.csv")
```

A.3. Exported Tables from Suspect Screening Workflow

Table A.3. $[M-H]^-$ feature groups along with the associated extract, retention time ("ret", in seconds), *m/z*, peak area, and peak intensity. Obtained from list fGroups@features@features.

group	extract	ret	mz	area	intensity
M215_R226_998	565	225.7	215.12904	72196620	13107810
M215_R226_998	566	226.5	215.12906	65193980	10241196
M215_R226_998	569	225.9	215.12914	37091390	6125400
M215_R226_998	570	226.7	215.12911	28588490	4968496
M249_R214_1652	569	212.9	249.02726	61151550	12129280
M249_R214_1652	570	211.9	249.02723	61316760	11895975
M253_R284_1796	585	283.2	253.08367	14649650	2757495
M253_R284_1796	586	282.7	253.08356	20104290	4246590
M253_R284_1796	589	282.5	253.08353	36347700	7596038
M253_R284_1796	590	284.4	253.08342	43153790	6480600
M253_R284_1796	593	283.6	253.08344	60379580	11588638
M253_R284_1796	594	283.4	253.08355	44433900	8751736
M299_R226_3160	577	227.1	298.94398	22629050	3466202
M299_R226_3160	578	226.1	298.94397	23658130	4269598
M311_R187_3452	569	186.4	311.09824	42966790	5279193
M311_R187_3452	570	187.0	311.09817	41120550	5660531
M311_R187_3452	577	185.6	311.09824	8592400	1637271
M311_R187_3452	578	185.2	311.09814	8855936	1666400
M311_R231_3453	573	231.9	311.09829	7254649	1330075
M311_R231_3453	574	230.5	311.09834	6549315	1140938
M324_R356_3802	573	355.6	324.12162	10690460	2095880
M324_R356_3802	574	355.3	324.12168	8048955	1589052
M339_R189_4098	561	188.3	338.97394	42896360	9014423
M339_R189_4098	562	188.3	338.97399	36077970	7448765
M339_R189_4098	573	188.4	338.97376	92131300	16250938
M339_R189_4098	574	188.0	338.97384	82620690	14774665
M339_R189_4098	581	188.6	338.97371	72212270	13177027
M339_R189_4098	582	188.4	338.97373	76491750	13828412
M339_R278_4094	561	277.6	338.97372	2.64E+08	43970892
M339_R278_4094	562	277.1	338.97380	2.11E+08	38359636
M339_R278_4094	573	277.5	338.97359	3.3E+08	58567444
M339_R278_4094	574	277.4	338.97366	2.79E+08	51478732
M339_R278_4094	581	277.0	338.97359	2.66E+08	50272780
M339_R278_4094	582	276.9	338.97357	2.77E+08	49641216
M339_R297_4097	561	296.4	338.97391	43163830	6210802
M339_R297_4097	562	296.1	338.97399	37938510	5738610
M339_R297_4097	573	296.7	338.97374	61484610	9015720

Table A.3. (Continued)

group	extract	ret	mz	area	intensity
M339_R297_4097	574	296.6	338.97378	55386100	8200772
M339_R297_4097	581	296.3	338.97374	63944160	8668043
M339_R297_4097	582	296.0	338.97375	66819840	9838696
M339_R313_4100	561	312.7	338.97391	25822570	2592019
M339_R313_4100	562	312.6	338.97400	20919980	2143995
M339_R313_4100	573	312.7	338.97387	44436460	3921307
M339_R313_4100	574	312.7	338.97395	38574480	3447967
M339_R313_4100	581	313.1	338.97377	38628410	3403457
M339_R313_4100	582	312.9	338.97380	39741550	3268622
M339_R333_4099	561	333.3	338.97390	69028120	11197056
M339_R333_4099	562	332.7	338.97399	53911250	9825996
M339_R333_4099	573	333.7	338.97381	140248000	22348412
M339_R333_4099	574	333.1	338.97390	120438300	19807698
M339_R333_4099	581	333.3	338.97373	134203400	20367226
M339_R333_4099	582	333.1	338.97375	141020000	23229428
M339_R369_4101	573	369.1	338.97394	13579980	1963891
M339_R369_4101	574	368.8	338.97401	11487860	1621609
M339_R369_4101	581	368.7	338.97387	13203140	1965595
M339_R369_4101	582	368.5	338.97388	13943890	1987064
M342_R363_4318	569	362.6	341.98643	40029480	7205217
M342_R363_4318	570	362.8	341.98632	38255790	6634388
M342_R363_4318	577	363.5	341.98625	38217060	6470455
M342_R363_4318	578	363.2	341.98615	44621490	7771161
M345_R195_4374	557	195.0	345.12524	17149880	2521788
M345_R195_4374	558	194.7	345.12519	10126870	1977631
M345_R195_4374	569	193.8	345.12502	78037200	16779670
M345_R195_4374	570	194.4	345.12492	90087380	17765376
M345_R195_4374	593	195.0	345.12500	18332270	2513681
M345_R195_4374	594	194.6	345.12502	14938490	2258678
M347_R213_4397	569	212.0	347.01050	5040632	1131933
M347_R213_4397	570	211.9	347.01038	5968689	1209138
M401_R259_5464	573	258.8	400.96683	16597250	2067165
M401_R259_5464	574	258.5	400.96696	10429090	2303107
M401_R259_5464	581	258.3	400.96673	10968200	2294019
M401_R259_5464	582	259.0	400.96673	10834250	2087161
M403_R259_5522	573	258.8	402.96378	17739060	2032217
M403_R259_5522	574	258.5	402.96395	10624160	2237954
M403_R259_5522	581	258.3	402.96372	10704790	2225335
M403_R259_5522	582	259.0	402.96372	10628140	2080527

Table A.3. (Continued)

group	extract	ret	mz	area	intensity
M421_R351_5883	573	351.4	420.97438	13014660	2135815.75
M421_R351_5883	574	351.0	420.97449	11202660	1912294.75
M421_R351_5883	581	351.1	420.97431	12035900	1897164.25
M421_R351_5883	582	350.9	420.97432	12506020	1972697.5
M427_R466_6072	577	466.8	426.96919	53241120	7321231.5
M427_R466_6072	578	466.9	426.96917	51529850	7050692.5
M443_R450_6484	538	448.3	442.96409	9285918	2031125.875
M443_R450_6484	539	450.3	442.96415	16040510	2210953.5
M443_R450_6484	553	449.9	442.96462	25982000	4339230.5
M443_R450_6484	554	449.7	442.96467	19166960	3551102
M473_R280_7120	573	279.8	472.92008	5231687	1063583.875
M473_R280_7120	574	279.6	472.92028	5407288	1059253
M473_R280_7120	581	278.5	472.92003	5695495	1102246.625
M473_R280_7120	582	279.2	472.91997	7033199	1118558.25
M473_R297_7119	561	297.2	472.92007	24015430	4628807.5
M473_R297_7119	562	296.9	472.92019	16653840	3539365.75
M473_R297_7119	573	297.5	472.91991	55799550	10915714
M473_R297_7119	574	296.6	472.91998	49479660	10701256
M473_R297_7119	581	296.3	472.91983	77072290	15812081
M473_R297_7119	582	296.0	472.91982	89093080	19914838
M497_R480_7670	569	480.3	497.05740	267871200	37264248
M497_R480_7670	570	480.8	497.05787	109126900	13990424
M499_R279_7723	561	279.2	498.96142	863041300	150866672
M499_R279_7723	562	279.4	498.96149	763239600	125171616
M499_R279_7723	573	279.0	498.96129	1435483000	226185696
M499_R279_7723	574	278.8	498.96134	1300273000	211880240
M499_R279_7723	581	279.3	498.96121	1338467000	195080048
M499_R279_7723	582	279.2	498.96114	1405276000	231850640
M511_R187_8005	561	186.7	510.96184	63601520	5557382
M511_R187_8005	562	185.8	510.96196	51130500	6246761.5
M511_R187_8005	573	186.0	510.96142	62847740	6026840
M511_R187_8005	574	186.4	510.96156	57027430	4077437.75
M511_R187_8005	581	186.2	510.96150	53210520	4277593
M511_R187_8005	582	186.7	510.96153	53968630	3951472.5
M511_R311_8004	561	311.1	510.96166	97915020	14805839
M511_R311_8004	562	311.0	510.96180	77856590	12062322
M511_R311_8004	573	311.1	510.96156	134288500	20702222
M511_R311_8004	574	311.1	510.96168	118749800	17597870

Table A.3. (Continued)

group	extract	ret	mz	area	intensity
M511_R311_8004	581	310.7	510.96143	109614900	16443596
M511_R311_8004	582	311.3	510.96148	116618300	16568737
M515_R671_8089	565	666.7	515.19867	80688090	7239526
M515_R671_8089	566	667.8	515.19879	98688850	7832605.5
M515_R671_8089	593	672.0	515.19852	14839910	1843443.875
M515_R671_8089	594	671.6	515.19859	18077970	2441485.5
M541_R321_8595	561	320.9	540.99143	7476533	1322275.25
M541_R321_8595	562	321.0	540.99165	5647043	1020480.375
M541_R321_8595	573	321.5	540.99127	12548640	2187333.75
M541_R321_8595	574	320.9	540.99142	10729270	1967379.25
M541_R321_8595	581	321.1	540.99114	10038430	1842041.75
M541_R321_8595	582	321.0	540.99119	10549360	1967202.25
M549_R226_8775	573	225.9	548.93588	18459180	3442769.5
M549_R226_8775	574	225.3	548.93610	14976500	2687319.75
M570_R296_9093	573	295.2	569.99940	38748080	5357097.5
M570_R296_9093	574	295.0	569.99951	34568800	3962217.5
M570_R296_9093	581	294.7	569.99935	32537480	3714957.75
M570_R296_9093	582	295.2	569.99938	33127610	3657376.5
M613_R213_9753	565	210.6	613.06692	9959665	2030188.875
M613_R213_9753	566	211.2	613.06703	9534366	2276262.75
M779_R368_11166	561	367.4	778.92346	42575080	5225745.5
M779_R368_11166	562	367.3	778.92355	32224790	4151963.5
M779_R368_11166	573	368.2	778.92304	115733100	14469100
M779_R368_11166	574	368.0	778.92312	89878910	12434373
M779_R368_11166	581	367.8	778.92285	120890000	15752031
M779_R368_11166	582	367.7	778.92278	118992300	16225086
M781_R290_11185	573	289.8	781.05196	89632550	13635511
M781_R290_11185	574	289.6	781.05204	80411920	14061565
M781_R368_11181	561	367.4	780.92066	34538200	4127362
M781_R368_11181	562	367.3	780.92072	26041150	3348622.25
M781_R368_11181	573	368.2	780.92021	93383240	11566195
M781_R368_11181	574	368.0	780.92027	73537830	10329330
M781_R368_11181	581	367.8	780.91991	92470570	12401940
M781_R368_11181	582	367.7	780.91995	94383320	13331368
M781_R385_11183	581	384.8	780.92039	33871680	4302266.5
M781_R385_11183	582	384.7	780.92039	36275220	4436025.5
M841_R343_11530	573	343.3	840.94011	11815920	1438659.75
M841_R343_11530	574	341.2	840.94126	8174679	1296516.5

Table A.4. $[M-H]^-$ feature groups with associated group retention time ("rts" in seconds) and group *m/z* ("mzs"). Obtained from fGroups@groupInfo.

Group	rts	mzs
M215_R226_998	226.1	215.12908
M249_R214_1652	214.3	249.02674
M253_R284_1796	283.5	253.08410
M299_R226_3160	226.2	298.94400
M311_R187_3452	186.8	311.09823
M311_R231_3453	231.2	311.09838
M324_R356_3802	355.9	324.12162
M339_R278_4094	277.5	338.97366
M339_R297_4097	296.6	338.97382
M339_R189_4098	188.6	338.97383
M339_R333_4099	333.4	338.97385
M339_R313_4100	313.0	338.97388
M339_R369_4101	369.1	338.97396
M342_R363_4318	363.3	341.98643
M345_R195_4374	194.9	345.12513
M347_R213_4397	213.2	347.01036
M401_R259_5464	259.1	400.96688
M403_R259_5522	258.9	402.96386
M421_R351_5883	351.5	420.97444
M427_R466_6072	465.6	426.96924
M443_R450_6484	449.8	442.96451
M473_R297_7119	297.0	472.91997
M473_R280_7120	279.6	472.92015
M497_R480_7670	480.3	497.05743
M499_R279_7723	279.4	498.96131
M511_R311_8004	311.3	510.96160
M511_R187_8005	186.6	510.96163
M515_R671_8089	671.0	515.19871
M541_R321_8595	321.3	540.99135
M549_R226_8775	225.8	548.93599
M570_R296_9093	295.6	569.99953
M613_R213_9753	213.3	613.06587
M779_R368_11166	368.0	778.92313
M781_R368_11181	368.0	780.92029
M781_R385_11183	385.2	780.92067
M781_R290_11185	289.9	781.05200
M841_R343_11530	342.6	840.94136

Table A.5. Selected columns from exported table of $[M-H]^-$ suspect compounds associated with each feature group. Showing the feature group, associated NIST suspect list compound and International Chemical Identifier (InChI). This was extracted from the data frame fGroups@screenInfo.

group	name_orig	InChI
M215_R226_998	2:1 Hydrogen-substituted fluorotelomer dimethyl ammonio butane	InChI=1S/C9H18F4N/c1-4-5-6-14(2,3)7-9(12,13)8(10)11/h8H,4-7H2,1-3H3/q+1
M249_R214_1652	3-(Heptafluoropropyl)-5-methyl-1H-pyrazole	InChI=1S/C7H5F7N2/c1-3-2-4(16-15-3)5(8,9)6(10,11)7(12,13)14/h2H,1H3,(H,15,16)
M253_R284_1796	1,1,1,2,2,3,3-Heptafluorononane	InChI=1S/C9H13F7/c1-2-3-4-5-6-7(10,11)8(12,13)9(14,15)16/h2-6H2,1H3
M299_R226_3160	1,1,2,2-Tetrafluoro-2-(1,1,2,2-tetrafluoroethoxy)ethane-1-sulfonyl fluoride	InChI=1S/C4HF9O3S/c5-1(6)2(7,8)16-3(9,10)4(11,12)17(13,14)15/h1H
M299_R226_3160	1,1,2,3,3,3-hexafluoro-2-(trifluoromethyl)propanesulfonic acid	InChI=1S/C4HF9O3S/c5-1(2(6,7)8,3(9,10)11)4(12,13)17(14,15)16/h(H,14,15,16)
M299_R226_3160	Perfluorobutanesulfonic acid	InChI=1S/C4HF9O3S/c5-1(6,3(9,10)11)2(7,8)4(12,13)17(14,15)16/h(H,14,15,16)
M311_R187_3452	2:2 fluorotelomer sulfinyl hydroxypropyl trimethyl ammonium	InChI=1S/C10H19F5NO2S/c1-16(2,3)6-8(17)7-19(18)5-4-9(11,12)10(13,14)15/h8,17H,4-7H2,1-3H3/q+1
M311_R231_3453	2:2 fluorotelomer sulfinyl hydroxypropyl trimethyl ammonium	InChI=1S/C10H19F5NO2S/c1-16(2,3)6-8(17)7-19(18)5-4-9(11,12)10(13,14)15/h8,17H,4-7H2,1-3H3/q+1
M324_R356_3802	2,2,3,3,4,4,4-Heptafluoro-N,N-bis(2-methylpropyl)butanamide	InChI=1S/C12H18F7NO/c1-7(2)5-20(6-8(3)4)9(21)10(13,14)11(15,16)12(17,18)19/h7-8H,5-6H2,1-4H3
M324_R356_3802	N,N-Dibutyl-2,2,3,3,4,4,4-heptafluorobutanamide	InChI=1S/C12H18F7NO/c1-3-5-7-20(8-6-4-2)9(21)10(13,14)11(15,16)12(17,18)19/h3-8H2,1-2H3
M339_R189_4098	Perfluoroalkyl Heptanedioic acid	InChI=1S/C7H2F10O4/c8-3(9,1(18)19)5(12,13)7(16,17)6(14,15)4(10,11)2(20)21/h(H,18,19)(H,20,21)
M339_R278_4094	Perfluoroalkyl Heptanedioic acid	InChI=1S/C7H2F10O4/c8-3(9,1(18)19)5(12,13)7(16,17)6(14,15)4(10,11)2(20)21/h(H,18,19)(H,20,21)
M339_R297_4097	Perfluoroalkyl Heptanedioic acid	InChI=1S/C7H2F10O4/c8-3(9,1(18)19)5(12,13)7(16,17)6(14,15)4(10,11)2(20)21/h(H,18,19)(H,20,21)
M339_R313_4100	Perfluoroalkyl Heptanedioic acid	InChI=1S/C7H2F10O4/c8-3(9,1(18)19)5(12,13)7(16,17)6(14,15)4(10,11)2(20)21/h(H,18,19)(H,20,21)
M339_R333_4099	Perfluoroalkyl Heptanedioic acid	InChI=1S/C7H2F10O4/c8-3(9,1(18)19)5(12,13)7(16,17)6(14,15)4(10,11)2(20)21/h(H,18,19)(H,20,21)
M339_R369_4101	Perfluoroalkyl Heptanedioic acid	InChI=1S/C7H2F10O4/c8-3(9,1(18)19)5(12,13)7(16,17)6(14,15)4(10,11)2(20)21/h(H,18,19)(H,20,21)

Table A.5. (Continued)

group	name_orig	InChI
M342_R363_4318	1,1,2,2,3,3,4,4,4-nonafluoro-N-(2-hydroxyethyl)-1-Butanesulfonamide	InChI=1S/C6H6F9NO3S/c7-3(8,5(11,12)13)4(9,10)6(14,15)20(18,19)16-1-2-17/h16-17H,1-2H2
M345_R195_4374	1,1,1,2,2,3,3,4,4-Nonafluorotridecane	InChI=1S/C13H19F9/c1-2-3-4-5-6-7-8-9-10(14,15)11(16,17)12(18,19)13(20,21)22/h2-9H2,1H3
M347_R213_4397	1,1,1,2,2,3,3-Heptafluoro-4,4-bis(trifluoromethyl)hexane	InChI=1S/C8H5F13/c1-2-3(6(13,14)15,7(16,17)18)4(9,10)5(11,12)8(19,20)21/h2H2,1H3
M347_R213_4397	1-(Perfluorohexyl)ethane	InChI=1S/C8H5F13/c1-2-3(9,10)4(11,12)5(13,14)6(15,16)7(17,18)8(19,20)21/h2H2,1H3
M401_R259_5464	Thiophene, 2-(tridecafluorohexyl)-	InChI=1S/C10H3F13S/c11-5(12,4-2-1-3-24-4)6(13,14)7(15,16)8(17,18)9(19,20)10(21,22)23/h1-3H
M401_R259_5464	3-(Tridecafluorohexyl)thiophene	InChI=1S/C10H3F13S/c11-5(12,4-1-2-24-3-4)6(13,14)7(15,16)8(17,18)9(19,20)10(21,22)23/h1-3H
M403_R259_5522	1,1,1,2,2,3,3,4,5,5,5-Undecafluoro-4-(pentafluoroethoxy)pentane	InChI=1S/C7F16O/c8-1(9,2(10,11)4(13,14)15)3(12,5(16,17)18)24-7(22,23)6(19,20)21
M421_R351_5883	Methyl perfluoro(3-(1-ethenyloxypropan-2-yloxy)propanoate)	InChI=1S/C9H3F13O4/c1-24-4(23)5(13,14)8(19,20)26-6(15,7(16,17)18)9(21,22)25-3(12)2(10)11/h1H3
M421_R351_5883	H-substituted Perfluoroalkyl (linear) dicarboxylic acid	InChI=1/C9H3F13O4/c10-1(2(23)24)4(11,12)6(15,16)8(19,20)9(21,22)7(17,18)5(13,14)3(25)26/h1H,(H,23,24)(H,25,26)
M427_R466_6072	6:2 Fluorotelomer sulfonic acid	InChI=1S/C8H5F13O3S/c9-3(10,1-2-25(22,23)24)4(11,12)5(13,14)6(15,16)7(17,18)8(19,20)21/h1-2H2,(H,22,23,24)
M443_R450_6484	1-hydroxy-6:2 fluorotelomer sulfonate	InChI=1S/C8H5F13O4S/c9-3(10,1-2(22)26(23,24)25)4(11,12)5(13,14)6(15,16)7(17,18)8(19,20)21/h2,22H,1H2,(H,23,24,25)
M443_R450_6484	6:2 fluorotelomer sulfate	InChI=1S/C8H5F13O4S/c9-3(10,1-2-25-26(22,23)24)4(11,12)5(13,14)6(15,16)7(17,18)8(19,20)21/h1-2H2,(H,22,23,24)
M473_R280_7120	1-Bromo-3-(tridecafluorohexyl)benzene	InChI=1S/C12H4BrF13/c13-6-3-1-2-5(4-6)7(14,15)8(16,17)9(18,19)10(20,21)11(22,23)12(24,25)26/h1-4H
M473_R280_7120	1-Bromo-4-(tridecafluorohexyl)benzene	InChI=1S/C12H4BrF13/c13-6-3-1-5(2-4-6)7(14,15)8(16,17)9(18,19)10(20,21)11(22,23)12(24,25)26/h1-4H
M473_R297_7119	1-Bromo-3-(tridecafluorohexyl)benzene	InChI=1S/C12H4BrF13/c13-6-3-1-2-5(4-6)7(14,15)8(16,17)9(18,19)10(20,21)11(22,23)12(24,25)26/h1-4H
M473_R297_7119	1-Bromo-4-(tridecafluorohexyl)benzene	InChI=1S/C12H4BrF13/c13-6-3-1-5(2-4-6)7(14,15)8(16,17)9(18,19)10(20,21)11(22,23)12(24,25)26/h1-4H

Table A.5. (Continued)

group	name_orig	InChI
M497_R480_7670	6:2 fluorotelomer sulfonamido propyl methyl amine	InChI=1S/C12H15F13N2O2S/c1-26-4-2-5-27-30(28,29)6-3-7(13,14)8(15,16)9(17,18)10(19,20)11(21,22)12(23,24)25/h26-27H,2-6H2,1H3
M499_R279_7723	Perfluoro tert-butylcyclohexane	InChI=1S/C10F20/c11-2(1(8(22,23)24,9(25,26)27)10(28,29)30)3(12,13)5(16,17)7(20,21)6(18,19)4(2,14)15
M499_R279_7723	Perfluorobutylcyclohexane	InChI=1S/C10F20/c11-1(4(16,17)7(22,23)9(26,27)10(28,29)30)2(12,13)5(18,19)8(24,25)6(20,21)3(1,14)15
M499_R279_7723	Perfluoro-1-decene	InChI=1S/C10F20/c11-1(2(12)13)3(14,15)4(16,17)5(18,19)6(20,21)7(22,23)8(24,25)9(26,27)10(28,29)30
M511_R187_8005	1-(Trifluoromethyl)perfluorodecalin	InChI=1S/C11F20/c12-1-2(13,6(19,20)10(27,28)9(25,26)4(1,15)16)5(17,18)8(23,24)7(21,22)3(1,14)11(29,30)31
M511_R187_8005	Perfluoro-2-methyldecalin	InChI=1S/C11F20/c12-1-2(13,7(21,22)10(27,28)9(25,26)6(1,19)20)5(17,18)8(23,24)3(14,4(1,15)16)11(29,30)31
M511_R311_8004	1-(Trifluoromethyl)perfluorodecalin	InChI=1S/C11F20/c12-1-2(13,6(19,20)10(27,28)9(25,26)4(1,15)16)5(17,18)8(23,24)7(21,22)3(1,14)11(29,30)31
M511_R311_8004	Perfluoro-2-methyldecalin	InChI=1S/C11F20/c12-1-2(13,7(21,22)10(27,28)9(25,26)6(1,19)20)5(17,18)8(23,24)3(14,4(1,15)16)11(29,30)31
M515_R671_8089	1,1,1,2,2,3,3,4,4,5,5,6,6-Tridecafluoroicosane	InChI=1S/C20H29F13/c1-2-3-4-5-6-7-8-9-10-11-12-13-14-15(21,22)16(23,24)17(25,26)18(27,28)19(29,30)20(31,32)33/h2-14H2,1H3
M541_R321_8595	9:3 fluorotelomer carboxylic acid	InChI=1S/C12H5F19O2/c13-4(14,2-1-3(32)33)5(15,16)6(17,18)7(19,20)8(21,22)9(23,24)10(25,26)11(27,28)12(29,30)31/h1-2H2,(H,32,33)
M549_R226_8775	perfluorononane phosphonic acid	InChI=1S/C9H2F19O3P/c10-1(11,2(12,13)4(16,17)6(20,21)8(24,25)26)3(14,15)5(18,19)7(22,23)9(27,28)32(29,30)31/h(H2,29,30,31)
M570_R296_9093	2,3,3,3-Tetrafluoro-2-[1,1,2,3,3,3-hexafluoro-2-(heptafluoropropoxy)propoxy]-N-phenylpropanamide	InChI=1S/C15H6F17NO3/c16-8(11(20,21)22,7(34)33-6-4-2-1-3-5-6)35-15(31,32)10(19,13(26,27)28)36-14(29,30)9(17,18)12(23,24)25/h1-5H,(H,33,34)
M613_R213_9753	1,1,1,2,2,3,3,4,4,5,5,6,6-Tridecafluoro-8-iodooctadecane	InChI=1S/C18H24F13I/c1-2-3-4-5-6-7-8-9-10-12(32)11-13(19,20)14(21,22)15(23,24)16(25,26)17(27,28)18(29,30)31/h12H,2-11H2,1H3
M779_R368_11166	DiHydrogen-substituted Perfluoro Ether pentadecane sulfonic acid	InChI=1S/C14H3F27O4S/c15-1-45-13(38,39)11(34,35)9(30,31)7(26,27)5(22,23)3(18,19)2(16,17)4(20,21)6(24,25)8(28,29)10(32,33)12(36,37)14(40,41)46(42,43)44/h1H2,(H,42,43,44)

Table A.5. (Continued)

group	name_orig	InChI
M781_R290_11185	12:1:2 fluorotelomer betaine	InChI=1S/C19H13F26NO2/c1-46(2,5-7(47)48)4-3-6(20)8(21,22)9(23,24)10(25,26)11(27,28)12(29,30)13(31,32)14(33,34)15(35,36)16(37,38)17(39,40)18(41,42)19(43,44)45/h6H,3-5H2,1-2H3/p+1
M781_R368_11181	Hydrogen-substituted PerFluoroTetradecane Sulfonate;	InChI=1S/C14H2F28O3S/c15-1(46(43,44)45)2(16,17)3(18,19)4(20,21)5(22,23)6(24,25)7(26,27)8(28,29)9(30,31)10(32,33)11(34,35)12(36,37)13(38,39)14(40,41)42/h1H,(H,43,44,45)
M781_R385_11183	Hydrogen-substituted PerFluoroTetradecane Sulfonate	InChI=1S/C14H2F28O3S/c15-1(46(43,44)45)2(16,17)3(18,19)4(20,21)5(22,23)6(24,25)7(26,27)8(28,29)9(30,31)10(32,33)11(34,35)12(36,37)13(38,39)14(40,41)42/h1H,(H,43,44,45)
M841_R343_11530	Perfluorotetramethyltetraoxapentadecanoicacidme	InChI=1S/C16H3F29O6/c1-47-2(46)3(17,8(23,24)25)48-14(40,41)5(20,10(29,30)31)50-16(44,45)7(22,12(35,36)37)51-15(42,43)6(21,11(32,33)34)49-13(38,39)4(18,19)9(26,27)28/h1H3

Table A.6. $[M+C_2H_3O_2]^-$ feature groups along with the associated extract, retention time ("ret", in seconds), *m/z*, peak area, and peak intensity. Obtained from list fGroups@features@features.

group	Extract	ret	mz	area	intensity
M219_R243_1109	561	243.5	219.0278666	31354760	4681557.5
M219_R243_1109	562	242.8	219.027898	29211180	3928405.75
M219_R243_1109	573	244.0	219.0277918	31065390	5050618
M219_R243_1109	574	242.7	219.0278581	28463750	4341493
M219_R243_1109	581	242.6	219.0277536	27646090	3840280.75
M219_R243_1109	582	243.2	219.0277582	28579950	4146775.75
M219_R260_1112	573	260.5	219.027893	36293920	4015567
M219_R260_1112	574	259.4	219.0279789	35011530	3937930.5
M219_R260_1112	581	259.1	219.0278514	37656230	4192081.75
M219_R260_1112	582	259.8	219.027836	38587450	4145234.25
M219_R277_1104	573	276.8	219.0275852	16752440	2253010.75
M219_R277_1104	574	276.6	219.0276337	17067010	2407372.5
M219_R277_1104	581	277.8	219.0275901	25845160	2895446.75
M219_R277_1104	582	278.4	219.0275786	25859650	3093079.5
M219_R297_1106	561	296.4	219.0278021	51896810	6511512.5
M219_R297_1106	562	296.1	219.0278582	51404880	6051759.5
M219_R297_1106	565	292.7	219.0278117	44768720	1224359
M219_R297_1106	566	293.2	219.0278098	46789150	1186428.125
M219_R297_1106	573	299.8	219.0276843	85598540	3205160.5
M219_R297_1106	574	299.7	219.0277563	84549130	2252814
M219_R297_1106	581	296.3	219.0276527	53891490	5442881.5
M219_R297_1106	582	296.8	219.0276603	48371840	5514271.5
M219_R656_1111	565	654.2	219.0278783	141453200	3410648.25
M219_R656_1111	566	655.3	219.0278619	154878200	3312163
M342_R363_4318	569	362.6	341.9864329	40029480	7205216.5
M342_R363_4318	570	362.8	341.9863189	38255790	6634388
M342_R363_4318	577	363.5	341.9862488	38217060	6470454.5
M342_R363_4318	578	363.2	341.9861494	44621490	7771161
M405_R262_5588	565	260.5	405.1467297	27652120	4041320
M405_R262_5588	566	260.8	405.146722	22783690	3435100.25
M405_R262_5588	569	260.2	405.146919	17444360	2370699.25
M405_R262_5588	570	261.3	405.1468108	17839070	2468139.25
M405_R286_5586	565	284.6	405.1467551	26228020	2422592.25
M405_R286_5586	566	284.2	405.1467582	23554370	2234508.5
M405_R286_5586	569	284.3	405.146902	19888750	2061118.125
M405_R286_5586	570	284.5	405.1466749	19517550	1937296.5
M405_R418_5566	585	418.7	405.0382636	11234240	1509022
M405_R418_5566	586	418.2	405.038187	13712660	2014961.625

Table A.6. (Continued)

group	Extract	ret	mz	area	intensity
M405_R418_5566	589	419.0	405.0383308	13728320	1729854.75
M405_R418_5566	590	418.3	405.0381972	13975780	1892763.5
M405_R418_5566	597	417.7	405.038487	11570430	1887062.125
M405_R418_5566	598	418.1	405.0384199	10571090	1586400.875
M407_R182_5618	565	181.4	407.125302	406147100	24658336
M407_R182_5618	566	181.9	407.1253171	383874900	25641842
M407_R182_5618	569	179.4	407.1256168	486355800	24512998
M407_R182_5618	570	180.6	407.1255061	489552800	25249690
M416_R452_5807	569	451.3	416.0239968	29322030	5170692
M416_R452_5807	570	451.6	416.0238602	29388540	4952654
M443_R450_6484	538	448.3	442.9640859	9285918	2031125.875
M443_R450_6484	539	450.3	442.9641463	16040510	2210953.5
M443_R450_6484	553	449.9	442.9646168	25982000	4339230.5
M443_R450_6484	554	449.7	442.9646713	19166960	3551102
M446_R395_6558	569	394.3	446.0343214	107740000	18341026
M446_R395_6558	570	394.6	446.0341232	94683950	16230693
M446_R395_6558	577	394.9	446.0344151	12491540	2154744.25
M446_R395_6558	578	395.0	446.0344519	16563090	2787970.5
M448_R330_6598	561	330.1	447.9853536	7025099	1086152.625
M448_R330_6598	562	329.5	447.9854864	5617387	1057815.25
M448_R330_6598	573	329.7	447.9851977	27451710	4624814.5
M448_R330_6598	574	330.0	447.9853349	24465000	3615448.25
M448_R330_6598	581	329.4	447.9851007	18915790	3083212
M448_R330_6598	582	329.2	447.9851512	20553850	3239778.25
M473_R273_7128	561	272.8	472.9879954	10852130	1789818.375
M473_R273_7128	562	272.2	472.9881031	8926441	1472082
M473_R273_7128	573	272.7	472.9878288	8316917	1402690.625
M473_R273_7128	574	272.5	472.9879013	7347010	1172402.5
M507_R563_7870	569	562.3	506.9594524	4978396	1090311.125
M507_R563_7870	570	562.5	506.9591433	4776477	1032779.813
M509_R187_7946	561	186.7	508.9648238	66381920	5703101
M509_R187_7946	562	185.8	508.9649493	53114930	6343116
M509_R187_7946	573	186.8	508.9645951	68781610	5105894.5
M509_R187_7946	574	185.6	508.9647074	58502720	6046125.5
M509_R187_7946	581	186.2	508.9645374	55595370	4438419
M509_R187_7946	582	186.7	508.9645532	57129390	4264998.5
M509_R311_7945	561	311.1	508.9646256	101955900	15357964
M509_R311_7945	562	311.0	508.9647634	81791520	12677892

Table A.6. (Continued)

group	Extract	ret	mz	area	intensity
M509_R311_7945	573	311.1	508.9645	1.49E+08	21658254
M509_R311_7945	574	311.1	508.9647	1.22E+08	18146354
M509_R311_7945	581	310.7	508.9644	1.13E+08	16865490
M509_R311_7945	582	310.5	508.9645	1.15E+08	17474314
M521_R213_8210	565	212.1	521.0556	51463890	9779527
M521_R213_8210	566	212.0	521.0556	49554140	8839252
M521_R213_8210	569	211.3	521.0558	35001160	7294670
M521_R213_8210	570	212.7	521.0556	36511210	7915569
M521_R213_8210	577	213.4	521.0554	33761140	8299529
M521_R213_8210	578	211.6	521.0555	36559000	7627571
M613_R213_9753	565	210.6	613.0669	9959665	2030189
M613_R213_9753	566	211.2	613.067	9534366	2276263
M625_R337_9882	573	336.8	624.9264	7218826	1193005
M625_R337_9882	574	336.3	624.9267	5661998	1016523
M633_R276_9973	561	275.2	632.9772	36990730	4752986
M633_R276_9973	562	275.5	632.9774	28846180	3644655
M633_R276_9973	573	275.2	632.9771	37043510	4622906
M633_R276_9973	574	275.0	632.9772	31947160	4132600
M633_R276_9973	581	275.4	632.9771	31308440	3723116
M633_R276_9973	582	275.3	632.9771	31559850	3865130
M741_R310_10949	573	310.3	740.9495	10119710	1830135
M741_R310_10949	574	309.5	740.9497	9193418	1434536
M741_R310_10949	581	310.0	740.9493	8618350	1305719
M741_R310_10949	582	309.8	740.9494	8649191	1265140
M741_R327_10948	561	326.9	740.9495	13466320	1829291
M741_R327_10948	562	326.2	740.9498	10795960	1451071
M741_R327_10948	573	326.5	740.9493	20207520	2907097
M741_R327_10948	574	326.0	740.9496	17360010	2525817
M741_R327_10948	581	326.1	740.9491	18571950	2521990
M741_R327_10948	582	326.0	740.9493	19483950	2756233
M839_R344_11515	573	344.1	838.947	15486150	1810647
M839_R344_11515	574	343.7	838.9473	12898960	1600833
M839_R344_11515	581	343.8	838.9468	14996250	1792474
M839_R344_11515	582	343.6	838.947	15438770	1831373
M841_R343_11530	573	343.3	840.9401	11815920	1438660
M841_R343_11530	574	341.2	840.9413	8174679	1296517

Table A.7. $[M+C_2H_3O_2]^-$ feature groups with associated group retention time ("rts" in seconds) and group *m/z* ("mzs"). This was data frame fGroups@groupInfo.

Group	rts	mzs
M219_R277_1104	277.3	219.02765
M219_R297_1106	296.9	219.02775
M219_R243_1109	243.4	219.02782
M219_R656_1111	655.6	219.02787
M219_R260_1112	259.9	219.02789
M342_R363_4318	363.3	341.98643
M405_R418_5566	418.3	405.03831
M405_R286_5586	285.6	405.14677
M405_R262_5588	262.0	405.14680
M407_R182_5618	182.2	407.12544
M416_R452_5807	451.7	416.02396
M443_R450_6484	449.8	442.96451
M446_R395_6558	395.4	446.03444
M448_R330_6598	329.9	447.98527
M473_R273_7128	272.8	472.98790
M507_R563_7870	563.0	506.95899
M509_R311_7945	311.2	508.96457
M509_R187_7946	186.6	508.96469
M521_R213_8210	213.1	521.05561
M613_R213_9753	213.3	613.06587
M625_R337_9882	336.6	624.92658
M633_R276_9973	275.5	632.97718
M741_R327_10948	326.5	740.94942
M741_R310_10949	310.1	740.94957
M839_R344_11515	343.9	838.94709
M841_R343_11530	342.6	840.94136

Table A.8. Selected columns from exported table of $[M+C_2H_3O_2]^-$ suspect compounds associated with each feature group. Showing the feature group, associated NIST suspect list compound and International Chemical Identifier (InChI). This was extracted from the data frame fGroups@screenInfo.

group	name_orig	InChI
M219_R243_1109	TriHydrogen-substituted perfluoroButanoic acid	InChI=1S/C4H4F4O2/c5-2(1-3(9)10)4(6,7)8/h2H,1H2,(H,9,10)
M219_R243_1109	C4H4O2F4	InChI=1S/C4H4F4O2/c5-1(3(7)8)2(6)4(9)10/h1-3H,(H,9,10)
M219_R260_1112	TriHydrogen-substituted perfluoroButanoic acid	InChI=1S/C4H4F4O2/c5-2(1-3(9)10)4(6,7)8/h2H,1H2,(H,9,10)
M219_R260_1112	C4H4O2F4	InChI=1S/C4H4F4O2/c5-1(3(7)8)2(6)4(9)10/h1-3H,(H,9,10)
M219_R277_1104	TriHydrogen-substituted perfluoroButanoic acid	InChI=1S/C4H4F4O2/c5-2(1-3(9)10)4(6,7)8/h2H,1H2,(H,9,10)
M219_R277_1104	C4H4O2F4	InChI=1S/C4H4F4O2/c5-1(3(7)8)2(6)4(9)10/h1-3H,(H,9,10)
M219_R297_1106	TriHydrogen-substituted perfluoroButanoic acid	InChI=1S/C4H4F4O2/c5-2(1-3(9)10)4(6,7)8/h2H,1H2,(H,9,10)
M219_R297_1106	C4H4O2F4	InChI=1S/C4H4F4O2/c5-1(3(7)8)2(6)4(9)10/h1-3H,(H,9,10)
M219_R656_1111	TriHydrogen-substituted perfluoroButanoic acid	InChI=1S/C4H4F4O2/c5-2(1-3(9)10)4(6,7)8/h2H,1H2,(H,9,10)
M219_R656_1111	C4H4O2F4	InChI=1S/C4H4F4O2/c5-1(3(7)8)2(6)4(9)10/h1-3H,(H,9,10)
M342_R363_4318	(S)-Perfluorobutanesulfinamide	InChI=1S/C4H2F9NOS/c5-1(6,3(9,10)11)2(7,8)4(12,13)16(14)15/h14H2
M405_R262_5588	1,1,1,2,2,3,3,4,4-Nonafluorotridecane	InChI=1S/C13H19F9/c1-2-3-4-5-6-7-8-9-10(14,15)11(16,17)12(18,19)13(20,21)22/h2-9H2,1H3
M405_R286_5586	1,1,1,2,2,3,3,4,4-Nonafluorotridecane	InChI=1S/C13H19F9/c1-2-3-4-5-6-7-8-9-10(14,15)11(16,17)12(18,19)13(20,21)22/h2-9H2,1H3
M405_R418_5566	3-Acetyl-5,5,6,6,7,7,8,8,8-nonafluorooctane-2,4-dione	InChI=1S/C10H7F9O3/c1-3(20)5(4(2)21)6(22)7(11,12)8(13,14)9(15,16)10(17,18)19/h5H,1-2H3
M405_R418_5566	3,3,4,4,5,5,6,6,7,7,8,8,8-tridecafluorooctan-1-ol	InChI=1S/C8H6F12O/c9-3(10)5(13,14)7(17,18)8(19,20)6(15,16)4(11,12)1-2-21/h3,21H,1-2H2
M407_R182_5618	(2S)-2-(Nonafluorobutyl)octan-1-ol	InChI=1S/C12H17F9O/c1-2-3-4-5-6-8(7-22)9(13,14)10(15,16)11(17,18)12(19,20)21/h8,22H,2-7H2,1H3
M407_R182_5618	1,1,1,2,2,3,3,4,4-Nonafluorododecan-5-ol	InChI=1S/C12H17F9O/c1-2-3-4-5-6-7-8(22)9(13,14)10(15,16)11(17,18)12(19,20)21/h8,22H,2-7H2,1H3
M407_R182_5618	9,9,10,10,11,11,12,12,12-Nonafluorododecan-1-ol	InChI=1S/C12H17F9O/c13-9(14,7-5-3-1-2-4-6-8-22)10(15,16)11(17,18)12(19,20)21/h22H,1-8H2

Table A.8. (Continued)

group	name_orig	InChI
M416_R452_5807	N-(2-hydroxyethyl)-N-methylperfluoro-2-methylpropanesulfonamide	InChI=1S/C7H8F9NO3S/c1-17(2-3-18)21(19,20)7(15,16)4(8,5(9,10)11)6(12,13)14/h18H,2-3H2,1H3
M416_R452_5807	1-Butanesulfonamide, 1,1,2,2,3,3,4,4,4-nonafluoro-N-(2-hydroxyethyl)-N-methyl-	InChI=1S/C7H8F9NO3S/c1-17(2-3-18)21(19,20)7(15,16)5(10,11)4(8,9)6(12,13)14/h18H,2-3H2,1H3
M443_R450_6484	perfluoroalkane-1-sulfinic acid;perfluorohexane sulfinate;perfluorohexane sulfinate	InChI=1S/C6HF13O2S/c7-1(8,3(11,12)5(15,16)17)2(9,10)4(13,14)6(18,19)22(20)21/h(H,20,21)
M446_R395_6558	1,1,2,3,3,3-Hexafluoro-N,N-bis(2-hydroxyethyl)-2-(trifluoromethyl)propane-1-sulphonamide	InChI=1S/C8H10F9NO4S/c9-5(6(10,11)12,7(13,14)15)8(16,17)23(21,22)18(1-3-19)2-4-20/h19-20H,1-4H2
M446_R395_6558	1,1,2,2,3,3,4,4,4-Nonafluoro-N,N-bis(2-hydroxyethyl)butane-1-sulphonamide	InChI=1S/C8H10F9NO4S/c9-5(10,7(13,14)15)6(11,12)8(16,17)23(21,22)18(1-3-19)2-4-20/h19-20H,1-4H2
M448_R330_6598	Perfluoro(3-(1-(ethenyloxy)propan-2-yloxy)propanenitrile)	InChI=1S/C8F13NO2/c9-2(10)3(11)23-8(20,21)5(14,6(15,16)17)24-7(18,19)4(12,13)1-22
M473_R273_7128	2,2,3,3,4,4,5,5,5-Nonafluoro-1-(pentafluorophenyl)pentan-1-one	InChI=1S/C11F14O/c12-2-1(3(13)5(15)6(16)4(2)14)7(26)8(17,18)9(19,20)10(21,22)11(23,24)25
M473_R273_7128	3,3,4,4,4-Pentafluoro-2,2-bis(pentafluoroethyl)butanoic acid	InChI=1S/C8HF15O2/c9-3(10,6(15,16)17)2(1(24)25,4(11,12)7(18,19)20)5(13,14)8(21,22)23/h(H,24,25)
M473_R273_7128	3,3,4,4,4-Pentafluoro-2-(1,1,1,2,3,3,3-heptafluoropropan-2-yl)-2-(trifluoromethyl)butanoic acid	InChI=1S/C8HF15O2/c9-3(6(15,16)17,7(18,19)20)2(1(24)25,5(12,13)14)4(10,11)8(21,22)23/h(H,24,25)
M473_R273_7128	3,3,4,4,5,5,5-Heptafluoro-2-(pentafluoroethyl)-2-(trifluoromethyl)pentanoic acid	InChI=1S/C8HF15O2/c9-3(10,5(13,14)8(21,22)23)2(1(24)25,6(15,16)17)4(11,12)7(18,19)20/h(H,24,25)
M473_R273_7128	4,4,4-Trifluoro-2,2,3,3-tetrakis(trifluoromethyl)butanoic acid	InChI=1S/C8HF15O2/c9-4(10,11)2(1(24)25,5(12,13)14)3(6(15,16)17,7(18,19)20)8(21,22)23/h(H,24,25)
M473_R273_7128	3,4,4,5,5,5-Hexafluoro-2,2,3-tris(trifluoromethyl)pentanoic acid	InChI=1S/C8HF15O2/c9-3(7(18,19)20,4(10,11)8(21,22)23)2(1(24)25,5(12,13)14)6(15,16)17/h(H,24,25)
M473_R273_7128	3,3,4,5,5,5-Hexafluoro-2,2,4-tris(trifluoromethyl)pentanoic acid	InChI=1S/C8HF15O2/c9-3(7(18,19)20,8(21,22)23)4(10,11)2(1(24)25,5(12,13)14)6(15,16)17/h(H,24,25)
M473_R273_7128	3,3,4,4,5,5,6,6,6-Nonafluoro-2,2-bis(trifluoromethyl)hexanoic acid	InChI=1S/C8HF15O2/c9-3(10,4(11,12)5(13,14)8(21,22)23)2(1(24)25,6(15,16)17)7(18,19)20/h(H,24,25)

Table A.8. (Continued)

group	name_orig	InChI
M473_R273_7128	2,3,4,4,4-Pentafluoro-2-(1,1,1,2,3,3,3-heptafluoropropan-2-yl)-3-(trifluoromethyl)butanoic acid	InChI=1S/C8HF15O2/c9-2(1(24)25,3(10,5(12,13)14)6(15,16)17)4(11,7(18,19)20)8(21,22)23/h(H,24,25)
M473_R273_7128	2,3,3,4,4,5,5,5-Octafluoro-2-(1,1,1,2,3,3,3-heptafluoropropan-2-yl)pentanoic acid	InChI=1S/C8HF15O2/c9-2(1(24)25,3(10,6(15,16)17)7(18,19)20)4(11,12)5(13,14)8(21,22)23/h(H,24,25)
M473_R273_7128	2,3,3,4,4,5,5,5-Octafluoro-2-(heptafluoropropyl)pentanoic acid	InChI=1S/C8HF15O2/c9-2(1(24)25,3(10,11)5(14,15)7(18,19)20)4(12,13)6(16,17)8(21,22)23/h(H,24,25)
M473_R273_7128	2,3,3,4,4,4-Hexafluoro-2-[1,1,1,3,3,3-hexafluoro-2-(trifluoromethyl)propan-2-yl]butanoic acid	InChI=1S/C8HF15O2/c9-2(1(24)25,4(10,11)8(21,22)23)3(5(12,13)14,6(15,16)17)7(18,19)20/h(H,24,25)
M473_R273_7128	2,3,4,4,5,5,5-Heptafluoro-2-(pentafluoroethyl)-3-(trifluoromethyl)pentanoic acid	InChI=1S/C8HF15O2/c9-2(1(24)25,4(11,12)7(18,19)20)3(10,6(15,16)17)5(13,14)8(21,22)23/h(H,24,25)
M473_R273_7128	2,3,3,4,5,5,5-Heptafluoro-2-(pentafluoroethyl)-4-(trifluoromethyl)pentanoic acid	InChI=1S/C8HF15O2/c9-2(1(24)25,5(13,14)8(21,22)23)4(11,12)3(10,6(15,16)17)7(18,19)20/h(H,24,25)
M473_R273_7128	2,3,3,4,4,5,5,6,6,6-Decafluoro-2-(pentafluoroethyl)hexanoic acid	InChI=1S/C8HF15O2/c9-2(1(24)25,4(12,13)7(18,19)20)3(10,11)5(14,15)6(16,17)8(21,22)23/h(H,24,25)
M473_R273_7128	2,4,4,5,5,5-Hexafluoro-2,3,3-tris(trifluoromethyl)pentanoic acid	InChI=1S/C8HF15O2/c9-2(1(24)25,5(12,13)14)3(6(15,16)17,7(18,19)20)4(10,11)8(21,22)23/h(H,24,25)
M473_R273_7128	2,3,4,4,5,5,5-Heptafluoro-3-(pentafluoroethyl)-2-(trifluoromethyl)pentanoic acid	InChI=1S/C8HF15O2/c9-2(1(24)25,6(15,16)17)3(10,4(11,12)7(18,19)20)5(13,14)8(21,22)23/h(H,24,25)
M473_R273_7128	2,3,4,5,5,5-Hexafluoro-2,3,4-tris(trifluoromethyl)pentanoic acid	InChI=1S/C8HF15O2/c9-2(1(24)25,5(12,13)14)3(10,6(15,16)17)4(11,7(18,19)20)8(21,22)23/h(H,24,25)
M473_R273_7128	2,3,4,4,5,5,6,6,6-Nonafluoro-2,3-bis(trifluoromethyl)hexanoic acid	InChI=1S/C8HF15O2/c9-2(1(24)25,6(15,16)17)3(10,7(18,19)20)4(11,12)5(13,14)8(21,22)23/h(H,24,25)
M473_R273_7128	2,3,3,5,5,5-Hexafluoro-2,4,4-tris(trifluoromethyl)pentanoic acid	InChI=1S/C8HF15O2/c9-2(1(24)25,5(12,13)14)4(10,11)3(6(15,16)17,7(18,19)20)8(21,22)23/h(H,24,25)
M473_R273_7128	2,3,3,4,5,5,6,6,6-Nonafluoro-2,4-bis(trifluoromethyl)hexanoic acid	InChI=1S/C8HF15O2/c9-2(1(24)25,6(15,16)17)4(11,12)3(10,7(18,19)20)5(13,14)8(21,22)23/h(H,24,25)
M473_R273_7128	2,3,3,4,4,5,6,6,6-Nonafluoro-2,5-bis(trifluoromethyl)hexanoic acid	InChI=1S/C8HF15O2/c9-2(1(24)25,6(15,16)17)4(11,12)5(13,14)3(10,7(18,19)20)8(21,22)23/h(H,24,25)
M473_R273_7128	2,3,3,4,4,5,5,6,6,7,7,7-Dodecafluoro-2-(trifluoromethyl)heptanoic acid	InChI=1S/C8HF15O2/c9-2(1(24)25,7(18,19)20)3(10,11)4(12,13)5(14,15)6(16,17)8(21,22)23/h(H,24,25)
M473_R273_7128	2,2,4,4,5,5,5-Heptafluoro-3-(pentafluoroethyl)-3-(trifluoromethyl)pentanoic acid	InChI=1S/C8HF15O2/c9-2(10,1(24)25)3(6(15,16)17,4(11,12)7(18,19)20)5(13,14)8(21,22)23/h(H,24,25)

Table A.8. (Continued)

group	name_orig	InChI
M473_R273_7128	2,2,4,5,5,5-Hexafluoro-3,3,4-tris(trifluoromethyl)pentanoic acid	InChI=1S/C8HF15O2/c9-2(10,1(24)25)3(5(12,13)14,6(15,16)17)4(11,7(18,19)20)8(21,22)23/h(H,24,25)
M473_R273_7128	2,2,4,4,5,5,6,6,6-Nonafluoro-3,3-bis(trifluoromethyl)hexanoic acid	InChI=1S/C8HF15O2/c9-2(10,1(24)25)3(6(15,16)17,7(18,19)20)4(11,12)5(13,14)8(21,22)23/h(H,24,25)
M473_R273_7128	2,2,3,4,4,5,5,5-Octafluoro-3-(1,1,1,2,3,3,3-heptafluoropropan-2-yl)pentanoic acid	InChI=1S/C8HF15O2/c9-2(10,1(24)25)3(11,5(13,14)8(21,22)23)4(12,6(15,16)17)7(18,19)20/h(H,24,25)
M473_R273_7128	2,2,3,4,4,5,5,6,6,6-Decafluoro-3-(pentafluoroethyl)hexanoic acid	InChI=1S/C8HF15O2/c9-2(10,1(24)25)3(11,5(14,15)7(18,19)20)4(12,13)6(16,17)8(21,22)23/h(H,24,25)
M473_R273_7128	2,2,3,5,5,5-Hexafluoro-3,4,4-tris(trifluoromethyl)pentanoic acid	InChI=1S/C8HF15O2/c9-2(10,1(24)25)4(11,8(21,22)23)3(5(12,13)14,6(15,16)17)7(18,19)20/h(H,24,25)
M473_R273_7128	2,2,3,4,5,5,6,6,6-Nonafluoro-3,4-bis(trifluoromethyl)hexanoic acid	InChI=1S/C8HF15O2/c9-2(10,1(24)25)3(11,6(15,16)17)4(12,7(18,19)20)5(13,14)8(21,22)23/h(H,24,25)
M473_R273_7128	2,2,3,4,4,5,6,6,6-Nonafluoro-3,5-bis(trifluoromethyl)hexanoic acid	InChI=1S/C8HF15O2/c9-2(10,1(24)25)3(11,6(15,16)17)5(13,14)4(12,7(18,19)20)8(21,22)23/h(H,24,25)
M473_R273_7128	2,2,3,4,4,5,5,6,6,7,7,7-Dodecafluoro-3-(trifluoromethyl)heptanoic acid	InChI=1S/C8HF15O2/c9-2(10,1(24)25)3(11,7(18,19)20)4(12,13)5(14,15)6(16,17)8(21,22)23/h(H,24,25)
M473_R273_7128	2,2,3,3,5,5,6,6,6-Nonafluoro-4,4-bis(trifluoromethyl)hexanoic acid	InChI=1S/C8HF15O2/c9-2(10,1(24)25)4(11,12)3(6(15,16)17,7(18,19)20)5(13,14)8(21,22)23/h(H,24,25)
M473_R273_7128	2,2,3,3,4,5,5,6,6,6-Decafluoro-4-(pentafluoroethyl)hexanoic acid	InChI=1S/C8HF15O2/c9-2(10,1(24)25)4(12,13)3(11,5(14,15)7(18,19)20)6(16,17)8(21,22)23/h(H,24,25)
M473_R273_7128	2,2,3,3,4,5,6,6,6-Nonafluoro-4,5-bis(trifluoromethyl)hexanoic acid	InChI=1S/C8HF15O2/c9-2(10,1(24)25)5(13,14)3(11,6(15,16)17)4(12,7(18,19)20)8(21,22)23/h(H,24,25)
M473_R273_7128	2,2,3,3,4,5,5,6,6,7,7,7-Dodecafluoro-4-(trifluoromethyl)heptanoic acid	InChI=1S/C8HF15O2/c9-2(10,1(24)25)4(12,13)3(11,7(18,19)20)5(14,15)6(16,17)8(21,22)23/h(H,24,25)
M473_R273_7128	2,2,3,3,4,4,6,6,6-Nonafluoro-5,5-bis(trifluoromethyl)hexanoic acid	InChI=1S/C8HF15O2/c9-2(10,1(24)25)4(11,12)5(13,14)3(6(15,16)17,7(18,19)20)8(21,22)23/h(H,24,25)
M473_R273_7128	2,2,3,3,4,4,5,6,6,7,7,7-Dodecafluoro-5-(trifluoromethyl)heptanoic acid	InChI=1S/C8HF15O2/c9-2(10,1(24)25)4(12,13)5(14,15)3(11,7(18,19)20)6(16,17)8(21,22)23/h(H,24,25)
M473_R273_7128	Perfluoro-6-(trifluoromethyl)heptanoic acid	InChI=1S/C8HF15O2/c9-2(10,1(24)25)4(12,13)6(16,17)5(14,15)3(11,7(18,19)20)8(21,22)23/h(H,24,25)
M473_R273_7128	Perfluorooctanoic acid	InChI=1S/C8HF15O2/c9-2(10,1(24)25)3(11,12)4(13,14)5(15,16)6(17,18)7(19,20)8(21,22)23/h(H,24,25)

Table A.8. (Continued)

group	name_orig	InChI
M507_R563_7870	Hydrogen-substituted Perfluoro Ether octane sulfonic acid	InChI=1S/C7H2F14O4S/c8-1(9)2(10,11)3(12,13)4(14,15)5(16,17)25-6(18,19)7(20,21)26(22,23)24/h1H,(H,22,23,24)
M509_R187_7946	perfluoroheptane phosphonic acid	InChI=1S/C7H2F15O3P/c8-1(9,2(10,11)4(14,15)6(18,19)20)3(12,13)5(16,17)7(21,22)26(23,24)25/h(H2,23,24,25)
M509_R311_7945	perfluoroheptane phosphonic acid	InChI=1S/C7H2F15O3P/c8-1(9,2(10,11)4(14,15)6(18,19)20)3(12,13)5(16,17)7(21,22)26(23,24)25/h(H2,23,24,25)
M521_R213_8210	3-(Perfluorohexyl)-5-phenyl-1H-pyrazole	InChI=1S/C15H7F13N2/c16-10(17,9-6-8(29-30-9)7-4-2-1-3-5-7)11(18,19)12(20,21)13(22,23)14(24,25)15(26,27)28/h1-6H,(H,29,30)
M613_R213_9753	[4-(3,3,4,4,5,5,6,6,7,7,8,8,9,9,10,10,10-Heptadecafluorodecyl)phenyl]methanol	InChI=1S/C17H11F17O/c18-10(19,6-5-8-1-3-9(7-35)4-2-8)11(20,21)12(22,23)13(24,25)14(26,27)15(28,29)16(30,31)17(32,33)34/h1-4,35H,5-7H2
M625_R337_9882	Chloro-perfluorooctane phosphonic acid	InChI=1S/C9H2ClF18O3P/c10-8(25,26)6(21,22)4(17,18)2(13,14)1(11,12)3(15,16)5(19,20)7(23,24)9(27,28)32(29,30)31/h(H2,29,30,31)
M633_R276_9973	Perfluoroperhydrofluorene	InChI=1S/C13F22/c14-1-2(15)4(17,9(26,27)13(34,35)11(30,31)7(2,22)23)5(18,19)3(1,16)8(24,25)12(32,33)10(28,29)6(1,20)21
M741_R310_10949	2,2,3,3,4,4,5,5,6,6,7,7,8,8,8-Pentadecafluorooctyl nonafluorobutane-1-sulfonate	InChI=1S/C12H2F24O3S/c13-2(14,1-39-40(37,38)12(35,36)9(27,28)8(25,26)11(32,33)34)3(15,16)4(17,18)5(19,20)6(21,22)7(23,24)10(29,30)31/h1H2
M741_R310_10949	Hydrogen-substituted PerFluoroDodecane Sulfonate	InChI=1S/C12H2F24O3S/c13-1(40(37,38)39)2(14,15)3(16,17)4(18,19)5(20,21)6(22,23)7(24,25)8(26,27)9(28,29)10(30,31)11(32,33)12(34,35)36/h1H,(H,37,38,39)
M741_R327_10948	2,2,3,3,4,4,5,5,6,6,7,7,8,8,8-Pentadecafluorooctyl nonafluorobutane-1-sulfonate	InChI=1S/C12H2F24O3S/c13-2(14,1-39-40(37,38)12(35,36)9(27,28)8(25,26)11(32,33)34)3(15,16)4(17,18)5(19,20)6(21,22)7(23,24)10(29,30)31/h1H2
M741_R327_10948	Hydrogen-substituted PerFluoroDodecane Sulfonate	InChI=1S/C12H2F24O3S/c13-1(40(37,38)39)2(14,15)3(16,17)4(18,19)5(20,21)6(22,23)7(24,25)8(26,27)9(28,29)10(30,31)11(32,33)12(34,35)36/h1H,(H,37,38,39)
M839_R344_11515	DiHydrogen-substituted Perfluoro Ether pentadecane sulfonic acid	InChI=1S/C14H3F27O4S/c15-1-45-13(38,39)11(34,35)9(30,31)7(26,27)5(22,23)3(18,19)2(16,17)4(20,21)6(24,25)8(28,29)10(32,33)12(36,37)14(40,41)46(42,43)44/h1H2,(H,42,43,44)
M841_R343_11530	Hydrogen-substituted PerFluoroTetradecane Sulfonate	InChI=1S/C14H2F28O3S/c15-1(46(43,44)45)2(16,17)3(18,19)4(20,21)5(22,23)6(24,25)7(26,27)8(28,29)9(30,31)10(32,33)11(34,35)12(36,37)13(38,39)14(40,41)42/h1H,(H,43,44,45)

Table A.9. MSMatch compound match results for extract 577, precursor *m/z* 298.944, retention time window of 3.70 min - 3.90 min.

Com-pound ID	Compound	MS1 Score	MS1 Score (Rev)	MS2 Score	MS2 Score (Rev)	# Annotated Fragments	# Annotated Structures	# Annotated Citations	Sample Class	Peak ID
3045	Perfluorobutane sulfonic acid	0.8216	0.9809	0.8916	0.9829	3	3	2	analytical standard	227
3045	Perfluorobutane sulfonic acid	0.8003	0.9405	0.8727	0.9397	2	0	2	aqueous film-forming foam (AFFF)	117
3045	Perfluorobutane sulfonic acid	0.8353	0.8341	0.8847	0.9755	1	1	0	analytical standard	220
3045	Perfluorobutane sulfonic acid	0.8339	0.8234	0.7965	0.9094	0	0	0	analytical standard	234
3045	Perfluorobutane sulfonic acid	0.7867	0.9545	0.8199	0.7193	2	0	2	aqueous film-forming foam (AFFF)	127
3045	Perfluorobutane sulfonic acid	0.7932	0.9488	0.7432	0.7028	2	0	2	aqueous film-forming foam (AFFF)	85
3045	Perfluorobutane sulfonic acid	0.795	0.9651	0.6896	0.7156	2	0	2	commercial formulation	154
3045	Perfluorobutane sulfonic acid	0.7959	0.9406	0.0151	0.8573	2	0	2	aqueous film-forming foam (AFFF)	108
3045	Perfluorobutane sulfonic acid	0.7952	0.9833			2	0	2	commercial formulation	60
3045	Perfluorobutane sulfonic acid	0.7955	0.9493			2	0	2	aqueous film-forming foam (AFFF)	96

Table A.10. MSMatch output of peaks identified in MS/MS fragmentation spectra derived for extract 577, precursor *m/z* 298.944, and retention time window of 3.70 min - 3.90 min.

Match Type	Mean m/z	Mean Intensity	n	Annotated Formula	Uncertainty (m/z)	Uncertainty (intensity)	Annotated Fragment ID	Has SMILES Notation
unknown	59.0124	0.005	3		0.0001	0.0007		
unknown	74.7351	0.004	3		0.0001	0.0008		
unknown	79.9526	0.003	2		0	0.0006		
structure	79.9561	0.103	3	O3S1	0.0001	0.0029	62, 96	true
structure	82.9596	0.009	3	F1O2S1	0	0.001	64, 66, 95	true
unknown	91.7321	0.003	2		0.0001	0.0006		
structure	98.9546	0.048	3	F1O3S1	0.0001	0.0054	63	true
unknown	100.9501	0.002	2		0.0004	0.0001		
structure	118.9915	0.003	2	C2F5	0	0.0004	48, 99	true
structure	168.9886	0.003	3	C3F7	0.0005	0.0007	49, 100	true
unknown	217.0022	0.003	2		0.0006	0.0014		
structure	298.9437	0.731	3	C4F9O3S1	0.0001	0.0042	61	true
unknown	299.0132	0.004	3		0.0003	0.0004		
unknown	299.9468	0.044	3		0.0001	0.0048		
unknown	300.9400	0.040	3		0.0002	0.0008		

Table A.11. Annotations from MSMatch for fragment peaks in the MS/MS spectra of extract 577, precursor *m/z* 298.944, and retention time window of 3.70 min - 3.90 min.

Annotated Fragment ID	Fragment	Measured at m/z	Exact Mass	Mass Error (ppm)	SMILES	Radical	Net Charge	Found in n Compounds	Found in n Peaks
96	O3S1	79.9561	79.9568	-9.1716	[O-]S(=O)=O	Not Recorded	-1	1	1
62	O3S1	79.9561	79.9568	-9.1716	[O-]S(=O)=O	Yes	-1	10	21
17	O3S1	79.9561	79.9568	-9.1716		No	Not Recorded	40	110
95	F1O2S1	82.9596	82.9603	-8.4378	[O-]S(F)=O	Not Recorded	-1	1	1
64	F1O2S1	82.9596	82.9603	-8.4378	[O-]S(F)=O	No	-1	4	5
66	F1O2S1	82.9596	82.9603	-8.4378	O-S(F)=O	No	0	1	1
46	F1O2S1	82.9596	82.9603	-8.4378		No	Not Recorded	1	1
63	F1O3S1	98.9546	98.9552	-6.4002	[O-]S(F)(=O)=O	No	-1	7	7
23	F1O3S1	98.9546	98.9552	-6.4002		No	Not Recorded	28	78
99	C2F5	118.9915	118.992	-4.202	F[C-](F)C(F)(F)F	Not Recorded	-1	1	1
48	C2F5	118.9915	118.992	-4.202	F[C-](F)C(F)(F)F	No	-1	18	35
13	C2F5	118.9915	118.992	-4.202		No	Not Recorded	8	26
100	C3F7	168.9886	168.9888	-0.9863	F[C-](F)C(F)(F)C(F)(F)F	Not Recorded	-1	1	1
49	C3F7	168.9886	168.9888	-0.9863	F[C-](F)C(F)(F)C(F)(F)F	No	-1	21	37
14	C3F7	168.9886	168.9888	-0.9863		No	Not Recorded	12	31
61	C4F9O3S1	298.9437	298.9424	4.4602	O=S(C(F)(F)C(F)(F)C(F)(F)C(F)(F)F)([O-])=O	No	-1	1	2

Table A.12. Manual annotations for fragment peaks in the MS/MS spectra of extract 577, with precursor *m/z* 298.944, and retention time window of 3.70 min - 3.90 min.

Measured *m/z*	Assigned Formula	Exact Mass	Mass Error (ppm)
59.0124	C2H3O2	59.01385	-24.57
299.9468	[13C]C3F9O3S	299.94635	1.50
300.9400	[34S]C4F9O3	300.93879	4.02

Table A.13. MSMatch output of peaks identified in MS/MS fragmentation spectra derived for extract 577, precursor *m/z* 341.986, and retention time window of 5.90 min – 6.20 min.

Match Type	Mean m/z	Mean Intensity	n	Annotated Formula	Uncertainty (m/z)	Uncertainty (intensity)	Annotated Fragment ID	Has SMILES Notation
unknown	59.0124	0.0024	1					
unknown	63.9611	0.0358	5		0	0.0025		
unknown	64.9689	0.2381	5		0.0001	0.0102		
unknown	64.9719	0.004	2		0	0.0011		
unknown	64.9751	0.0038	2		0.0013	0.003		
unknown	65.9568	0.0028	3		0.0001	0.0004		
unknown	66.9647	0.0108	5		0.0001	0.0006		
unknown	69.4264	0.0023	2		0.0013	0.0003		
structure	82.9596	0.0027	2	F1O2S1	0.0001	0.0003	64, 66, 95	true
unknown	85.4956	0.0026	3		0.0001	0.0007		
unknown	91.7288	0.0031	3		0.0013	0.0005		
unknown	91.9799	0.0936	5		0	0.0037		
unknown	93.9758	0.0046	4		0.0002	0.0012		
unknown	121.9818	0.004	2		0.0001	0.0014		
unknown	121.9906	0.0645	5		0.0001	0.0025		
unknown	123.9862	0.0034	2		0.0001	0.0016		
unknown	187.994	0.0032	3		0.0007	0.0006		
unknown	204.1396	0.0023	2		0.0002	0.0001		
structure	218.9862	0.0053	4	C4F9	0.0003	0.0007	50, 101	True
unknown	297.961	0.0037	3		0.0005	0.0006		
unknown	341.9861	0.4647	5		0.0001	0.0116		
unknown	342.9889	0.0423	5		0.0002	0.0028		
unknown	343.983	0.0238	5		0.0007	0.0025		

Table A.14. Annotations from MSMatch for fragment peaks in the MS/MS spectra of extract 577, precursor *m/z* 341.986, and retention time window of 5.90 min – 6.20 min.

Annotated Fragment ID	Fragment	Measured at m/z	Exact Mass	Mass Error (ppm)	SMILES	Radical	Net Charge	Found in n Compounds	Found in n Peaks
95	F1O2S1	82.9596	82.9603	-8.4378	[O-]S(F)=O	Not Recorded	-1	1	1
64	F1O2S1	82.9596	82.9603	-8.4378	[O-]S(F)=O	No	-1	4	5
66	F1O2S1	82.9596	82.9603	-8.4378	O-S(F)=O	No	0	1	1
46	F1O2S1	82.9596	82.9603	-8.4378		No	Not Recorded	1	1
101	C4F9	218.9862	218.9856	2.6257	FC(F)([C-](F)F)C(F)(F)C(F)(F)F	Not Recorded	-1	1	1
50	C4F9	218.9862	218.9856	2.6257	FC(F)([C-](F)F)C(F)(F)C(F)(F)F	No	-1	13	27
15	C4F9	218.9862	218.9856	2.6257		No	Not Recorded	4	16

Table A. 15. Manual annotations for fragment peaks in the MS/MS spectra of extract 577, precursor *m/z* 341.986, and retention time window of 5.90 min – 6.20 min.

Measured *m/z*	Assigned Formula	Exact Mass	Mass Error (ppm)
59.0124	C2H3O2	59.01385	-24.57
63.9611	SO2	63.96245	-21.11
64.9689	O2SH	64.97027	-21.09
66.9647	FOS	66.96594	-18.52
91.9799	O2SNCH2	91.98117	-13.81
121.9906	O2SNCH2CH2O	121.99174	-9.34
341.9861	C6F9H5NO3S	341.98519	2.66
342.9889	[13C]C5F9H5NO3S	342.98855	1.02
343.983	[34S]C6F9H5NO3	343.98099	5.84

Table A.16. MSMatch compound match results for extract 577, precursor *m/z* 426.969, and retention time window of 7.70 min - 7.85 min.

Com-pound ID	Compound	MS1 Score	MS1 Score (Rev)	MS2 Score	MS2 Score (Rev)	# Annotated Fragments	# Annotated Structures	# Annotated Citations	Sample Class	Peak ID
3052	6:2 Fluorotelomer sulfonic acid	0.9647	0.9973	0.7238	0.895	2	2	1	analytical standard	284
3052	6:2 Fluorotelomer sulfonic acid	0.9688	0.995	0.6911	0.778	3	3	2	analytical standard	287
3052	6:2 Fluorotelomer sulfonic acid	0.9747	0.9738	0.6645	0.7676	1	1	0	analytical standard	337
3052	6:2 Fluorotelomer sulfonic acid	0.8728	0.882	0.1579	0.9731	2	0	2	aqueous film-forming foam (AFFF)	139
3052	6:2 Fluorotelomer sulfonic acid	0.9708	0.9957	0.2998	0.331	2	2	2	analytical standard	290
3052	6:2 Fluorotelomer sulfonic acid	0.9708	0.9957	0.2998	0.331	2	2	2	analytical standard	290

Table A.17. MSMatch output of peaks identified in MS/MS fragmentation spectra derived for extract 577, precursor *m/z* 426.969, and retention time window of 7.70 min - 7.85 min.

Match Type	Mean m/z	Mean Intensity	n	Annotated Formula	Uncertainty (m/z)	Uncertainty (intensity)	Annotated Fragment ID	Has SMILES Notation
unknown	59.0125	0.0081	4		0.0001	0.0023		
structure	79.9561	0.1340	4	O3S1	0	0.0082	62, 96	true
unknown	79.9609	0.0040	3		0	0.0006		
structure	80.9639	0.2867	4	H1O3S1	0	0.0087	86, 98	true
unknown	81.9519	0.0054	4		0.0001	0.0012		
structure	82.9596	0.0131	4	F1O2S1	0.0001	0.0014	64, 66, 95	true
unknown	91.7286	0.0029	3		0.0001	0.0004		
unknown	216.9894	0.0039	4		0.0001	0.0013		
unknown	254.0328	0.0037	4		0.0009	0.0007		
unknown	254.9865	0.0034	3		0.001	0.0005		
unknown	282.9813	0.0038	4		0.0008	0.0004		
formula	292.9839	0.0048	4	C7F11	0.0013	0.0006	40	false
unknown	386.9554	0.0116	2		0.0003	0.0009		
unknown	386.9569	0.0118	3		0.0012	0.0009		
unknown	406.9627	0.0954	4		0.0002	0.0056		
unknown	407.9663	0.0116	4		0.0011	0.002		
unknown	408.962	0.0069	3		0.0015	0.0014		
unknown	408.9631	0.0069	3		0.001	0.0013		
structure	426.9691	0.3343	4	C8F13H4O3S1	0.0001	0.0059	88	true
unknown	427.9725	0.0385	4		0.0004	0.0024		
unknown	428.9694	0.0237	4		0.0009	0.0028		

Table A.18. Annotations from MSMatch for fragment peaks in the MS/MS spectra of extract 577, precursor *m/z* 426.969, and retention time window of 7.70 min - 7.85 min.

Annotated Fragment ID	Fragment	Measured at m/z	Exact Mass	Mass Error (ppm)	SMILES	Radical	Net Charge	Found in n Compounds	Found in n Peaks
96	O3S1	79.9561	79.9568	-8.7547	[O-]S(=O)=O	Not Recorded	-1	1	1
62	O3S1	79.9561	79.9568	-8.7547	[O-]S(=O)=O	Yes	-1	10	21
17	O3S1	79.9561	79.9568	-8.7547		No	Not Recorded	40	110
98	H1O3S1	80.9639	80.9646	-8.6458	[O-]S(=O)O	No	-1	1	1
86	H1O3S1	80.9639	80.9646	-8.6458	[O-]S(=O)O	No	-1	3	10
44	H1O3S1	80.9639	80.9646	-8.6458		No	Not Recorded	2	2
95	F1O2S1	82.9596	82.9603	-7.8351	[O-]S(F)=O	Not Recorded	-1	1	1
64	F1O2S1	82.9596	82.9603	-7.8351	[O-]S(F)=O	No	-1	4	5
66	F1O2S1	82.9596	82.9603	-7.8351	O-S(F)=O	No	0	1	1
46	F1O2S1	82.9596	82.9603	-7.8351		No	Not Recorded	1	1
40	C7F11	292.9839	292.9824	5.2904		No	Not Recorded	1	1
88	C8F13H4O3S1	426.9691	426.9674	3.923	O=S(CCC(F)(F)C(F)(F)C(F)(F)C(F)(F)C(F)(F)C(F)(F)C(F)(F)F)([O-])=O	Yes	-1	1	2

Table A.19. Manually annotated MS/MS fragmentation peaks in the spectra for extract 577, precursor *m/z* 426.969, and retention time window of 7.70 min - 7.85 min.

Measured *m/z*	Assigned Fragment	Exact Mass	Mass Error (ppm)
59.0125	C2H3O2	59.01385	-22.88
386.9554	C8F11H2O3S1	386.95545	-0.13
406.9627	C8F12H3O3S1	406.96168	2.51
427.9725	[13C]C7F13H4O3S	427.97126	2.90
428.9694	[34S]C8F13H4O3	428.96370	13.29

Table A.20. MSMatch output of peaks identified in MS/MS fragmentation spectra derived for extract 553, precursor *m/z* 442.965, and retention time window of 7.40 min – 7.75 min.

Match Type	Mean m/z	Mean Intensity	n	Annotated Formula	Uncertainty (m/z)	Uncertainty (intensity)	Annotated Fragment ID	Has SMILES Notation
structure	79.9561	0.0041	3	O3S1	0.0001	0.0004	62, 96	true
unknown	91.73	0.0036	3		0.0014	0.0018		
unknown	96.9589	0.7588	4		0	0.0115		
unknown	96.9719	0.0068	3		0.0001	0.0004		
unknown	97.9582	0.0065	4		0.0001	0.001		
unknown	97.9638	0.0018	3		0.0002	0.0002		
structure	98.9547	0.0303	4	F1O3S1	0.0001	0.0019	63	true
unknown	98.9625	0.0047	4		0.0011	0.001		
unknown	442.9642	0.1588	4		0.0001	0.0102		
unknown	443.9662	0.0164	1					
unknown	443.9673	0.0165	4		0.0008	0.0014		
unknown	444.9602	0.0087	3		0.0009	0.0005		
unknown	444.9638	0.0062	1					

Table A.21. Annotations from MSMatch for fragment peaks in the MS/MS spectra of extract 553,with precursor *m/z* 442.965, and retention time window of 7.40 min – 7.75 min.

Annotated Fragment ID	Fragment	Measured at m/z	Exact Mass	Mass Error (ppm)	SMILES	Radical	Net Charge	Found in n Compounds	Found in n Peaks
96	O3S1	79.9561	79.9568	-8.7547	[O-]S(=O)=O	Not Recorded	-1	1	1
62	O3S1	79.9561	79.9568	-8.7547	[O-]S(=O)=O	Yes	-1	10	21
17	O3S1	79.9561	79.9568	-8.7547		No	Not Recorded	40	110
63	F1O3S1	98.9547	98.9552	-5.3054	[O-]S(F)(=O)=O	No	-1	7	7
23	F1O3S1	98.9547	98.9552	-5.3054		No	Not Recorded	28	78

Table A.22. Manual annotations for fragment peaks in the MS/MS spectra of extract 553, with precursor *m/z* 442.965, and retention time window of 7.40 min – 7.75 min.

Measured *m/z*	Assigned Formula	Exact Mass	Mass Error (ppm)
96.9589	HSO4	96.96010	-12.38
98.9547	[^{34}S]HO4	98.95590	-12.13
442.9642	C8H4F13O4S	442.96282	3.12
443.9673	[^{13}C]C7H4F13O4S	443.96617	2.55
444.9602	[^{34}S]C8H4F13O4	444.95862	3.55

Table A.23. MSMatch fragment match annotations for peaks in the MS/MS spectra of extract 569,with precursor *m/z* 416.024, and retention time window of 7.40 min – 7.75 min.

Match Type	Mean m/z	Mean Intensity	n	Annotated Formula	Uncertainty (m/z)	Uncertainty (intensity)	Annotated Fragment ID	Has SMILES Notation
unknown	59.0011	0.0025	3		0.0017	0.0011		
unknown	59.0069	0.007	5		0.0008	0.0007		
unknown	59.0125	0.9533	5		0	0.0049		
unknown	59.0186	0.0074	4		0.0001	0.0006		
unknown	59.0247	0.0028	3		0.0007	0.0003		
unknown	60.0159	0.0238	5		0	0.0025		
unknown	61.0168	0.0043	4		0.0001	0.0009		
unknown	91.7293	0.0058	3		0.0006	0.0037		

Table A.24. Manual annotations for fragment peaks in the MS/MS spectra of extract 569,with precursor *m/z* 416.024, and retention time window of 7.40 min – 7.75 min.

Measured *m/z*	Assigned Formula	Exact Mass	Mass Error (ppm)
59.0125	[C2H3O2]-	59.01385	-22.88
60.0159	[[^{13}C]-CH3O2]-	60.01721	-21.83
61.0168	[[^{18}O]-CH3O2]-	61.01810	-21.31

Table A.25. MSMatch fragment match annotations for peaks in the MS/MS spectra of extract 569, with precursor *m/z* 446.034, and retention time of window of 6.53 min – 6.83 min.

Match Type	Mean m/z	Mean Intensity	n	Annotated Formula	Uncertainty (m/z)	Uncertainty (intensity)	Annotated Fragment ID	Has SMILES Notation
unknown	59.0078	0.0044	3		0.0015	0.0004		
unknown	59.0126	0.5074	5		0.0001	0.0048		
unknown	59.0191	0.0033	4		0.0009	0.0007		
unknown	60.0159	0.0117	5		0.0000	0.0022		
unknown	61.0168	0.0027	3		0.0002	0.0003		
structure	79.9561	0.0663	5	O3S1	0.0000	0.0022	62, 96	true
structure	80.9640	0.0050	5	H1O3S1	0.0001	0.0011	86, 98	true
unknown	81.9521	0.0025	3		0.0002	0.0005		
structure	82.9597	0.0070	5	F1O2S1	0.0001	0.0006	64, 66, 95	true
unknown	91.7281	0.0066	4		0.0009	0.0030		
unknown	121.9910	0.0031	3		0.0001	0.0004		
unknown	135.9980	0.0015	2		0.0000	0.0003		
unknown	136.0065	0.1192	5		0.0000	0.0035		
unknown	137.0000	0.0029	1					
unknown	137.0097	0.0034	4		0.0006	0.0004		
unknown	138.0027	0.0046	5		0.0003	0.0008		
unknown	140.0014	0.0036	5		0.0002	0.0005		
unknown	166.0028	0.0032	3		0.0002	0.0007		
unknown	166.0060	0.0021	2		0.0001	0.0001		
unknown	166.0173	0.1268	5		0.0001	0.0044		
unknown	166.0317	0.0041	3		0.0001	0.0011		
unknown	167.0207	0.0060	5		0.0003	0.0013		
unknown	168.0132	0.0051	5		0.0005	0.0015		
unknown	186.0238	0.0539	5		0.0001	0.0021		
unknown	187.0246	0.0018	1					
unknown	187.0272	0.0032	2		0.0000	0.0010		

Table A.25. (continued)

Match Type	Mean m/z	Mean Intensity	n	Annotated Formula	Uncertainty (m/z)	Uncertainty (intensity)	Annotated Fragment ID	Has SMILES Notation
unknown	188.0200	0.0029	3		0.0006	0.0007		
unknown	196.9846	0.0030	1					
structure	218.9863	0.0316	5	C4F9	0.0001	0.0026	50, 101	true
unknown	282.9487	0.0167	5		0.0004	0.0015		
unknown	386.0139	0.0036	4		0.0016	0.0006		
unknown	446.0372	0.0043	4		0.0012	0.0011		

Table A.26. MSMatch fragment match annotations for fragment peaks in the MS/MS spectra of extract 569,with precursor *m/z* 442.965, and retention time of window of 6.53 min – 6.83 min.

Annotated Fragment ID	Fragment	Measured at m/z	Exact Mass	Mass Error (ppm)	SMILES	Radical	Net Charge	Found in n Compounds	Found in n Peaks
96	O3S1	79.9561	79.9568	-8.7547	[O-]S(=O)=O	Not Recorded	-1	1	1
62	O3S1	79.9561	79.9568	-8.7547	[O-]S(=O)=O	Yes	-1	10	21
17	O3S1	79.9561	79.9568	-8.7547		No	Not Recorded	40	110
98	H1O3S1	80.9640	80.9646	-7.6577	[O-]S(=O)O	No	-1	1	1
86	H1O3S1	80.9640	80.9646	-7.6577	[O-]S(=O)O	No	-1	3	10
44	H1O3S1	80.9640	80.9646	-7.6577		No	Not Recorded	2	2
95	F1O2S1	82.9597	82.9603	-6.7502	[O-]S(F)=O	Not Recorded	-1	1	1
64	F1O2S1	82.9597	82.9603	-6.7502	[O-]S(F)=O	No	-1	4	5
66	F1O2S1	82.9597	82.9603	-6.7502	O-S(F)=O	No	0	1	1
46	F1O2S1	82.9597	82.9603	-6.7502		No	Not Recorded	1	1
101	C4F9	218.9863	218.9856	3.2879	FC(F)([C-](F)F)C(F)(F)C(F)(F)F	Not Recorded	-1	1	1
50	C4F9	218.9863	218.9856	3.2879	FC(F)([C-](F)F)C(F)(F)C(F)(F)F	No	-1	13	27
15	C4F9	218.9863	218.9856	3.2879		No	Not Recorded	4	16

Table A.27. Manual annotations for fragment peaks in the MS/MS spectra of extract 569,with precursor m/z 442.965, and retention time of window of 6.53 min – 6.83 min.

Measured *m/z*	Formula	Exact Mass	Mass Error (ppm)
59.0126	[C2H3O2]-	59.01385	-21.18
60.0159	[[^{13}C]-CH3O2]-	60.01721	-21.83
61.0168	[[^{18}O]-CH3O2]-	61.0181	-21.31
81.9521	[34S]O3	81.95316	-12.93
82.9597	[34S]O3H	82.96098	-15.43
121.991	O2SNCH2CH2O	121.99174	-6.07
136.0065	O2SNCH2CH2CH2O	136.00739	-6.54
166.0173	O2SNCH2CH2OCH2CH2O	166.01795	-3.92
186.0238	O2SNCH2CH2OCH2CH2OHF	186.02418	-2.04
282.9487	C4F9SO2	282.94808	2.19
386.0139	C8H9F9NO4S	386.01141	6.45
446.0372	C8H10F9NO4S-C2H3O2	446.03253	10.47

A.4. Extracted Ion Chromatograms and Mass Spectra

(a)

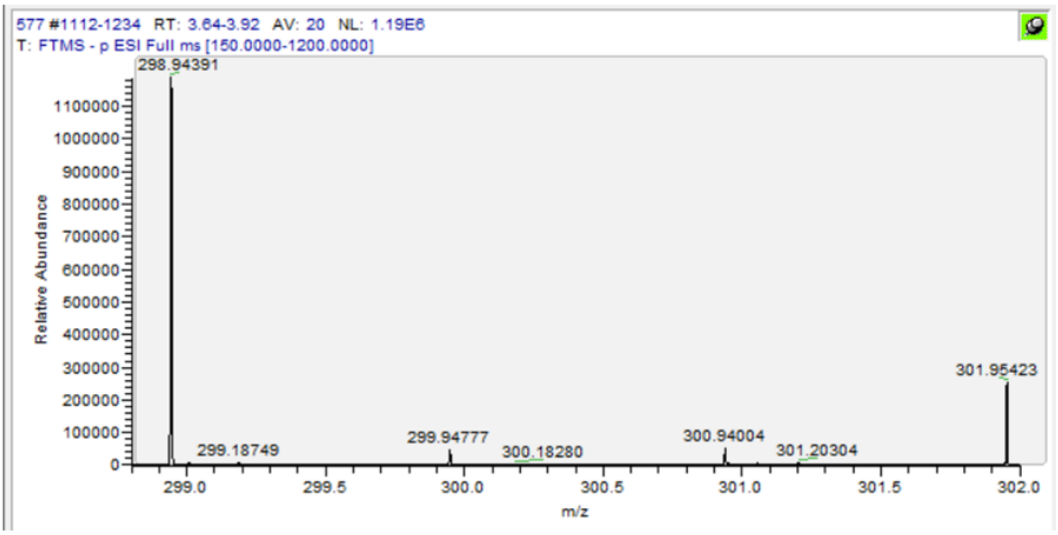

(b)

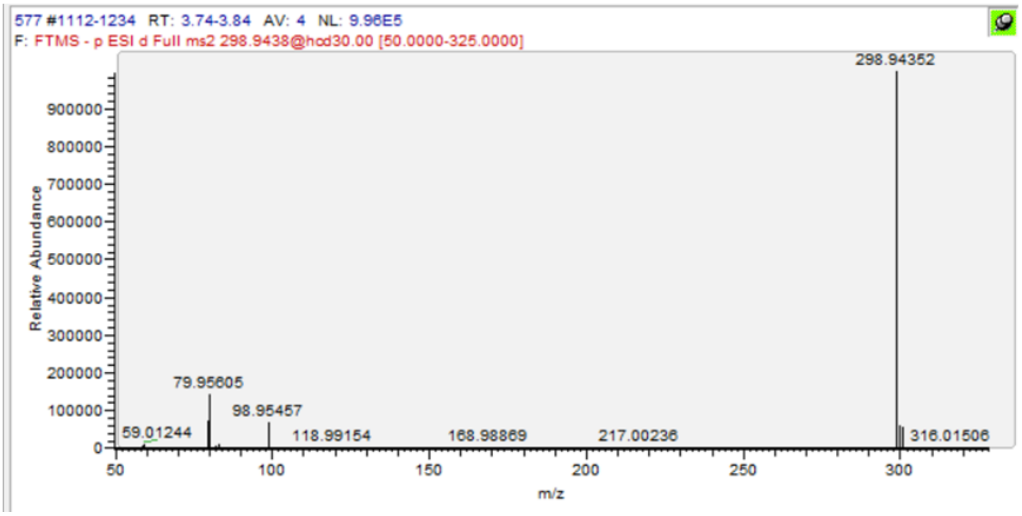

Figure A.1. (a) Mass spectra from extract 577 (MB-E), integrated from 3.64 min - 3.92 min, (b) MS/MS fragmentation spectra, from extract 577 (MB-E), averaged from 4 scans, collected from 3.74 min - 3.84 min with precursor *m/z* 298.9438.

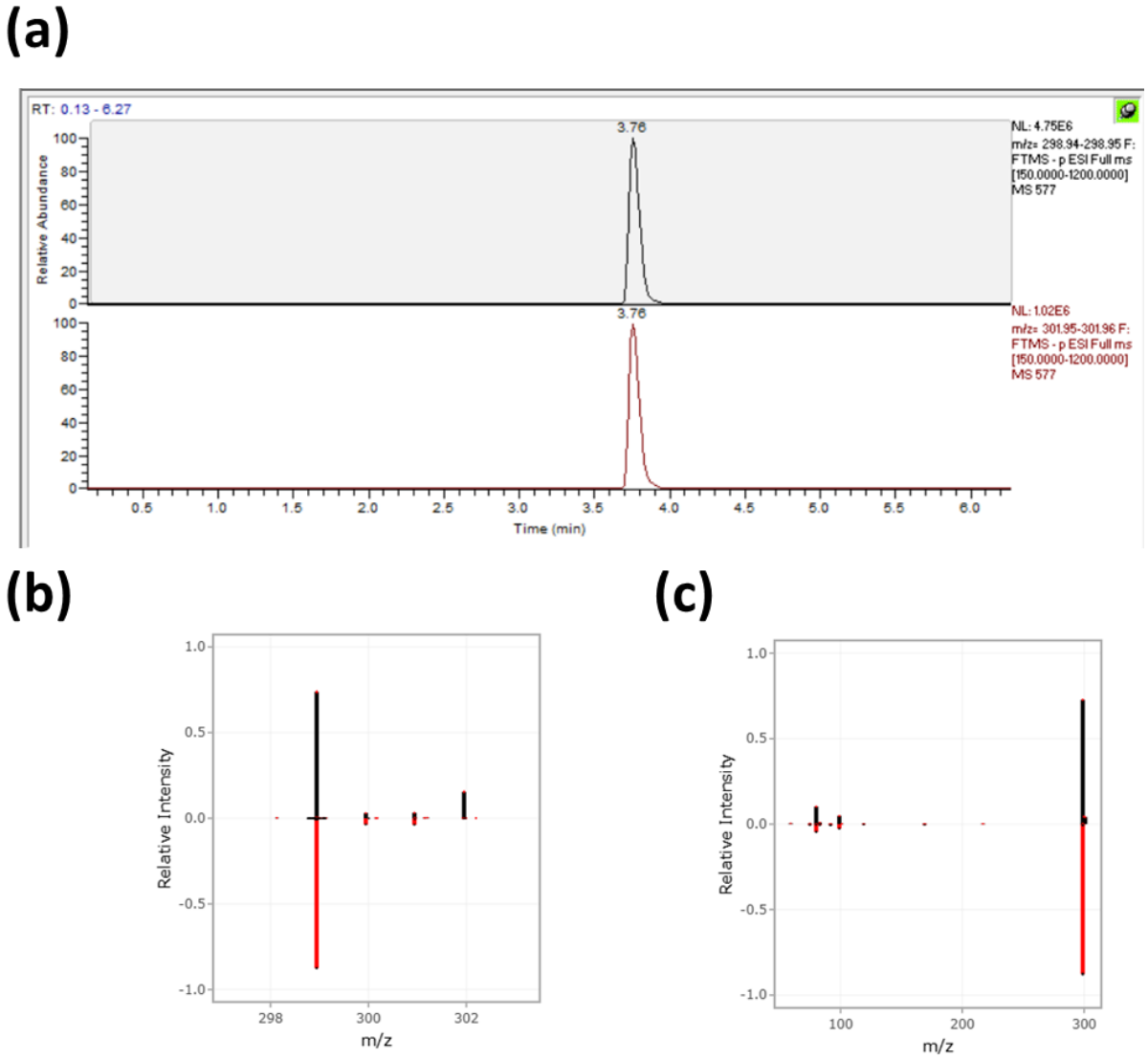

Figure A.2. (a) Comparison of the extracted ion chromatograms with *m/z* 298.94 - 298.95 (top; the feature annotated as PFBS) and *m/z* 301.95 - 301.96 (bottom; derived from $^{13}C_3$-PFBS internal standard) in extract 577. (b) Comparison MS1 spectrum and (c) MS2 spectrum with the spectrum determined here in black and the previously annotated spectrum in red. The red spectrum was the previously uploaded spectrum in MSMatch that produced the highest MS2 score (0.8916). From MSMatch regarding the red spectra: " This reference spectrum was measured by LC (ThermoFisher Scientific) quadrupole orbitrap MS (ThermoFisher Scientific), separated by octadecyl (C18) analytical column in negative ESI mode at 2500 volts and fixed fragmentation by HCD (higher energy collision-induced dissociation) at 30 normalized volts."

(a)

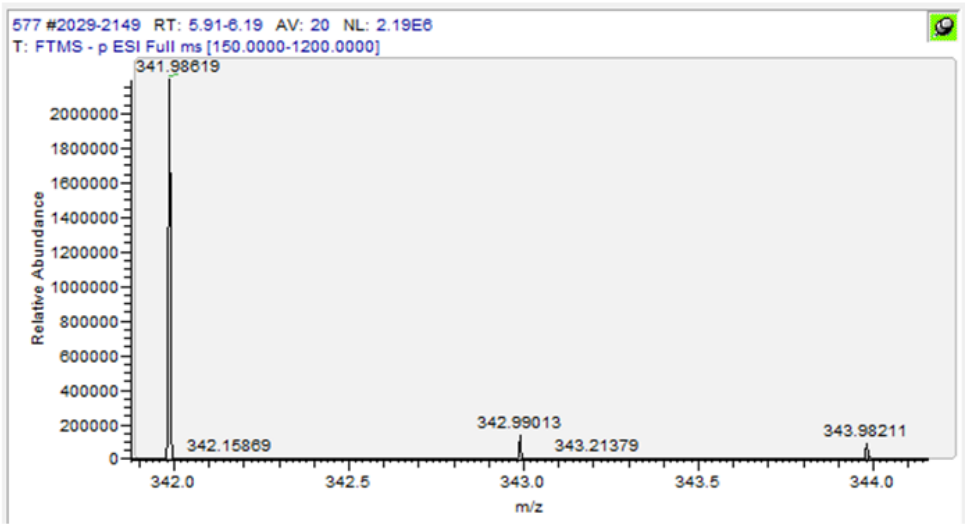

(b)

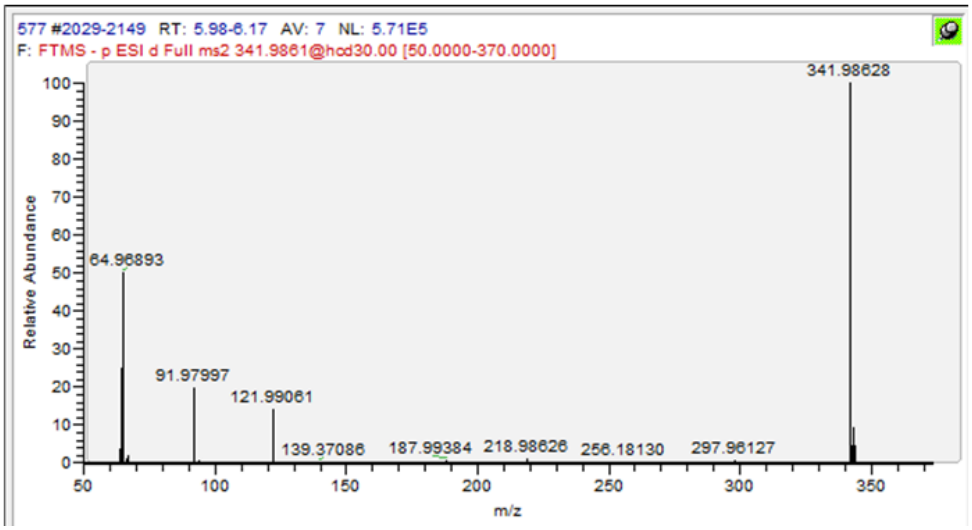

Figure A.3. (a) Mass spectra from extract 577 (MB-E), integrated from 5.91 min - 6.19 min, (b) MS/MS fragmentation spectra, from extract 577 (MB-E), averaged from 7 scans, collected from 5.98 min - 6.17 min with precursor *m/z* 341.9861.

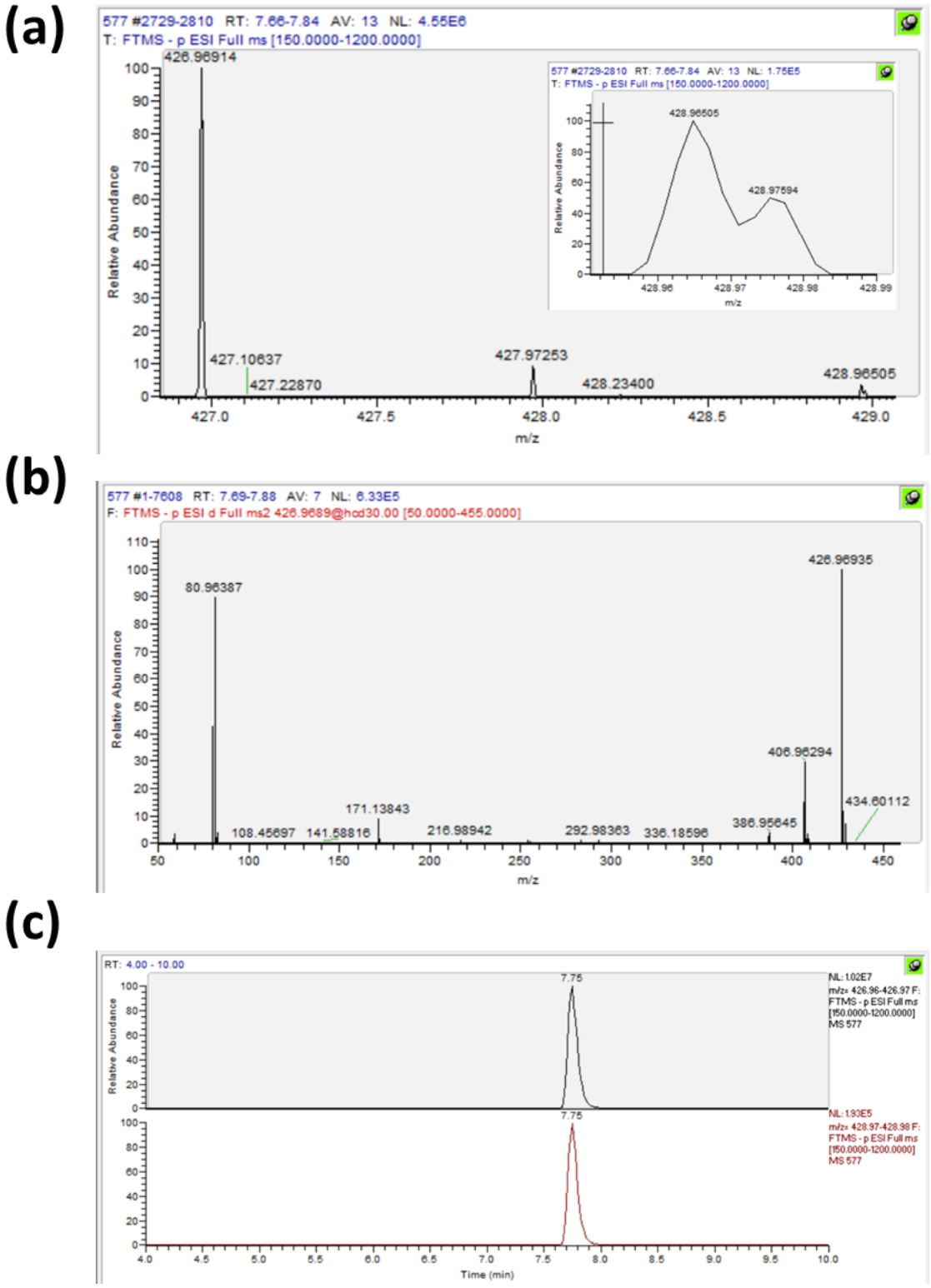

Figure A.4. (a) Mass spectra from extract 577 (MB-E), integrated from 7.66 min – 7.84 min and (b) MS/MS fragmentation spectra, from extract 577 (MB-E), averaged from 7 scans, collected from 7.69 min – 7.88 min with precursor *m/z* 426.9689. (c) Comparison of the extracted ion chromatograms of *m/z* 426.96 – 426.97 (black; feature annotated as 6:2 FTS) and *m/z* 428.97 – 428.98 (derived from $^{13}C_2$-6:2 FTS internal standard).

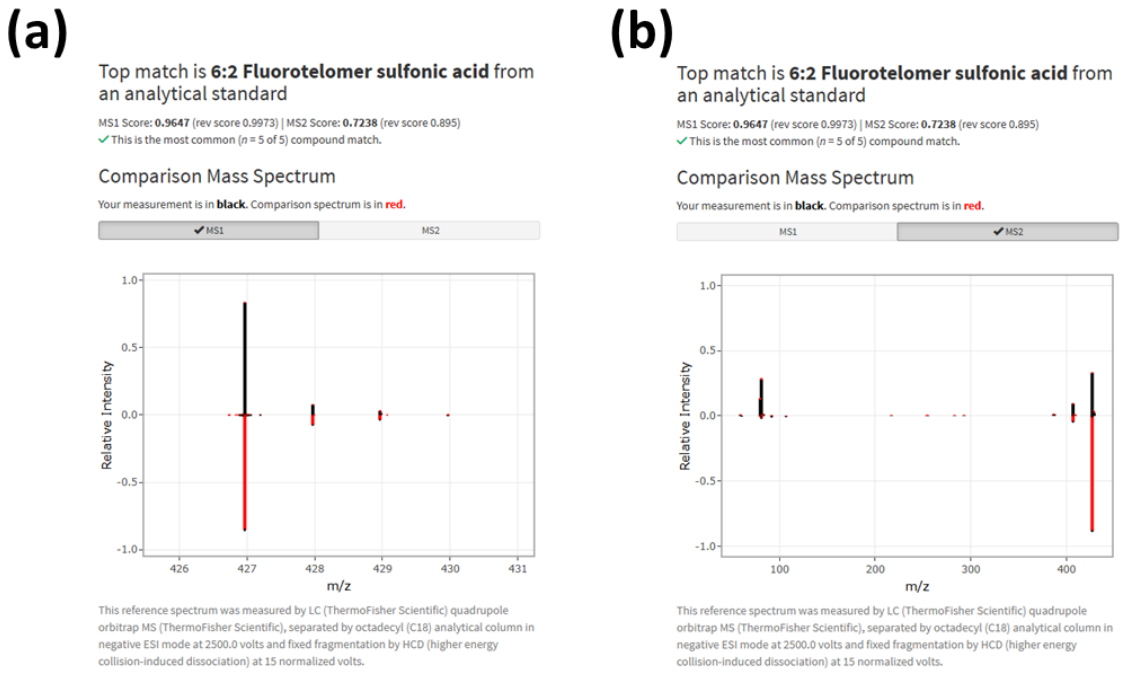

Figure A.5. (a) Comparison MS1 spectrum and (b) MS2 spectrum with the spectrum determined here in black and the previously annotated spectrum in red. The red spectrum was a previously uploaded spectrum in MSMatch that produced the highest MS2 score (0.7238). From MSMatch regarding the red spectra: "This reference spectrum was measured by LC (ThermoFisher Scientific) quadrupole orbitrap MS (ThermoFisher Scientific), separated by octadecyl (C18) analytical column in negative ESI mode at 2500 volts and fixed fragmentation by HCD (higher energy collision-induced dissociation) at 15 normalized volts.

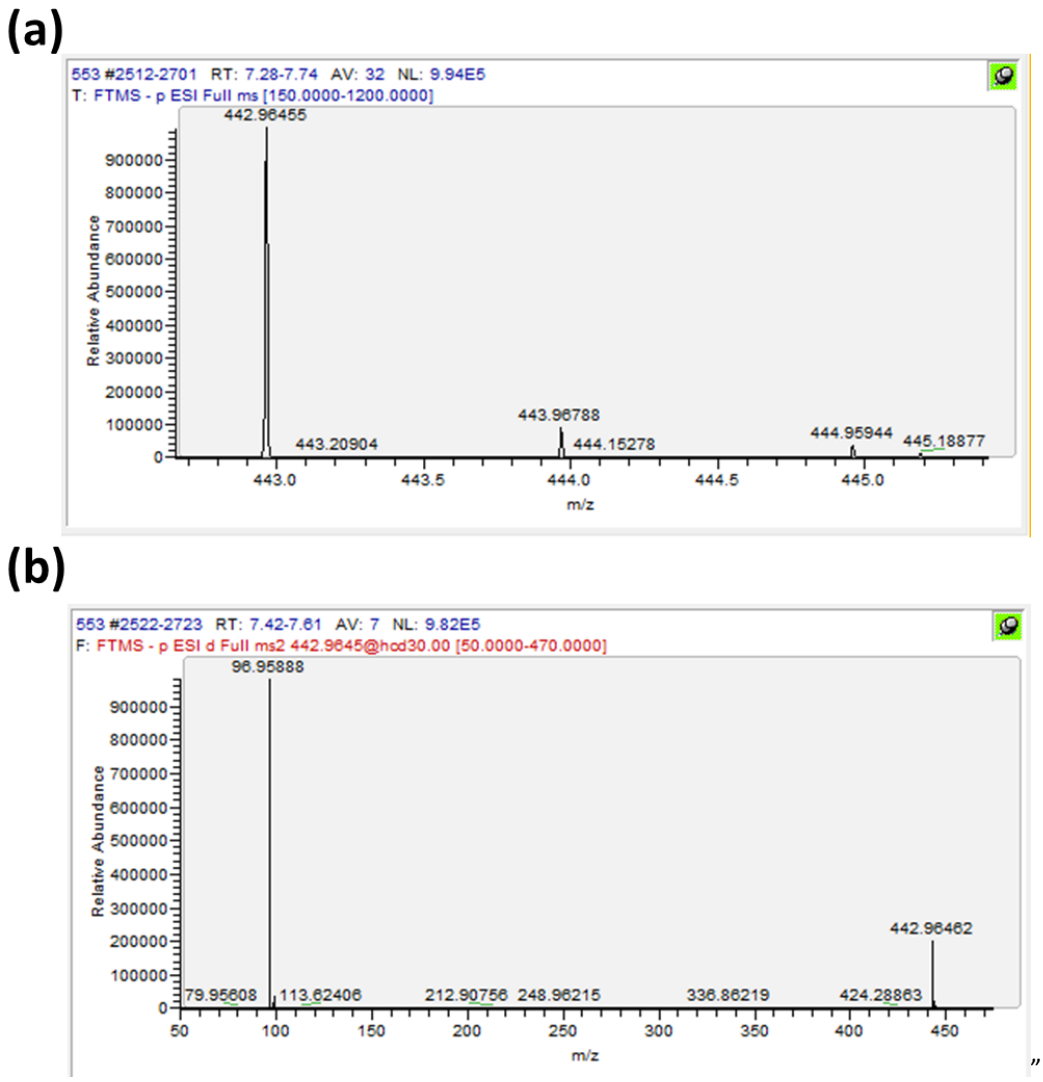

Figure A.6. (a) Mass spectra from extract 553 (OS-F), integrated from 7.28 min -7.74 min and (b) MS/MS fragmentation spectra, from extract 553 (MB-F), averaged from 7 scans, collected from 7.42 min – 7.61 min with precursor *m/z* 442.9645.

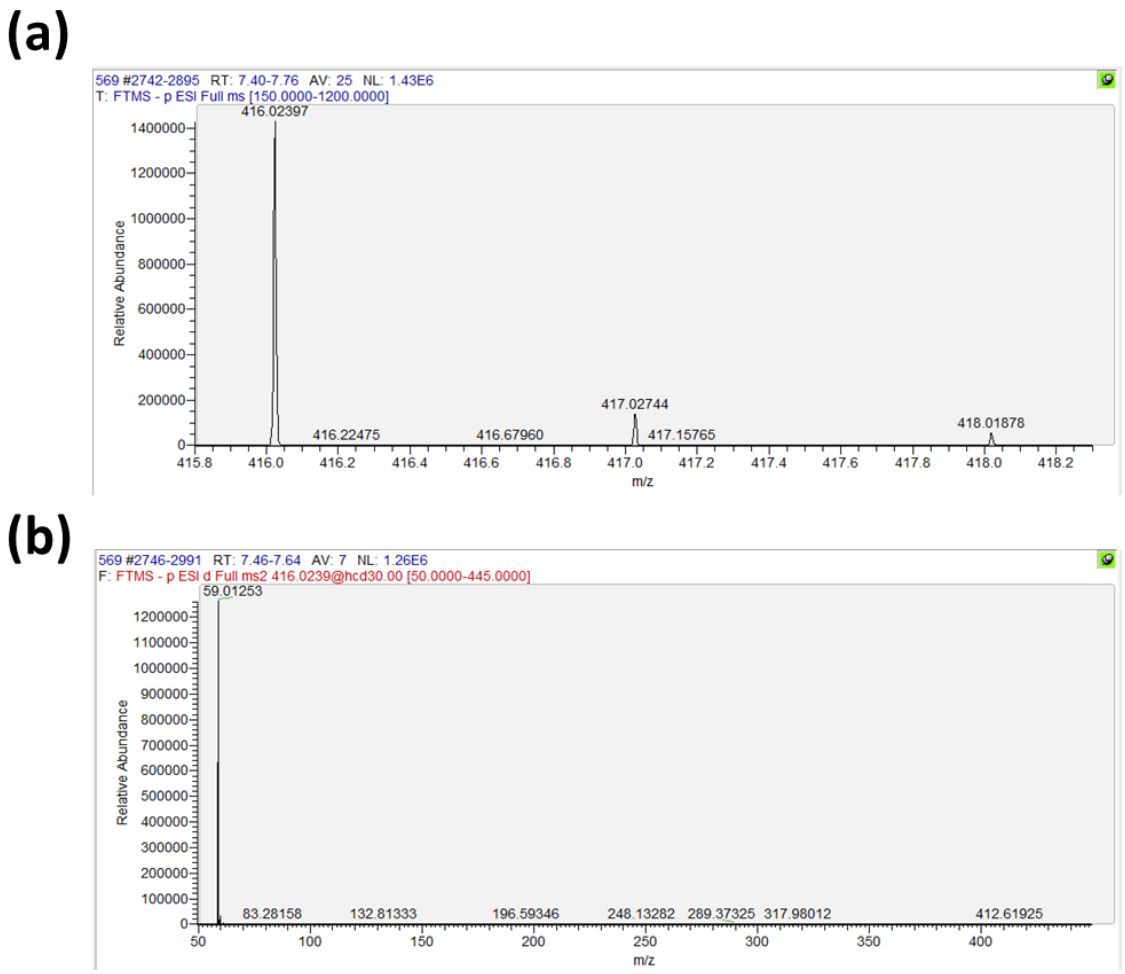

Figure A.7. (a) Mass spectra from extract 569 (MB-C), integrated from 7.40 min – 7.76 min and (b) MS/MS fragmentation spectra, from extract 569 (MB-C), averaged from 7 scans, collected from 7.46 min – 7.64 min with precursor *m/z* 416.0239.

(a)

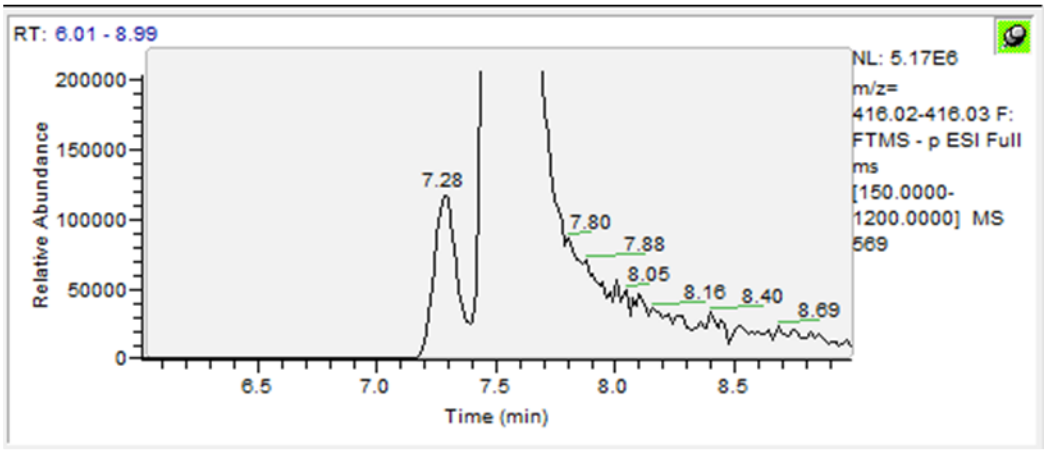

(b)

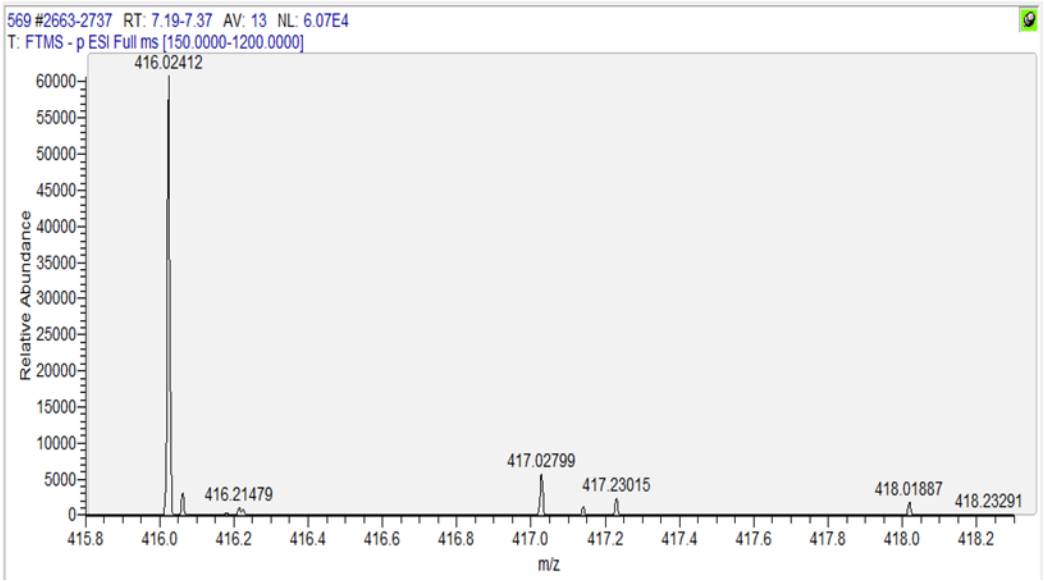

Figure A.8. (a) Extracted ion chromatogram of *m/z* 416.00-416.04 in extract 569, showing two peaks and (b) mass spectra from extract 569, integrated over 7.19 min – 7.37 min, the approximate timing of the first peak in the above chromatogram.

(a)

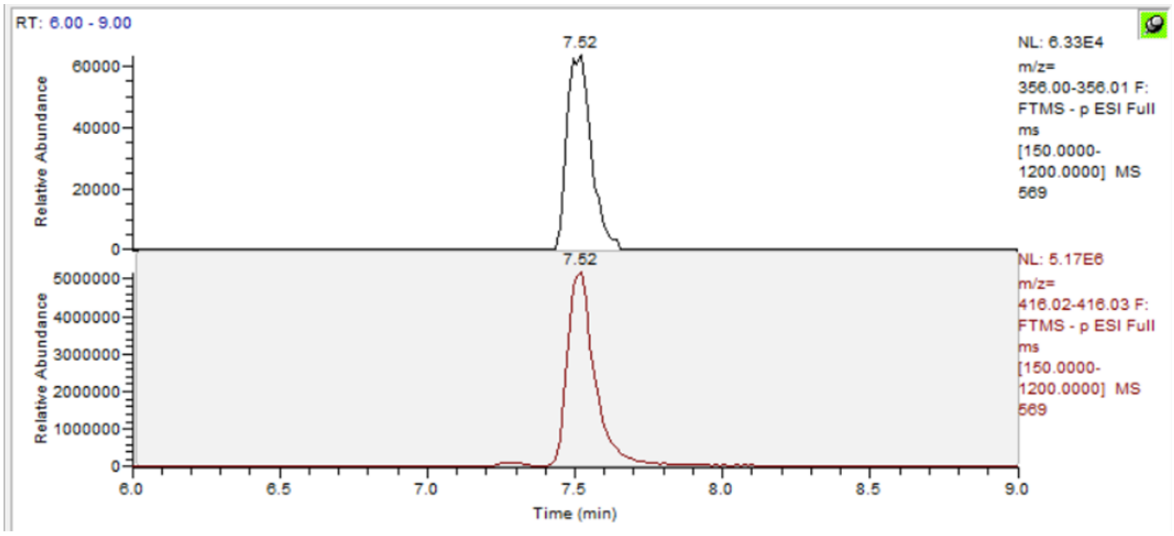

(b)

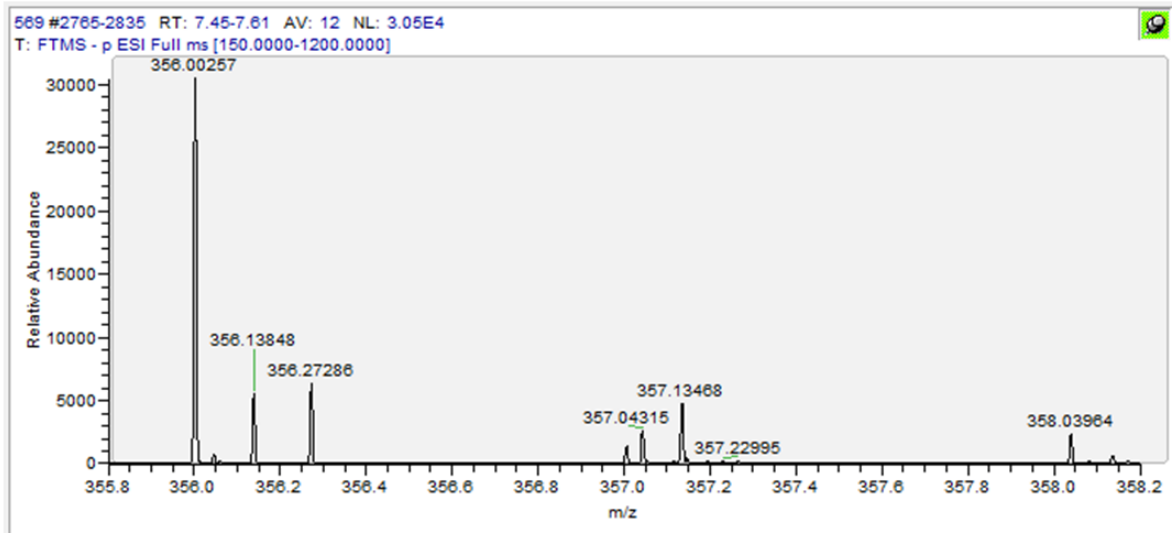

Figure A.9. (a-top) Extracted ion chromatogram of *m/z* 355.9 -356.1 and (a-bottom) *m/z* 415.9 - 416.1, both in extract 569 (b) mass spectra from *m/z* 355.8 – 358.2 from extract 569, integrated over 7.45 min - 7.61 min.

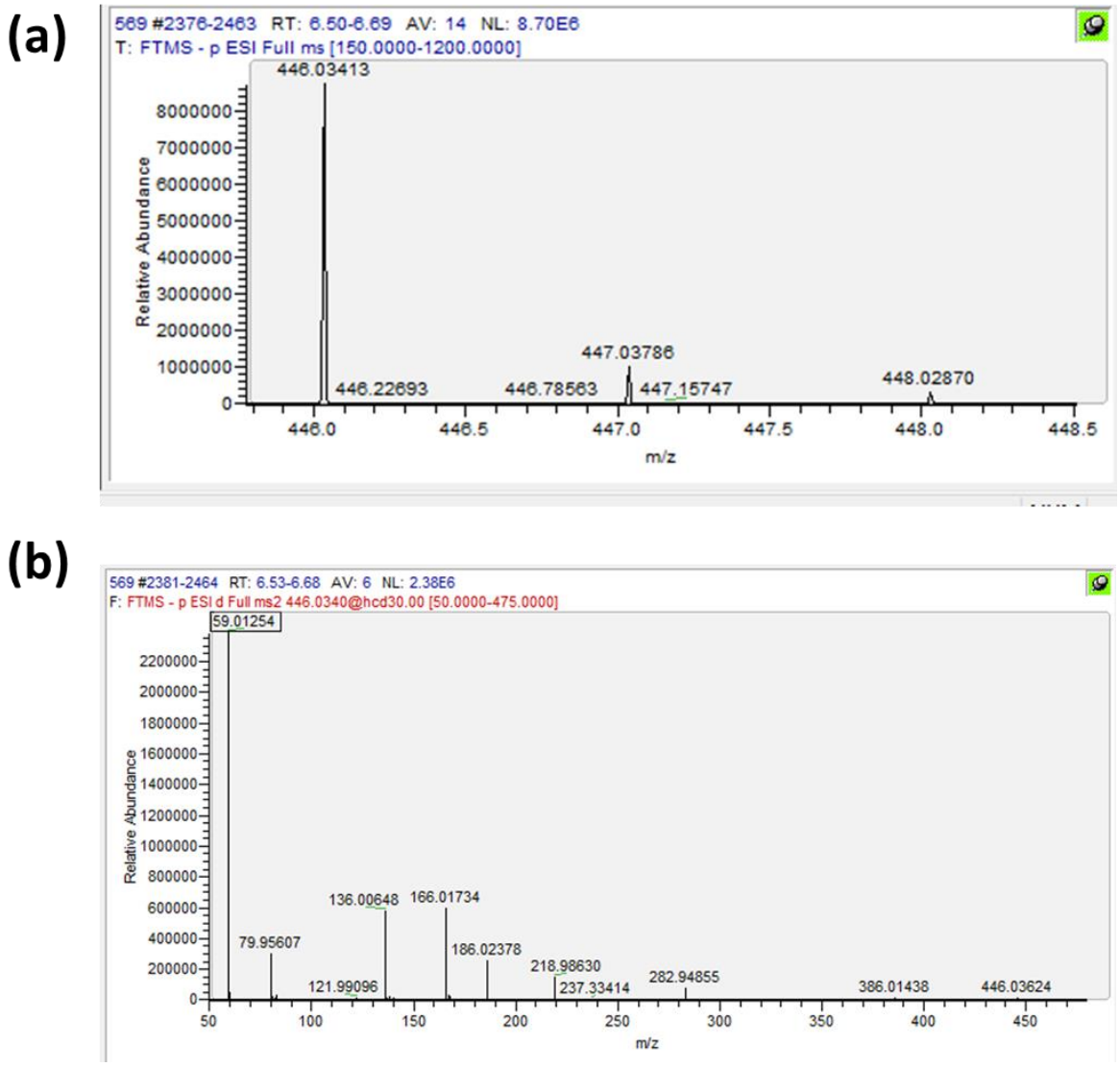

Figure A.10. (a) Mass spectra from extract 569 (MB-C), integrated from 6.50 min - 6.69 min and (b) MS/MS fragmentation spectra, from extract 569 (MB-C), averaged from 6 scans, collected from 6.53 min - 6.68 min with precursor *m/z* 446.0340.

(a)

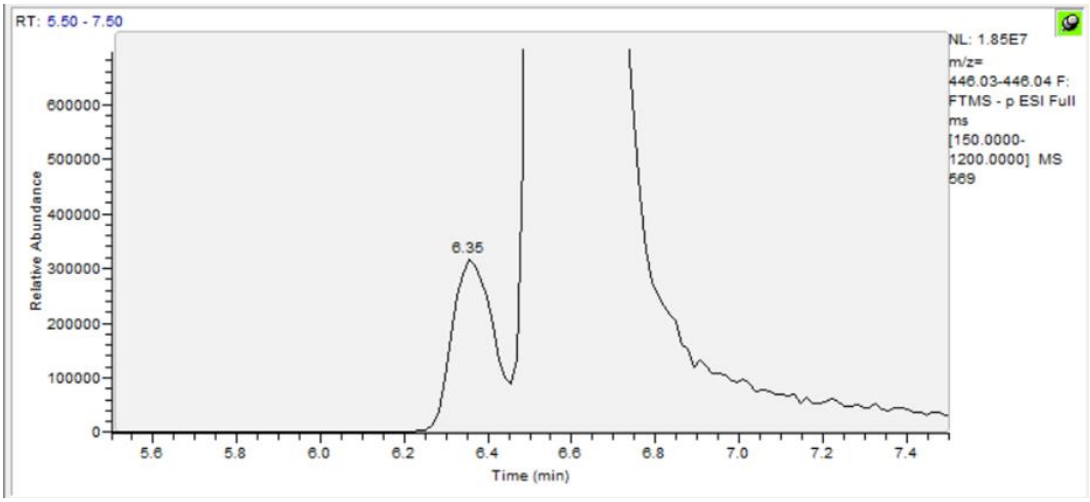

(b)

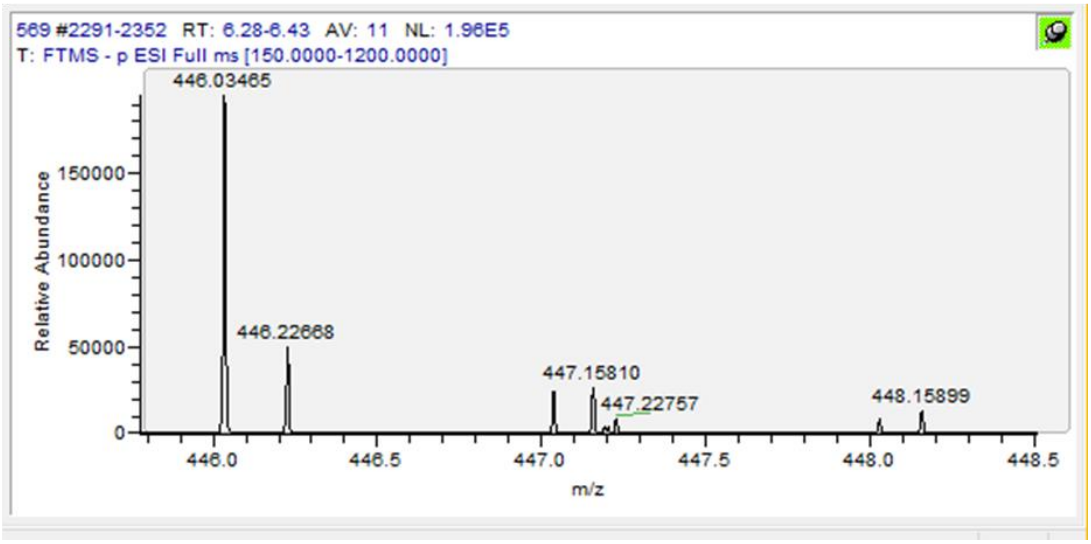

Figure A. 11. Extracted ion chromatogram of *m/z* 446.03 – 446.04 in extract 569, showing two peaks and (b) mass spectra from extract 569, integrated over 6.28 min - 6.43 min, the approximate timing of the first peak in the above chromatogram.

(a)

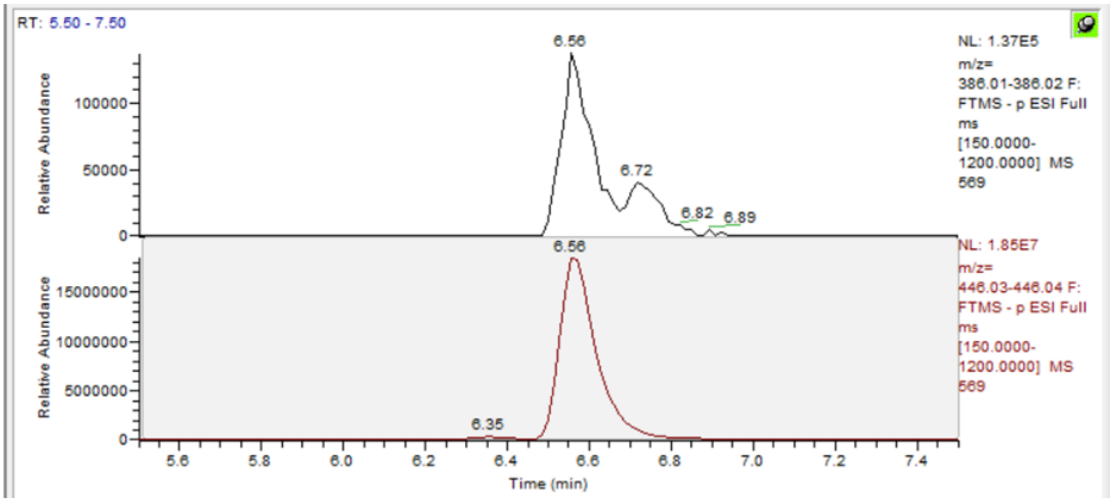

(b)

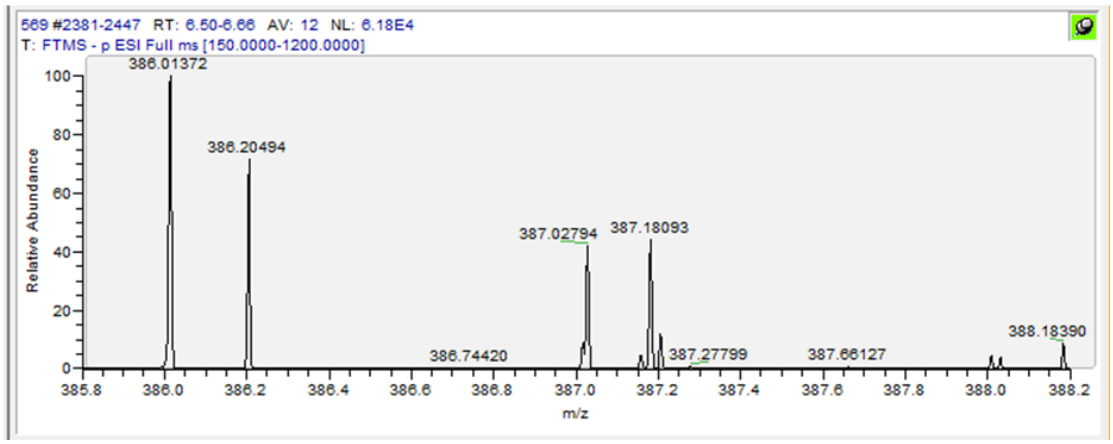

Figure A. 12. (a-top) Extracted ion chromatogram of *m/z* 386.01 – 386.02 and (a-bottom) *m/z* 446.03 – 446.04, both in extract 569 (b) mass spectra from *m/z* 385.8 – 388.2 2 from extract 569, integrated over 6.50 min - 6.66 min.

Appendix B. List of Abbreviations, and Acronyms

6:2 FTSulfate
6:2 Fluorotelomer sulfate

6:2 FTS
6:2 Fluorotelomer sulfonate

br-FBSEE
Branched-perfluorobutane sulfonamido diethanol

br-MeFBSE
Branched-methyl perfluorobutanesulfonamido ethanol

ESI
Electrospray ionization

FASE
Perfluoroalkanesulfonamido ethanol

FBSE
Perfluorobutane sulfonamido ethanol

FBSEE
Perfluorobutane sulfonamido diethanol

GC-MS
Gas chromatography mass spectrometry

GC-QTOF-MS
Gas chromatography quadrupole time-of-flight mass spectrometry

HPLC
High-performance liquid chromatography

INAA
Instrumental neutron activation analysis

IS
Internal standard

LC
Liquid chromatography

LC-HRMS
Liquid chromatography high-resolution mass spectrometry

LC-MS/MS
Liquid chromatography tandem mass spectrometry

LC-QTOF-MS
Liquid chromatography quadrupole time-of-flight mass spectrometry

MeFBSE
Methyl perfluorobutane sulfonamido ethanol

MeFOSE
Methyl perfluorooctane sulfonamido ethanol

MS
Mass spectrometry

m/z
Mass-to-charge ratio

n-FBSEE
Linear-perfluorobutane sulfonamido diethanol

n-MeFBSE
Linear-methyl perfluorobutanesulfonamido ethanol

NIST
National Institute of Standards and Technology

PFAS
Per- and polyfluoroalkyl substances

PFBS
Perfluorobutane sulfonic acid

PIGE
Particle-induced gamma ray emission spectroscopy

TN
Technical note